Lenzinger Berichte

93 | **2017**

Scientific Reports on Wood, Pulp and Regenerated Cellulose

www.lenzing.com

LENZING

LEADING FIBER INNOVATION

LENZINGER BERICHTE

Scientific Reports on Wood, Pulp and Regenerated Cellulose

„Das Experiment, dem nicht eine Theorie, d.h. eine Idee vorausgeht, verhält sich zur Naturforschung wie das Rasseln einer Kinderklapper zur Musik.“

Justus Freiherr von Liebig
(1803 - 1873), deutscher Chemiker

Dedicated to the retirement of
Johann Männer (Lyocell expert Lenzing AG) and
Dr. Gregor Kraft (Viscose expert Lenzing AG).

AU-ISSN 0024-0907
Published by Lenzing AG
4860 Lenzing, Austria
Phone +43 7672 701-0

Editor: Dr. Thomas Röder
Printed in Austria, May 2017

Front page: Copyright Lenzing AG
Fotos: Franz Neumayr, Thomas Röder, Sandra Schlader, Vogel AV
Layout: MMS Werbeagentur

Additional copies can be obtained by contacting the following address:

Dr. Thomas Röder
c/o Lenzing AG, R&D, 4860 Lenzing, Austria
Phone: +43 7672 701-3082, Fax: +43 7672 918-3082
E-mail: t.roeder@lenzing.com

All papers are available online at:
http://www.lenzing.com
and
http://www.lenzinger-berichte.com

Foreword

It was discovered in the middle of the 19th century already, that cellulose can be dissolved and regenerated again to produce fibers. Industrial production started at the beginning of the 20th century and therefore man-made cellulose fibers were the first artificial fibers long before petrol-based synthetic fibers. Also Lenzing AG is producing woodbased cellulose fibers since nearly 80 years and has set standards ever since – following the slogan "Leading Fiber Innovation".
Although man-made cellulose fibers have quite a history, there is still enough room for further research and development. Especially during the last years these fibers are experiencing a renaissance as they are made from the renewable resource wood and thus fulfilling the requirement for sustainability, which is becoming more and more important. However, just the raw material does not make a sustainable product; rather the whole production chain must follow this principle.
Consequently R&D within Lenzing AG covers the whole value chain, from wood and pulp to fibers and the final products made from them. This wide spectrum of topics related to cellulose fibers are also covered in this volume of Lenzinger Berichte. The papers include co-products from the pulping process, new developments in dyeing cellulose or comfort properties of nonwovens. There will be new and surprising developments in dissolving and shaping of cellulose and in related fields also in the future, so challenges for research will continue. The well-positioned R&D, including process and product development, is a strategic asset for Lenzing AG to keep its leading position within the industry in the future also.

Dr. Gert Kroner
Vice President Global R&D
Product Innovation
Lenzing AG

Lenzing, April 2017

Vorwort

Fasern aus gelöster und anschließend wieder regenerierter Cellulose wurden Mitte des 19. Jahrhunderts entdeckt und ab Beginn des 20. Jahrhunderts im industriellen Maßstab hergestellt. Damit waren sie lange vor den auf Erdöl basierenden Synthetik Fasern die ersten Fasern, die industriell hergestellt und modifiziert werden konnten. Auch die Lenzing AG produziert seit beinahe 80 Jahren holzbasierte Cellulose Fasern und hat in dieser Zeit immer wieder Impulse gesetzt – nicht umsonst ist der Slogan der Lenzing AG „Leading Fiber Innovation".
Auch wenn regenerierte Cellulose Fasern bereits auf eine lange Geschichte zurückblicken, sind noch nicht alle Möglichkeiten bekannt und erforscht. Gerade in letzter Zeit erleben diese Fasern eine Renaissance, da sie aus dem nachwachsenden Rohstoff Holz gewonnen werden und somit den immer wichtiger werdenden Aspekt Nachhaltigkeit erfüllen. Der Rohstoff allein macht jedoch noch kein nachhaltiges Produkt, sondern die gesamte Produktionskette muss diesem Anspruch folgen.
Daher deckt die R&D der Lenzing AG auch die gesamte Wertschöpfungskette vom Holz über den Zellstoff bis zur Faser und den daraus hergestellten Produkten ab. Diese Bandbreite an Themen im Umfeld der Cellulose Fasern sind auch in dieser Ausgabe der Lenzinger Berichte zu finden. Die Artikel umfassen Co-Produkte aus dem Zellstoff Prozess, neue Entwicklungen beim Färben von Cellulose oder Komfort Eigenschaften von Nonwovens.
Es wird auch in Zukunft überraschende neue Entwicklungen im Bereich Lösen und Formen von Cellulose und den damit verbundenen Bereichen geben und die Fragestellungen an die Forschung werden nicht so schnell abnehmen. Die Lenzing AG setzt weiterhin auf eine gut aufgestellte R&D, sowohl in Prozess- als auch in Produktentwicklung, um auch in Zukunft die Spitzenposition innerhalb der Industrie innezuhaben.

Dr. Gert Kroner
Vice President Global R&D
Product Innovation
Lenzing AG

Lenzing, April 2017

Composition of Pulp Mill Bark Waste

Danuta J. Mozdyniewicz[1], Richard Herchl[2], Stefan Böhmdorfer[3] and Antje Potthast[3]
[1] Kompetenzzentrum Holz GmbH, Linz, Austria
[2] Lenzing AG, Lenzing, Austria
[3] University of Natural Resources and Life Sciences (BOKU), Wien, Austria
e-mail: d.mozdyniewicz@kplus-wood.at

Abstract

Softwood bark is an interesting raw material with high potential due to its availability in considerable quantities. Several studies have already been performed on the constituents of bark, resulting in findings of bioactive components, specific carbohydrates, or raw materials for bio-based adhesives. Conversely, so far hard woods received less attention due to their thinner bark, which cannot be separated from wood without some limitations. The extraction of bio-based materials with solvents of varying properties results in a wide spectrum of components grouped by their characteristics dependent on the solvents used. In our study, beech and spruce pulp mill debarking residues were investigated to reveal the influence of different solvent sequences on carbohydrate isolation and the composition of lipophilic extractives.

Introduction

Bark is available in large quantities at pulp production sites, but up to now it is mainly utilized thermally for energy generation. Implementation of a bio-refinery concept makes a previous separation of valuable components from all available sources necessary. Furthermore, the substitution of petrochemical industry products by more sustainable ones should be achieved in future. Especially softwood bark was found to contain a large amount of extractives, which can be assigned to various substance groups. Generally, hydrophilic as well as lipophilic components may be extracted using different solvents. Spruce bark, for example, contains ca. 15 - 20% of water soluble substances, e.g. sugars and phenols as well as polyphenols and polysaccharides, which are largely and inadvertently extracted in the course of wet bark removal [1].

Further, the presence of bio-active polyphenols with proven anti-oxidative effect has been lately described by Co [2]. However, very small amounts are used worldwide by now in rather niche products like dietary supplements. Another product group which can be found in bark with interesting properties and high future potential are stilbene glucosides. They may easily be extracted with pressurized hot water and are present in fresh bark in large quantities. However, their amount decreases with increased bark storage time, affecting the feasibility of commercial exploitation [3]. Lignin derived aromatic compounds and tannins may be considered as further potential valuable products. They can be found in bark extracts in a great variety. Especially their conversion into bio based adhesives for fibreboard manufacture may play a role in the future [4]. However, only few commercial applications are known so far, due to higher material and energy costs in comparison with oil-based adhesives.

Another component group worth mentioning are carbohydrates. Bark or debarking residues contain considerable amounts of carbohydrates, present both as bound sugars in cellulose or pectin and as easily extractable free mono- and oligosaccharides [5]. Differences between softwood and hardwood in bark thickness and structure demand an adjustment of the debarking intensity, resulting in varying amounts of wood fragments found in the debarking residues. Generally, debarking of hardwood provides a product with higher wood content and may therefore be utilized for carbohydrate isolation, e. g. for further fermentation, while using the wood trunks might be used for entirely different applications.

The use of an appropriate solvent allows the extraction of particular component groups with hydrophilic or hydrophobic characteristics [2, 6, 7]. Successive extraction with solvents of changing polarity may result in a diversity of new products. Peltonen described

successive extraction of spruce and pine bark with a series of various solvents, however, some of the solvents are not applicable in the industry due to environmental and health risks [6, 8]. Nowadays, water, acetone and ethanol rate as the most popular extraction agents due to high availability, low costs and easy recyclability.

With very few exceptions, most of the extraction experiments were performed using softwood bark [9, 10]. So far hard woods have received less attention due to their thinner bark, which cannot be easily separated from wood. The high wood content in the industrial hardwood bark (up to 20%) may also be advantageous for carbohydrate extraction. Therefore, an investigation of beech bark extraction might point out new sources of industrial products.

Several interesting components were found in fresh spruce bark. However, immediate removal and utilization of bark after cutting is not always possible due to wood storage, which is unavoidable in most cases. In this work, the extraction of bark from two dissolving pulp production sites was performed and the obtained extracts were investigated. Bark was removed from the logs after several months of storage. A comparison of the composition of the several obtained extracts of debarking residues originating from beech (Fagus sylvatica) and spruce (Picea abies) was performed. Also, the influence of prior lipophilic components removal on the yield and composition of the carbohydrate fraction content was investigated.

Materials and Methods

Industrial bark waste from beech (Fagus sylvatica) and spruce (Picea abies) was used for the experiments. Beech wood debarking residues contained large amounts of wood splinters, due to the more intense debarking procedure. In the first step, the samples were defrosted, left to dry at room temperature for two days and subsequently milled (60 mesh). The carbohydrate compositions and ash contents of the raw materials are shown in Table 1.

The extraction was carried out in a lab-scale Parr reactor station with a reactor volume of 450 ml, mechanical stirring and temperature control. 20 g of the bark were placed in the reactor and the content was heated to a temperature exceeding the boiling point of the solvent. A pressure increase up to 5 bar was observed depending on the solvent. After 10 minutes at the specified temperature the reactor was quenched using ice water. The extraction scheme of the experiments is shown in Figure 1. Spruce bark was used for the experiments V1 & V2, and beech debarking residues were used in V3 & V4. The particular extracts in the sequence were named in the order of the sampling (E1 to E3).

After cooling, the solids were separated by filtration using a crucible (Porosity 4), washed with fresh solvent and filled in the reactor for the next experiment. After the completion of the solvent sequence, the bark residues were air dried and weighed. Dry content was determined to allow the total yield calculation in relation to the initial bark amount.

The solid content of the extracts was determined after blowdown evaporation with nitrogen or freeze drying of the aqueous solutions. The determination of neutral sugar monomers was performed by anion exchange chromatography (AEC) with pulsed amperometric detection (PAD) after a two-step total hydrolysis with H_2SO_4 according to Sixta [11].

The amounts of fatty acids (including resin acids), sterols, sterol esters and triglycerides were detected by GC-MS using the modified method by Örsa [12]. Samples with similar solid concentrations were used for the analysis. Heneicosanoic acid, cholesterol, cholesteryl palmitate and 1,3-dipalmitoyl-2-oleoyl-glycerol (Sigma-Aldrich) were used as group markers and the peak areas of the groups were compared.

Results and Discussions

Raw Material Analyses

The raw materials were examined with regard to the carbohydrate composition and the ash content. The results are shown in Table 1. Carbohydrates represented 35.1% of the analysed spruce bark, with glucose as the highest concentrated sugar. Arabinose, xylose, mannose and galactose displayed significantly lower concentrations in the range of 1.8 – 3.7%, rhamnose content was even below 1%. A significantly higher xylose content of 11.6% was found in beech bark residues, which was not surprising if one considers the high wood content in the pulp mill bark waste due to harsh debarking and the generally high glucuronoxylan content in hardwoods [13, 14]. The other sugars were in a similar range as in spruce bark, with the exception of mannose, which was below 1%. Although the difference in glucose content between the wood species is less than 1%, different sources may be identified. In case of beech bark residues, the value may be attributed to the high cellulose content in the present wood fraction, whereas the presence of galactoglucomannan explains the fact in case of spruce [15]. The total amount of hydrolysable carbohydrates of 35.1% in spruce bark was consistent with the previously described holocellulose content, which usually refers to the residual carbohydrate fraction after lignin removal from wood [6]. Generally, the high proportion of car-

Table 1. *Initial carbohydrate composition of the raw materials.*

	Glc [%]	Xyl [%]	Man [%]	Ara [%]	Rha [%]	Gal [%]	∑[%]	Ash [%]
Spruce bark	25.2	2.2	1.8	3.7	0.4	1.8	35.1	2.8
Beech bark	26.0	11.6	0.9	2.2	0.5	1.4	42.6	9.1

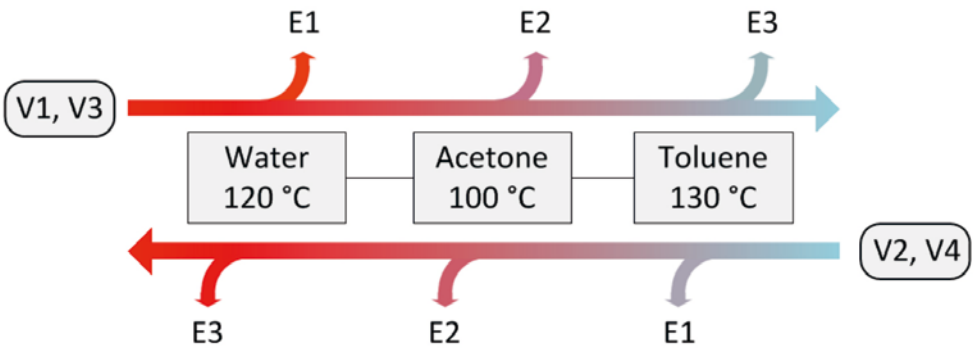

Figure 1. *Extraction scheme (V1 & V2: spruce; V3 & V4: beech).*

bohydrates in bark makes its extracts after further conversion a potential source sugars for biotechnological processing. Spruce bark displayed significantly lower ash content, and also a lower total amount of carbohydrates was found. Carbohydrates may even be obtained more efficiently from beech bark residues, as a content of 42.6% of hydrolysable carbohydrates was found (Table 1), a value in good agreement with literature results [10]. However, the particular sugars are present in different proportions. Significantly higher amounts of glucose and xylose were found compared to previous analyses. The presence of large quantities of wood splinters due to extensive debarking offer an explanation for the discrepancy. Glucose was the predominant carbohydrate with 26% of the bark, followed by 11.6% xylose. The concentrations of arabinose and galactose were 2.2%, and 1.4% respectively, which is an indication for the presence of considerable amounts of pectin. The other sugars displayed values below 1%. The relatively high ash content of the beech bark was linked to the outside storage in the wood yard, earlier analyses revealed significantly less ash in fresh bark [10].

Generally, considerable amounts of hydrolysable carbohydrates were found in both examined debarking residues, confirming their suitability as a source for subsequent biotechnological conversion.

Extraction Yields

Two experiments with varying solvent sequences were performed for each wood species to reveal the solvent sequence influence on the yield and composition of the fractions. Solvents were selected according to environmental and economic demands and therefore differed from previously investigations [10]. In V1 and V3, water was used as the first solvent, followed by acetone and toluene, while the sequence started with toluene and ended with water in V2 and V4. A schematic illustration is shown in Figure 1. Relatively mild extraction conditions were chosen to prevent undesired side reactions. The extraction yield was determined by the quantification of the dry content present in the extracts.

Similar fractionation trends were found for equal solvent sequences for both wood species, especially regarding the non-aqueous solvents. An initial toluene extraction resulted in higher toluene extract yield and decreased acetone extractive content, whereas yields were below 1% for both bark samples with toluene as the last extraction step (Table 2). In the latter case, a large portion of toluene soluble components had already been extracted by acetone in the previous step, indicating an insufficient solvent amount or selectivity to clearly differentiate both component groups. The sums of the yields of both non-aqueous extracts were comparable within one wood species, however, the values were significantly lower in the case of beech bark residuals. In case of spruce, around 7% of the initial bark was removed by the non-aqueous solvents and around 2% in case of beech, which is in accordance with the amount of lipophilic extractives in beech wood [16].

Beech bark water extracts uniformly contained about 14% of solids in the initial as well as in the final water phase. In case of spruce bark, however, the yield increased from 14.7% to 16.3% when toluene and

Table 2. *Solid yields of the obtained fractions.*

	final bark yield [%]	water extract [%]	aceton extract [%]	toluene extract [%]	total [%]
V1 (spruce)	72.1	14.7	6.9	0.7	94.5
V2 (spruce)	73.4	16.3	2.2	4.8	96.8
V3 (beech)	89.0	14.0	2.1	0.2	105.3
V4 (beech)	89.6	14.0	1.1	1.0	105.7

acetone extractions were performed initially, which may indicate an increased accessibility after removal of hydrophobic components. In the literature, significantly higher water extract yields of the inner spruce bark were reported, however, at higher temperature and longer treatment time (up to 24 h)[17]. In general, the yield of the spruce bark solid residue was slightly below values found in the literature, which might be ascribed to different experimental conditions, undesired losses during handling, wood storage, or wood source. Further, volatile components were not quantified in the experiments. Beech bark water extract on the other hand, contained less solids compared to previous results [10]. Limited accessibility was caused by the high wood content in the sample.

Next to varying extract yields, the samples showed distinct visual differences. Spruce bark extracts obtained during the experiment V2 are shown as an example in Figure 2. All the obtained water extracts had an intense brown color, which may primarily be attributed to lignin and lignin fragments. Further, a strong foam formation was observed, indicating a presence of pectin and protein in the aqueous phase. Beech bark toluene extracts displayed the least intense coloration of all the liquids obtained, concurrently very low amounts of residual solids were found after solvent removal.

Figure 2. *Spruce bark extracts (toluene-acetone-water).*

Carbohydrate Extraction

A closer look at the concentrations of hydrolysable carbohydrates in the water extracts revealed a dependence on the wood species and the pretreatment. Figure 3 shows the fractions of extractable carbohydrates with regard to the total determined carbohydrate content and bark mass. Generally, the extraction of spruce bark yielded significantly higher amounts, with 14.2% in the fraction obtained by an initial aqueous treatment. Performing the water extraction as the last step decreased the value to 12.3%. The yields for beech bark extraction were significantly lower with 9.4 and 7.1%, due its high wood content and the resulting low accessibility. Generally, 3 - 5% of bark could be identified as water extractable carbohydrates under the applied conditions, which is a rather small amount. The application of acid hydrolysis as the first step would allow increasing the carbohydrate yield, however potentially undesired by-reactions cannot be ruled out. As a possible option, a hydrolysis could be performed after solvent extraction, so that the obtained extractives remain unaffected.

Besides the carbohydrate yield, the accessibility of the particular sugar components was of a great interest, as an accumulation of a single component in a fraction could be advantageous for isolation. Generally, water extraction of spruce bark resulted in higher carbohydrate yields up to 33.8% after total hydrolysis (Table 3). Significantly lower values of around 24% were found in beech bark extracts. Glucose was the dominating

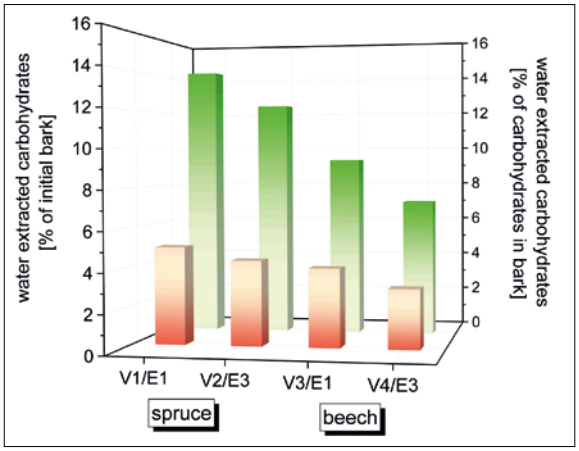

Figure 3. *Percentage of water extracted carbohydrates as a fraction of bark (front columns) and as a fraction of the determined carbohydrate content in the bark (back columns).*

Table 3. *Carbohydrate content of the water extracts determined after total hydrolysis.*

	Glc [%]	Xyl [%]	Man [%]	Ara [%]	Rha [%]	Gal [%]	∑[%]
V1 water extract	25.7	0.4	1.4	3.8	0.4	2.1	33.8
V2 water extract	21.0	0.2	1.2	2.2	0.3	1.7	26.6
V3 water extract	14.3	2.1	1.0	3.1	1.3	3.1	24.9
V4 water extract	13.1	2.0	1.1	3.3	1.2	3.1	23.8

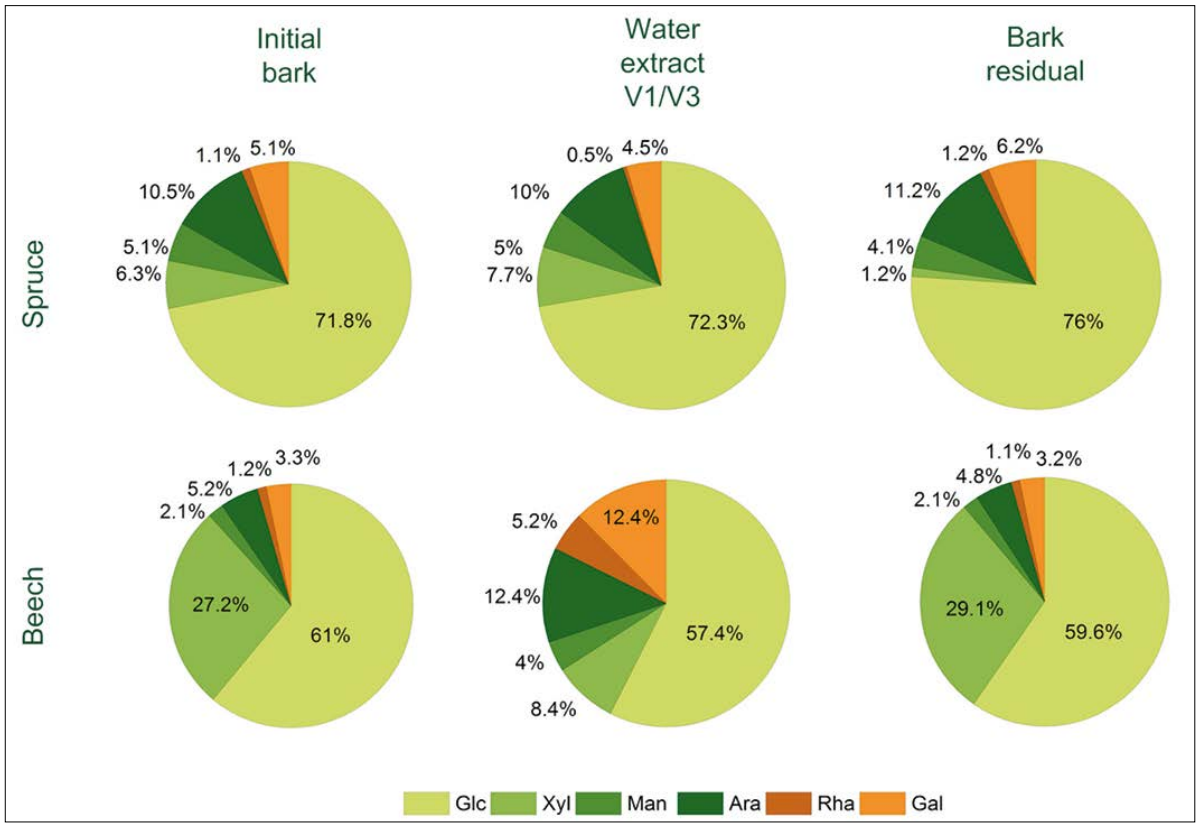

Figure 4. *Sugar patterns of the different fractions.*

sugar in all the water dissolved fractions in both bark residues, which was consistent with previous results [1, 18, 19]. Predominantly non-cellulosic polysaccharides provided the source for glucose, as cellulose is hardly affected by auto-hydrolysis at temperatures below 150 °C [20]. However, hemicellulose degraded to form soluble oligosaccharides, which is industrially used as a pre-hydrolysis step to obtain high purity pulp. However, the temperature during our experiments was insufficient for extensive hemicellulose removal, which is reflected in the extract composition shown in Table 3.

Looking at the carbohydrate content in the bark residue after the extraction, an increased relative carbohydrate content is noticeable (Table 4). However, no drastic increase or decrease was detected for any particular sugar. The limited impact is not a surprise, considering, that maximally 5% of the initial bark was removed as carbohydrates. The solvent sequence played a role solely with respect to the yield. In Figure 4 a comparison of sugar patterns of the particular fractions is shown. Water extract compositions of experiments V2 and V4 were excluded in this diagram, as the differences to the other experiments were negligible. Spruce fractions exhibited minimal differences in the sugar distribution in the particular fractions. A slightly lower xylose proportion may again indicate stability of xylan under the applied

Table 4. *Carbohydrate content of the extraction residues determined after total hydrolysis.*

	Glc [%]	Xyl [%]	Man [%]	Ara [%]	Rha [%]	Gal [%]	∑[%]
Spruce bark after V1	31.8	3.4	2.2	4.4	0.2	2.0	44.0
Spruce bark after V2	31.6	3.5	2.3	3.9	0.3	2.1	43.7
Beech bark after V3	26.0	12.7	0.9	2.1	0.5	1.4	43.6
Beech bark after V4	27.8	13.5	0.9	2.0	0.5	1.4	46.1

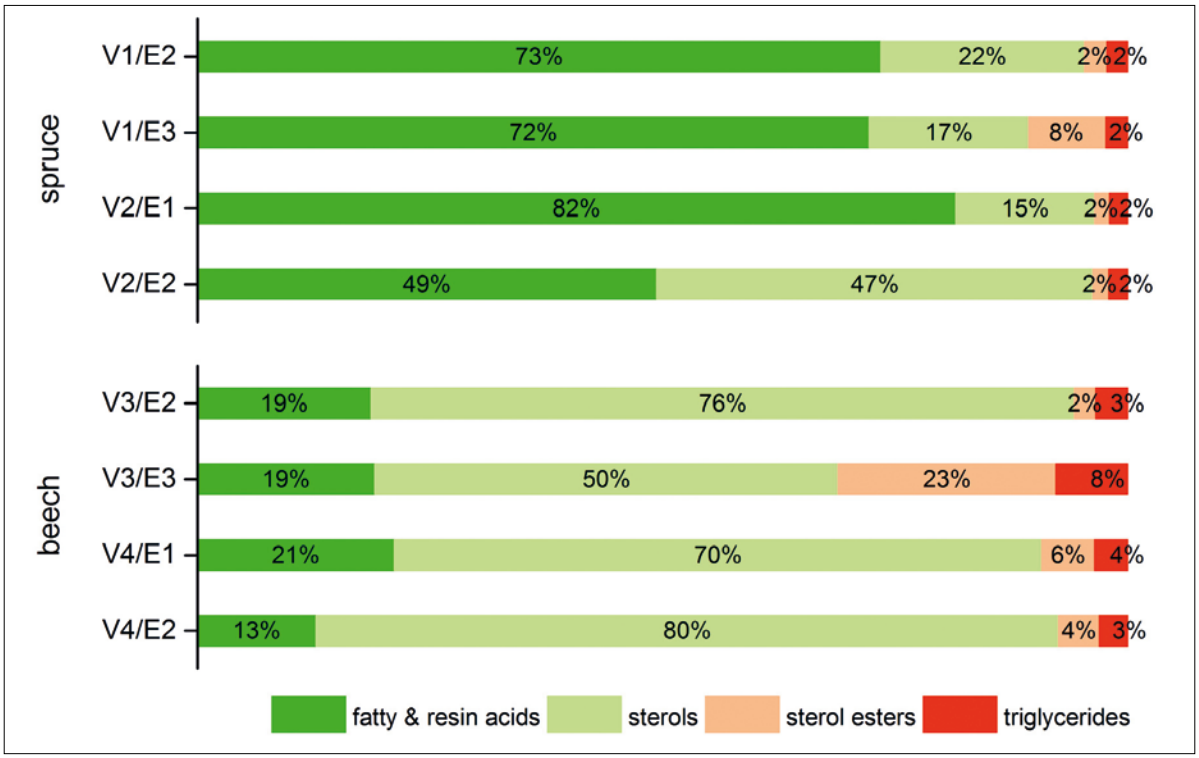

Figure 5. *Comparison PID versus QEPAS, black: QEPAS measurement directly probing sample gas from the process stream, red: PID measurement of pre-treated gas sample.*

conditions. In beech bark extract, significantly reduced content of xylose and glucose was found, attributed to the high amount of cellulose and hemicellulose in the present wood and their stability, leading to an apparent enrichment of the other constituents. Since this reduction is more pronounced for xylose, an increased amount is found in the residual bark.

Lipophilic Extractives

Finally, the behaviour of the lipophilic extractives in dependence of the extraction sequence was investigated by GC-MS. The limited availability of standard substances prevented a complete component quantification. Therefore, a comparison of cumulative peak areas for particular component groups was the method of choice in our case [12]. In Figure 5, the results are presented in percent of peak areas of particular regions in the chromatogram in relation to the total lipophilic fraction. In this way, only an approximation of the relative composition within the group was possible. The obtained patterns varied in dependency of the applied solvent sequence. After previous acetone extraction, a higher ratio of sterol esters was found dissolved in toluene (V1/E3 & V3/E3). The significantly reduced yields of toluene extracts in those experiments in comparison with the reversed sequence (Table 2) suggest previous extraction of the other components rather than a higher accessibility to the solvent. The relative share of the fatty and resin acids remained constant in these trials. The situation was quite different if the reverse sequence was considered. Fatty and resin acids were the predominant group in the initial toluene extraction of spruce, decreasing in the subsequent acetone extract. In beech bark, sterols were identified as the largest group in all fractions. The portions of sterol esters and triglycerides remained unchanged.

Conclusions

1. Initial water extraction results in higher carbohydrate yield independent of the species. 3 - 5% of the bark used in the experiments were extractable carbohydrates.
2. Fatty acids and resin acids are dominating lipophilic components in spruce bark, sterols in beech bark.
3. Similar changes in group profiles are found in equal solvent sequences.

Acknowledgements

Financial support was provided by the Austrian government, the provinces of lower Austria, upper Austria, and Carinthia as well as by Lenzing AG. We also express our gratitude to the Johannes Kepler University, Linz, the University of Natural Resources and Life Sciences (BOKU), Vienna, and Lenzing AG for their in-kind contributions.

References

[1] Kylliäinen, O. and B. Holbom, Chemical composition of components in spruce bark waters. Pap Puu, 2004. 86(4): p. 289 - 292.

[2] Co, M., et al., Extraction of antioxidants from spruce (Picea abies) bark using eco-friendly solvents. Phytochem Anal, 2012. 23: p. 1 - 11.

[3] Krogell, J., et al., Extraction and chemical characterization of Norway spruce inner and outer bark. Nord Pulp Paper Res, 2012. 27(1): p. 6-17.

[4] Pizzi, A., Recent developments in eco-efficient bio-based adhesives for wood bonding: opportunities and issues. J Adhesion Sci Technol, 2006. 20(8): p. 829 - 846.

[5] Kemppainen, K., et al., Spruce bark as an industrial source of condensed tannins and non-cellulosic sugars. Ind Crops Prod, 2014. 52: p. 158 - 168.

[6] Peltonen, S., Studies on bark extracts from scots pine (Pinus silvestris) and norway spruce (Picea abies). Part I. Main chemical composition. Pap Puu, 1981. 63(10): p. 593 - 595.

[7] Sjöström, E. and R. Alén, Analytical methods in wood chemistry, pulping and papermaking. Springer Series in Wood Science. 1999: Springer Verlag.

[81] Peltonen, S., Studies on bark extracts from scots pine (Pinus sylvestris) and norway spruce (Picea abies). Part II. Chromatographic analysis of hot water and alkali soluble polyflavonoids. Pap Puu, 1981. 63(11): p. 681 - 687.

[9] Ekman, R. and A. Academy, The suberin monomers and triterpenoids from the outer bark of betula verrucosa Ehrh. Holzforschung, 1983. 37: p. 205-211.

[10] Dietrichs, H.H., et al., Untersuchungen über die Kohlenhydrate der Rinden einheimischer Holzarten. Holzforschung, 1978: p. 60-67.

[11] Sixta, H., et al. Characterization of alkali-soluble pulp fractions by chromatography. in 11th ISWPC. 2001. Nice, France.

[12] Örsa, F. and B. Holmbom, A convenient method for the determination of wood extractives in papermaking process waters and effluents. J Pulp and Pap Sci, 1994. 20(12): p. J361-J366.

[13] Sixta, H., Handbook of Pulp Vol. 1. 2006. 3-1352.

[14] Willför, S., et al., Polysaccharides in some industrially important hardwood species. Wood Science and Technology, 2005. 39: p. 601-617.

[15] Willför, S., et al., Polysaccharides in some industrially important softwood species. Wood Sci Technol, 2005. 39(4): p. 245 - 257.

[16] Pietarinen, S.P., et al., Knotwood and bark extracts: strong antioxidants from waste materials. J Wood Sci, 2006. 52(5): p. 436 - 444.

[17] Balas, a., et al. Bioactive compounds from bark and knotwood of Norway spruce (Picea abies). in 10th European Workshop on Lignocellulosics and Pulp. 2008. KTH Stockholm, Schweden.

[18] Dietrichs, H.H., M. Sinner, and J. Puls, Potential of Steaming Hardwoods and Straw for Feed and Food Production. Holzforschung, 1978. 6: p. 193-199.

[19] Le Normand, M., et al., Hot-water extraction and characterization of spruce bark non-cellulosic polysaccharides. Nord Pulp Paper Res, 2012. 27(1): p. 18-23.

[20] Tunc, M.S. and A. Van Heiningen, Hydrothermal dissolution of mixed southern hardwoods. Holzforschung, 2008. 62: p. 539-545.

Preparation of Xylan Derivatives from Hemi-Rich Alkaline Process Lye

Vasken Kabrelian[1*], Kateryna Wöss[1], Richard Herchl[2], Thomas Röder[2] and Karin Fackler[2]

[1] Kompetenzzentrum Holz GmbH, Altenberger Str. 69, 4040 Linz, Austria
[2] Lenzing AG, Werkstraße 2, 4860 Lenzing, Austria
[*] Contact: v.kabrelian@kplus-wood.at

Abstract

The Lenzing Group has been committed to the fundamental principles of sustainability for many years. Profit-ably operating is equally important to achieve a social balance and safeguard the ecological basis of life. One of the key issues is the more extensive use of the raw material wood for valuable products. The biopolymer xylan, a co-product from cellulose production, has been neglected over decades. Hemicelluloses have come into focus for special applications as well as for further processes. A process stream with a high xylan concentration pro-vides a high potential as starting material for new products.
Wood based hemicelluloses can be used as a sustainable material in different applications. They originate from renewable non-food material. In addition, it is possible to extract them from side streams of existing production processes. Thus, they would offer an eco-friendly alternative for applications by providing polysaccharide backbone and OH-groups for diversity of modifications. The chemical modification of xylan is a promising path to new biopolymer ethers and esters with specific properties depending on the functional groups, the degree of substitution, and the substitution pattern.
The hydrophilic and hydrophobic derivatizations have been studied directly in hemi-rich alkaline media (hemilye) with respect to the effects of reaction parameters, such as reaction medium, time, and molar ratio, on the reaction outcome. Major benefit of the process is the enhanced reactivity of xylan in the extraction liquor without intermediate separation and, especially, drying. The synthesized products were characterized by FT-IR, ^{1}H-NMR, ^{13}C-NMR spectroscopy and HPLC and the results have been demonstrated in this work. The synthesized xylan derivatives were: carboxymethylxylan (CMX), hydroxypropyltrimethylammonium-xylan (HPTMAX), 3-butoxy-2-hydroxypropyl xylan ether (BHPXE), carboxyethylxylan (CEX), carboxy-propylxylan (CPX), xylansulphonate, xylansulfate.

Keywords: *hemicellulose, xylan derivatives, synthesis, modification*

Introduction

Wood polysaccharides are potential sources of environmentally compatible polymers for versatile future materials [1,2]. Dissolving pulp for textiles has become a growing industry. However, these products are based on pure cellulose and thus open up possibilities for hemicellulose streams. Production of sugars for biofuels or platform chemicals from wood resources are also processes that have the potential to include isolated hemicellulose or hemicellulose sugars as a co-product [3]. Due to the increasing demand for advanced renewable materials and green technologies, investigating the substantial polymer reserves in forests is of great interest.
The hemicellulose xylan is mainly composed of glucuronoxylans (GX), in which **β**-(1→4)-linked xylopyranosyl units (Xylp) from a linear chain that carries (1→2)-linked 4-O-methyl-**α**-D-glucopyranosyl uronic acid residues (MeGlcpA) and acetyl groups (Fig.1). The MeGlcpA : Xylp ratio in the investigated xylan is about 1 : 20 [4].

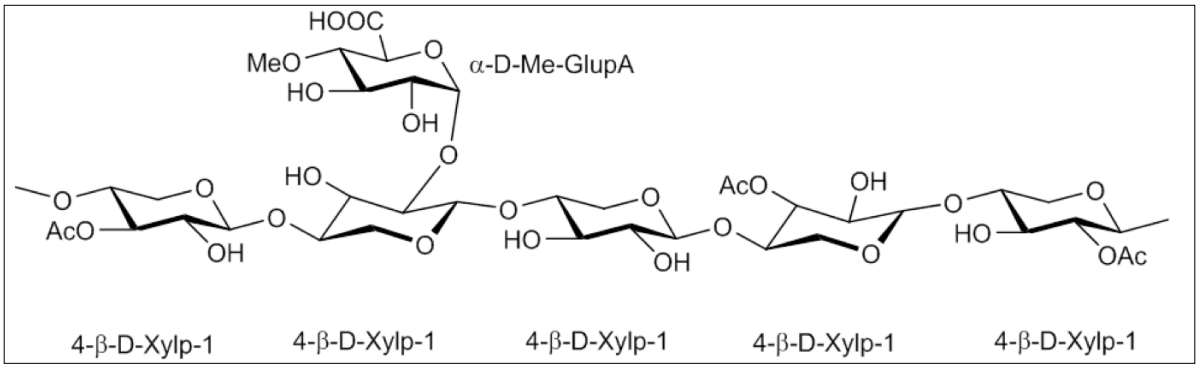

Figure 1. *Structure of alkali extracted xylan from bleached beech pulp.*

Recently, xylan derivatives gained increasing importance as new biopolymeric based materials and functional polymers [5,6]. Due to the functional properties of natural xylans, various application fields are considered, eg. xylan has a relatively low solubility in water [5]; this can be significantly improved by a suitable chemical modification. Water soluble xylan derivatives can be used also in construction materials, food, pharmaceutical and cosmetics industries, as binder or suspending agents, as a protective colloid or special-coating, or in hydrogels [7,8,9,10]. In addition to cellulose or starch derivatives, which are already being widely used, water-soluble xylan derivatives qualify because of their lower molar masses specifically for such applications, in which a lower viscosity or a higher consistency is desired. From xylan derivatives such as xylan and xylan-sulfonates and -sulfates micro particles were prepared as a drug carrier for colonic specific applications in anti-inflammatory and -toxic drugs [11,12]. Other possible applications of the hydrophobic xylan derivatives are known from packaging industry, e. g. as coating for packaging and paper [13,14].

It is known that the property and structure of xylan by substitution reaction of the hydroxyl groups of the monomeric units can change with different functional groups [5]. So both etherification (e.g. carboxymethylation) and esterification (e.g. sulfatation) were checked for their suitability. Carboxymethylation of polysaccharides is one of the most versatile functionalization procedures as it provides access to biobased materials with valuable properties [15]. Up to now the derivatization of polysaccharide xylan was observed only with xylan powder after the isolation from pulping processes. In this study, the derivatizations were performed directly in hemi lye from viscose processes.

Materials and Methods

Materials

Xylan containing hemilye was provided by Lenzing AG (www.lenzing.com)

All the reagents that were used for xylan derivatization were from Sigma-Aldrich: The synthesized hydrophilic and hydrophobic xylan derivatives results are listed in figure 2.

Methods

^{1}H-NMR Spectroscopy

The samples were characterized by liquid ^{1}H NMR spectroscopy in their composition by Bruker Avance III 300 MHz NMR spectrometer, 7.05 T magnetic field strength. 0.06 g sample 1-7 were dissolved in 600 μl D_2O and degassed 2 min in an ultrasonic bath. Reference (xylan) is sparingly soluble in D_2O, therefore 0.06 g were dissolved in 600 μl DMSO-d6.

^{13}C- NMR Spectroscopy

Quantitative ^{13}C NMR experiments were carried out according to Tezuka et al. (Polymer 1989, 30:2288–91) at 25 °C on a Bruker Avance III 500 MHz instrument equipped with a z-gradient doubleresonance probe. NMR samples were prepared by dissolving approximately 40 mg of the sample in 0.7 ml DMSO-d6. Spectra were acquired with inverse-gated decoupling pulse sequence, 3 s pulse delays, 4096 scans and chromium(III)acetylacetonate (0.015 M) for complete relaxation of all nuclei. The data were processed with standard Bruker Topspin-NMR software.

HPLC

Analyses of HPLC-Monnosaccharide determinations were carried out using following devices: HPLC auxiliary pump (Kontron 420), 2 pulse dampener as SSI (Scientific Systems Inc.), Gradient Pump IC-compatible (Dionex GS50), autosampler (Kontron 460), CarboPac PA10 column (Dionex), PEEK blend Cross, Electrochemical Detector (Dionex ED 40) and gold working electrode, and Dionex Chromeleon version 6.60.

FTIR Spectroscopy

Analyses of FTIR were carried out using these devices:

Bruker Tensor 27 FTIR spectrometer, MCT detector, resolution 2 cm^{-1}, 64 scans.
Specac Single Reflection Diamond ATR "Golden Gate".
The samples were measured as original ATR spectra without sample preparation (in each case 2 measurements). The spectra were averaged and the mean value spectrum was baseline-corrected (rubber band method).

FT-Raman Spectroscopy
Analyses of FT-Raman were carried out using these devices:
Bruker Multiram FT-Raman Spectrometer, NdYagLaser 1064 nm excitation wavelength,
500 mW laser power; Resolution 4 cm^{-1}, 100 scans. The samples were compressed without dilution and measured directly (in each case 2 measurements). The spectra were averaged and the mean value spectrum was baseline-corrected (inverse rubber band method).

Results and Discussion

For derivatization of the xylan contained in the hemi lye, homogeneous reaction pathways were investigated (Figure 2).

Synthesis of Derivative 1 (Carboxymethylxylan, CMX):
100 ml hemi lye (6.6 g xylan) were placed in a glass flask and 19 g sodiummonochloroacetate (SMCA, 4 equivalents) were added, and the mixture was vigorously stirred for 2 hours at 60°C. Afterwards, the reaction mixture was neutralized with diluted hydrochloric acid; the gel-like polymer was precipitated with ethanol and centrifuged, washed with 80/20 ethanol: water (vol/vol) and dried under vacuum, yielding 85% with and DS_{NMR} of 0.2. The yield was calculated by comparing the produced xylan derivative weight with the xylan content in the applied hemi lye. By using press lye, same results for the synthesis of CMX were found. Applying 5 equivalents of SMCA, a DS_{NMR} of 0.25 and a yield of 80% could be achieved (see figure 3). Repeating the syntheses several times showed, that the xylan derivatization was reproducible.
^{1}H NMR (300 MHz, δ, DMSO-d6, 298 K): 4.51-4.25 (1H, br, H-1), 4.11-3.94 (1H, br,H-5eq), 3.82 (2H, s,-CH_2-), 3.75-3.64 (1H, br, H-4), 3.57-3.17 (3H, br, H-3.2,5ax) ppm; IR (film): ν = 2919, 2880, 1588, 1414, 1323 cm^{-1}.

Synthesis of Derivative 2 (Carboxy Ethyl Xylan, CEX):
100ml hemi lye (6.1 g xylan) were mixed with 16 g 3-chloropropionic acid (4 equivalents) in a 250ml glass flask. The mol equivalence was calculated by comparison with mol weight of xylan unit 132 g/mol. The sample was stirred at 60°C for 2 hours and worked up as described above by syntheses of derivative 1. The yield was 70% (figure 3).
1H NMR (300 MHz, δ, DMSO-d6, 298 K): 5.33-4.94 (1H, br, H-red δ), 4.35-4.21 (1H, br, H-1), 4.03-3.81 (1H, br,H-5eq), 3.65-2.91 (4H, br, H-4,3,2,5ax), 2.86-2.69 (2H, t, J=6.3 Hz, -O-**CH**$_2$-CH_2-COOH) ppm.
-O-CH_2-**CH**$_2$-COOH signals overlap with the xylan region and therefore they cannot be recognized. IR (film): ν = 1575, 1404, 1316, 995, 900 cm^{-1}.

Synthesis of Derivative 3 (Carboxy Propyl Xylan, CPX):
100ml hemi lye (6.1 g xylan) were mixed with 18.5 g 4-chlorobutyric acid (4 equivalents) in a 250ml flask. The sample was stirred at 60°C for two hours and worked up as described above by syntheses of derivative 1. The yield was 70% (figure 3).
1H NMR (300 MHz, δ, DMSO-d6, 298 K): 5.24-4.99 (1H, br, H-red δ), 4.37-4.19 (1H, br, H-1), 4.03-3.79 (1H, br,H-5eq), 3.56-3.45 (1H, br, H-4), 3.45-2.91 (3H, br, H-3,2,5ax), 2.21-2.08 (2H, m, Hz, -O-CH2-**CH2**-CH2-COOH) ppm.
-O-**CH**$_2$-CH_2-CH_2-COOH and -O-CH_2-CH_2-**CH**$_2$-COOH signals overlap with peaks from the xylan region and are therefore not visible. IR (film): ν = 1604, 1412, 1050, 995, 900 cm^{-1}.

Synthesis of Derivative 4 (Hydroxypropyltrimethyl Ammoniumxylan Xylan, HPTMAX):
100 ml hemi lye (6.6 g xylan) were placed in glass reactor flask and then 18 mml glycidyltrimethylammonium chloride (4 equivalents) were transferred into the reaction vessel via dropping funnel. After stirring at 60°C for 7 hours the reaction was stopped by dilution and the reaction was adjusted to pH 5.0 with HCl. The gel-like polymer was precipitated with ethanol and centrifuged washed with 80/20 ethanol: water (vol/vol) and dried under vacuum, yielding 80% with a DS_{NMR} of 0.3 (see figure 3).
^{1}H NMR (300 MHz, δ, DMSO-d6, 298 K): 4.51-4.25 (1H, br, H-1), 4.11-3.94 (1H, br,H-5eq), 3.75-3.64 (1H, br, H-4), 3.57-3.17 (3H, br, H-3,2,5ax), 3.12 (2H, s,-N(CH3)3-) ppm.
CH_2-CH (OH) -CH_2 peaks overlap with xylan peaks and therefore they cannot be seen clearly in the spectrum. IR (film): ν = 2919, 2880, 1604, 1476, 919 cm^{-1}.

Synthesis of Derivative 5 (Xylansulfate):
2 g xylan powder were dissolved in LiCl /DMAc (1 g/100 ml) in a glass flask (xylan powder was used

according to the fact, that the sulfation reaction is only successful in non-aqueous media). The reaction vessel was heated to 60°C and stirred. Then 8 g SO_3/pyridine complex were added dropwise via dropping funnel. Thereafter, the mixture was stirred for 1 hour at 60°C. The precipitated xylansulfate powder was then filtered off and washed with methanol and acetone, and dried under vacuum, yielding 50% (see figure 3). Because the sulfate group has no protons, it is not detectable via ^{1}H-NMR spectroscopy. The DS determination was not possible. IR (film): ν = 2948, 2895, 1634, 1398.5, 1230, 1103, 993, 806, 615.9 cm^{-1}.

Synthesis of Derivative 6 (Xylansulphonate):
100 ml hemi lye (6.0 g xylan) and 31 g of 3-chloro-2-hydroxy-1-propanesulfonic acid sodium salt hydrate (4 equivalents) were stirred in a glass flask (250 ml) at 60°C for 2 hours. Afterwards, the reaction mixture was adjusted to pH 8 with HCl. Subsequently, the xylan derivative was precipitated with ethanol, centrifuged, and filtered, then washed several times with ethanol /water (90/10) mixture, and dried under vacuum, yielding 60% (figure 3).
^{1}H NMR (300 MHz, δ, DMSO-d6, 298 K): 5.23-4.94 (1H, br, H-red δ), 4.33-4.22 (1H, br, H-1), 3.94-3.81 (1H, br,H-5eq), 3.73-3.64 (2H, m, -CH_2-SO_3Na), 3.57-3.42 (1H, br, H-4), 3.50-3.95 (3H, br, H-3,2,5ax) ppm. CH_2-CH (OH) - signals of propyl residue overlap with xylan peaks and therefore they are not visible in spectrum. IR (film): ν = 1604, 1414, 1380, 1163.8, 1031.8, 981.5, 896.6, 652.9 cm^{-1}.

Synthesis of Derivative 7 (3-Butoxy-2-Hydroxypropyl Xylan Ether, BHPEX):
Method 1: A 2 L Radley reactor was equipped with reflux condenser and dropping funnel and 385 ml hemi lye (18.0 g xylan as dry matter) was added to the reactor. 118 ml butyl glycidyl ether (0.90 mol, 6 equivalents) was added dropweise at 45°C during 20 minutes under stirring. Stirring was continued overnight at 45°C. The pH was regulated to 11.5 with 50% sulfuric acid yielding a precipitate. The precipitate was collected by centrifugation and washed with ethanol/water 80/20 and dried, yielding 70% with an DS_{NMR} of 1.6 (see figures 2,3).
Method 2: In a glass flask (250 ml) 100 ml hemi lye (6.28 g xylan) and 24.77 g butyl glycidyl ether are weighed and stirred at 65°C (4 equivalent) for 3 hours. After the end of reaction, the reaction mixture was adjusted to pH 8 by 50% sulfuric acid. Subsequently, the xylan derivate was precipitated with ethanol and centrifuged, washed with 80/20 ethanol: water (v/v) several times and filtered. At the end the product was dried under vacuum, yielding 70%.

^{1}H NMR (300 MHz, δ, D_2O, 298 K): 1.52-1.41 (1H, m, CH_3-CH_2-**C**$\mathbf{H}_2$-CH_2-O-), 1.38-1.22 (2H, m, CH_3-**C**$\mathbf{H}_2$-CH_2-CH_2-O-), 0.91-084 (2H, m, **C**$\mathbf{H}_3$-CH_2-CH_2-CH_2-O-) ppm. Signals in the 2.8-5.5 ppm range overlap strongly and therefore their assignment of residual protons of the 3-butoxy-2-hydroxypropyl radical is not possible.
^{13}C-NMR (500 MHz, δ, DMSO-d6): 101.763, 70.207, 31.331, 18.841, 13.790 ppm. Signals for the butyl residue -$CH_2CH_2CH_2CH_3$, DS 1.6 (average of three integrals of 3 signals below 39.5 ppm (aliphatic carbons of butyl group) divided by the signal for C1 of xylan backbone at 102 ppm)

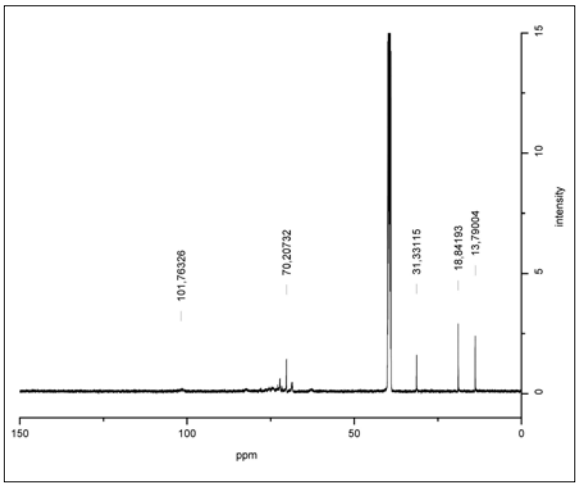

Figure 2. *^{13}C-NMR spectra of 3-Butoxy 2-hydroxypropyl ether xylan.*

The successful derivatization of the xylan was confirmed by ^{1}H-NMR, ^{13}C-NMR and FTIR studies.

The monosaccharides determinations like xylan, glucan and mannan of xylan powder, CMX and HPTMAX were detected by anion-exchange chromatography combined with pulsed amperometry and the results are shown in table 1.
The method of glucose determination is suitable for determining the xylan part in substrates. The method is calibrated on the recovery of xylan and mannan, the glucan value is therefore limited in accuracy. In general, only unsubstituted monomer parts are detected. This explains the low xylan parts for hemi powder of about 82% (each 10th unit has a glucoronic acid side chain). Starting with a degree of substitution of 0.2 (NMR), this would mean that every 5th unit carries a substituent, thus, an expected xylan value of about 60% would result. The measured values are remarkably lower.

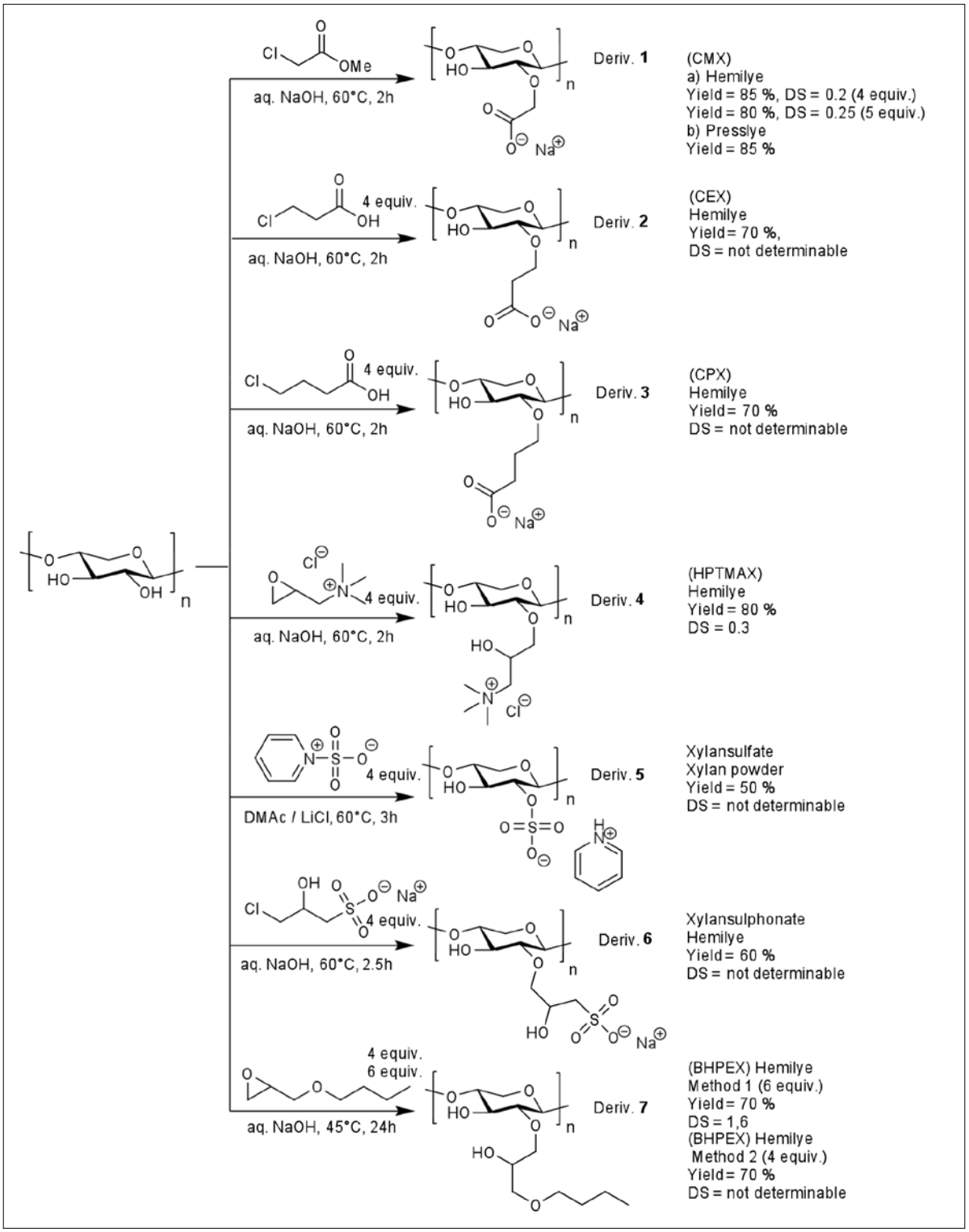

Figure 3. *Reaction paths for the preparation of xylan derivatives.*

Table 1. *Carbohydrate content of the water extracts determined after total hydrolysis.*

Product	Glucan [%]	Xylan [%]	Mannan[%]	sum total
Xylan powder	2,9	82,0	0,1	85,0
CMX deriv.	2,9	23,7	2,3	28,9
HPTMAX deriv.	2,6	31,8	2,9	37,3

Discussion

Following the FTIR and NMR experimental results, it can be concluded that the derivatization of xylan in hemi liquor took place successfully. Furthermore, according to the results of NMR analyses the separation of inorganic salts in the hemi liquor can be a major challenge. By comparing the sugar analysis of xylan of CMX and HPTMX with xylan powder used as reference sample, it has been found that 28-38% of xylan units were not derivatized, after the derivatization process.

Conclusion

In this work it was shown that the synthesis of new xylan derivatives directly from industrial hemi liquor without prior xylan precipitation under the applied reaction conditions is possible. Six hydrophilic and one hydrophobic xylan derivatives were synthetized. The preparation of the xylan derivatives is reproducible and the yields were acceptable. By chemical modification of xylan, manifold functionalities could be introduced into the polymeric chain. The distribution of the functional groups could be controlled by the reaction conditions and the molar ratio of the used reagents. As an example we observed an increasing DS at the synthesis of carboxymethylxylan (CMX) with increasing molar ratio of xylan: sodiummonochloroacetate (SMCA). We found the same results by the synthesis of CMX from hemi and press lye. Xylan derivatives possess an interesting spectrum of possible applications. They may be used as paper additive and flocculation aid, as antimicrobial agent in case of HPMAX, whereas CMX can act as fiber modifying agent. Xylan derivatives may act as polymeric tensides like methyl xylan and could be used as carrier of drugs (nanoparticles of xylan esters). Xylan sulphate may be applied as antiviral drugs and as blood coagulation inhibitor [12].

Acknowledgements

Financial support was provided by the Austrian government, the provinces of Lower Austria, Upper Austria and Carinthia as well as by the Lenzing AG. We also express our gratitude to the Johannes Kepler University, Linz, the University of Natural Resources and Applied Life Sciences, Vienna, and the Lenzing AG for their in kind contributions.

References

[1] Ebringerova A. Structural Diversity and Application Potential of Hemicelluloses. Macromol. Symp. 2006, 232, 1-12.

[2] Mikkonen KS., Laine C., Kontro I., Talja RA., Serimaa R. Tenkanen M. Combination of internal and external plasticization of hydroxypropylated birch xylan tailors the properties of sustainable barrier films. European Polymer Journal. 2015, 66, 307-318.

[3] Jacobsen S. E., Wyman C.E. Cellulose and Hemicellulose Hydrolysis Models for Application to Current and Novel Pretreatment Processes. Applied Biochemistry and Biotechnology. 2000, Vol. 84-86, 81-96

[4] Mais U., Sixta H. Characterization of Alkali-Soluble hemicellulose of Hardwood dissolving Pulps. American Chemical Society. 2004, 94-107.

[5] Heinze T., Koschella A., Ebringerova A. Chemical functionalization of xylan: A short review. Science and technology. ACS symposium series, 2004, Vol. 864, pp.312-325.

[6] Petzold -Welcke K., Schwikal K., Daus S., Heinze T. Xylan derivatives and their application potential – Mini review of own results. Carbohydrate Polymers. 2014, 100, 80-88.

[7] Pohjanlehto H., Setälä H., Kammiovirta K., Harlin A. Carbohydrate Research. 2011, 346, 2736-2745.

[8] Hansen N.M.L., Plackett D. Sustainable film and coatings from hemicellulos. Biomacromolecules. 2008, 9, 1493-1505.

[9] Simkovic I., Tracz A., Kelnar I., Uhliarikova I., Mendichi R. Carbohydrate polymers. Quaternized and sulfated xylan derivative films. 2014, 99, 356-364.

[10] Peng X., Ren J., Zhong L., Sun R., Shi W., Hu B. Cellulose. Glycidyl methacrylate derivatized xylan-rich hemicellulose: synthesis and characterizations. 2012, 19: 1361-1372.

[11] Daus S., Petzold-Welcke K., Köttritzsch M., Baumgaertel A., Schubert U., Heinze H. Macromolecular Materials and Engineering. 2011, 296, 551-561.

[12] Eduardo da siva A., RodriguesMarcelino H., Gomes M., Oliveira E., Nagashima T., Egito E. Products and Applications of Biopolymers. www.intechopen.com

[13] Laine C., Harlin A., Hartman J., Hyvärinen S., Kammiovirta K., Krogerus B., Pajari H., Rautkoski H., Setälä H., Sievänen J., Uotila J., Nissi M. Hydroxyalkylated xylans – Their synthesis and application in coatings for packaging and paper. Industrial Crops and Products. 2013, 44, 692-704.

[14] Mikkonen K., Laine C., Kontro I., Talja R.A., Serimaa R., Tenkanen M. European Polymer Journal. 2015, 66, 307-318.

[15] Heinze T. Macromol.Chem. Phys. New ionic polymers by cellulose functionalization. 1998, 199, 2341-2364.

Studies on the Regiochemistry of Acetylation of Xylan

Annett Pfeifer, Andreas Koschella and Thomas Heinze*

Friedrich Schiller University of Jena, Institute for Organic Chemistry and Macromolecular Chemistry, Center of Excellence for Polysaccharide Research, Humboldtstraße 10, D-07743 Jena, Germany
*E-mail: thomas.heinze@uni-jena.de Tel: +49 3641 948270, Fax: +49 3641 948272
Member of European Polysaccharide Network of Excellence (EPNOE, http://www.epnoe.eu)

Abstract

A low molecular weight xylan dissolved in *N,N*-dimethyl acetamide/LiCl was allowed to react with acetic anhydride with and without pyridine as base. Depending on the reaction conditions applied, xylan acetates with degree of substitution of acetyl groups (DS_{Ac}) between 0.33 and 2.00 could be synthesized. Almost all samples were soluble in *N,N*-dimethyl formamide, independent on the DS_{Ac}. The functionalization pattern of the xylan acetates depends on the reaction conditions. Position 2 appears to be higher reactive if no pyridine is added, while the reactivity of both hydroxyl groups is equalized in the presence of pyridine. SEC measurements revealed loss of low molecular weight fractions and, hence, a slight shift towards higher molecular masses.

Keywords: *Xylan, acetylation, homogeneous reaction, functionalization pattern, molecular weight distribution*

Introduction

Xylans are important hemicelluloses occurring in wood and other plants, which mediate between hydrophilic cellulose and hydrophobic lignin in the cell wall [1,2]. Although approximately 25% of the dry wood consist of xylan, the biopolymer is not reasonable used. Usually it is degraded to soluble products during the pulping process. In addition to cellulose, the structural variability of xylan makes it to an interesting starting material that merits to be converted into value added products [3-5]. However, the chemistry of xylan is not well understood.

Various esters and ethers of xylan using different synthesis approaches including homogeneous or heterogeneous conversions have been described in the literature. From a commercial point of view, sulfuric acid half esters are most important, which impart water-solubility to the polymer, on one hand. On the other, xylan sulfates possess a broad spectrum of bioactivity. It is the only xylan derivative commercially produced based on beech wood xylan [6,7].

Xylan carboxylic acid esters have found interest that may be soluble in organic solvents and, hence, enable shaping it into films and particles. The esterification of xylan with pharmaceutically active carboxylic acids like ibuprofen yields the corresponding prodrug [8]. Moreover, nanoparticles from xylan esters can be formed as well [9].

Acetylation of hemicelluloses, obtained from sugar cane bagasse, with acetic anhydride in presence of *N*-bromosuccinimide could be realized under almost solvent-free conditions. The polymer was swollen with water and *N,N*-dimethyl formamide (DMF). Products with values of degree of substitution (DS) of up to 1.15 could be obtained [10]. Moreover, esterification of xylan applying the so-called impeller method was carried out. Xylan was allowed to react with different carboxylic acids in the presence of trifluoroacetic anhydride [11]. The conversion of xylan from bagasse with acetic anhydride in acetic acid as medium and *p*-toluenesulfonic acid as catalyst yields products of low DS of about 0.2 only [12]. Ionic liquids like 1-allyl-3-methylimidazolium chloride were used as reaction medium for esterification of xylan. It was found that conversion of the dissolved polymer with acetic anhydride proceeds without any catalyst yielding products with DS up to 1.28. [13]. Higher DS values could be achieved by homogeneous

acylation of xylan in *N,N*-dimethyl acetamide (DMA)/LiCl. The conversion of xylan in DMA/LiCl with acetic anhydride in the presence of pyridine yields xylan acetates with high DS values of up to complete functionalization. The xylan used was obtained from Eucalyptus kraft pulp [14,15]. Based on NMR measurements, the authors claim an equal reactivity of the secondary hydroxyl groups at positions 2 and 3 of the repeating unit. However, in most cases the regiochemistry of the acylation was not studied in detail.

In the present work, the influence of reaction medium and reaction conditions on the DS and on regiochemistry was studied. In particular, the investigations were focused on the influence of pyridine as base on the functionalization pattern of xylan acetates obtained by homogeneous acetylation in DMA/LiCl of the biopolymer with acetic anhydride.

Materials and Methods

Materials

Xylan (**1**, 78.8% xylose, 6.5% glucose, 5.1% rhamnose, 4.0% 4-*O*-methylglucuronic acid, and 5.6% xylooligomers determined by HPLC after acidic hydrolysis) was kindly provided by Bene Pharmachem GmbH & Co. KG (Geretsried, Germany). It was dried for 2 h at 100 °C in vacuum. DMA (dried over molecular sieves), LiCl (dried for 2 h at 105 °C in vacuum), acetic anhydride, propionic anhydride, and pyridine were purchased from Sigma Aldrich and used as received.

Measurements

FTIR spectra were recorded on a Nicolet Avatar 370 DTGS spectrometer using the KBr technique. The ^{1}H- and ^{13}C-NMR spectra were acquired with Bruker Avance 400 (400 MHz) spectrometer in $CDCl_3$ at room temperature with a concentration of at least 5% (w/w) of polymer in solution using the chloroform peak as internal reference. The carbonyl peaks in the ^{13}C-NMR spectra were integrated using a line fitting method. Partial values of DS of acetyl groups (DS_{Ac}) were calculated according to eq. 1 [14].

$$DS_{Ac}(\text{Position}) = \frac{I_{C=O(Ac_{2or3})}}{I_{C=O(Ac_2)} + I_{C=O(Ac_3)} + I_{C=O(Prop_2)} + I_{C=O(Prop_3)}} \cdot 2 \quad \text{eq. 1}$$

I refer to the integrals of the carbonyl peaks of acetyl (Ac)- and propionyl groups (Prop) at the positions 2 and 3 in the modified anhydroxylose unit (AXU).

Size exclusion chromatography was conducted on a JASCO RT 930 applying dimethyl sulfoxide (DMSO)/0.5% LiBr as eluent. Novema columns 300 and 3000 were used. The elugrams were calibrated with pullulan standards. The molar mass distribution of the xylan acetates was normalized to the molar mass of the unfunctionalized AXU unit according to eq. 2.

$$M_{normalized} = \frac{M}{M_{mod.AXU}} \cdot M_{AXU} \quad \text{eq. 2}$$

M: Molar mass from SEC

$M_{mod.\ AXU}$: Molar mass of the modified AXU bearing acetyl moieties, depending on degree of substitution

M_{AXU}: Molar mass of the AXU, 132.05 g/mol

Methods

Homogeneous Synthesis of Xylan Acetate in DMA/LiCl (Sample 12)

In a typical procedure, xylan **1** (2.0 g, 0.015 mol) was slurried in 40 ml DMA for 2 h at 120 °C under exclusion of moisture. After cooling to 80 °C, 3.6 g LiCl were added and stirring was continued without further heating until complete dissolution of the polymer occurred. Pyridine (5.9 mL, 0.073 mol, 4.8 mol/mol AXU) and acetic anhydride (5.8 mL, 0.061 mol, 4.0 mol/mol AXU) were added and the reaction was allowed to proceed for 6 h at 50 °C under stirring. After cooling to room temperature, the mixture was poured into 300 mL ethanol. After collecting the precipitated polymer, it was washed 5 times with 150 mL ethanol and dried at 80 °C in vacuum.

Yield: 1.42 g

DS_{Ac}: 1.73 (determined by ^{1}H NMR spectroscopy of the perpropionylated polymer).

The polymer is soluble in DMF and chloroform.

Perpropionylation of Xylan Acetate (Sample 12prop)

In a typical procedure, 0.4 g of xylan acetate **12** was mixed with 5.0 mL pyridine and 5.0 mL propionic anhydride. After stirring for 20 h at 60 °C, the polymer was isolated by precipitation in 150 mL ethanol, washed 5 times with 100 mL ethanol, and dried at 80 °C in vacuum.

Yield: 0.30 g

DS_{Ac}: 1.73 (determined by ^{1}H NMR spectroscopy of the perpropionylated polymer).

FTIR spectroscopy: No ν(OH).

^{1}H-NMR spectroscopy ($CDCl_3$, 400 MHz, δ, ppm): 1.10 H-10 (CH_3, Propyl); 2.02 H-7 (CH_3, Acetyl); 2.29 H-9 (CH_2, Propyl); 3.30 H-5b; 3.76 H-4; 3.90 H-5a; 4.48 H-1; 4.73 H-2; 5.04 H-3.

^{13}C-NMR spectroscopy ($CDCl_3$, 100.63 MHz, δ, ppm): 9.0 C-10 (CH_3, Propyl); 20.7 C-7 (CH_3, Acetyl); 27.4 C-9 (CH_2, Propyl); 62.5 C-5; 70.8 C-2; 71.8 C-3; 74.7 C-4; 100.1 C-1, 169.3 C-6 (C=O, Acetyl at position 2); 169.8 C-6 (C=O, Acetyl at position 3); 172.7 C-8 (propionyl at position 2); 173.2 C-8 (propionyl at position 3).

The polymer is soluble in chloroform.

Results and Discussion

Acetylation of Xylan

Xylan acetates have been synthesized homogeneously in DMA/LiCl by conversion with acetic anhydride at 50 °C (Scheme 1). The reaction was conducted without or with addition of pyridine as base and varying the reaction time from 0.5 to 16 h (Table 1). The xylan acetates were isolated by precipitation in ethanol. For determination of the DS_{Ac} by means of ^{1}H-NMR spectroscopy, perpropionylation of the samples was carried out.

From the results summarized in Table 1, it become obvious that the DS_{Ac} increased with increasing reaction time. Furthermore, a strong influence of the base on the DS reached was observed. While a DS_{Ac} of 0.33 was realized after 0.5 h at 60 °C by a conversion of the xylan in DMA/LiCl without pyridine (sample **2**), the presence of pyridine lead to a significant increase of the DS_{Ac} to 0.60 (sample **8**). At a reaction time of 16 h, the DS_{Ac} is increased to 1.41 (sample **7**) without applying pyridine. On the contrary, a completely acetylated product (DS_{Ac} 2.00, sample **13**) could be obtained in presence of pyridine. Thus, pyridine increased the DSAc

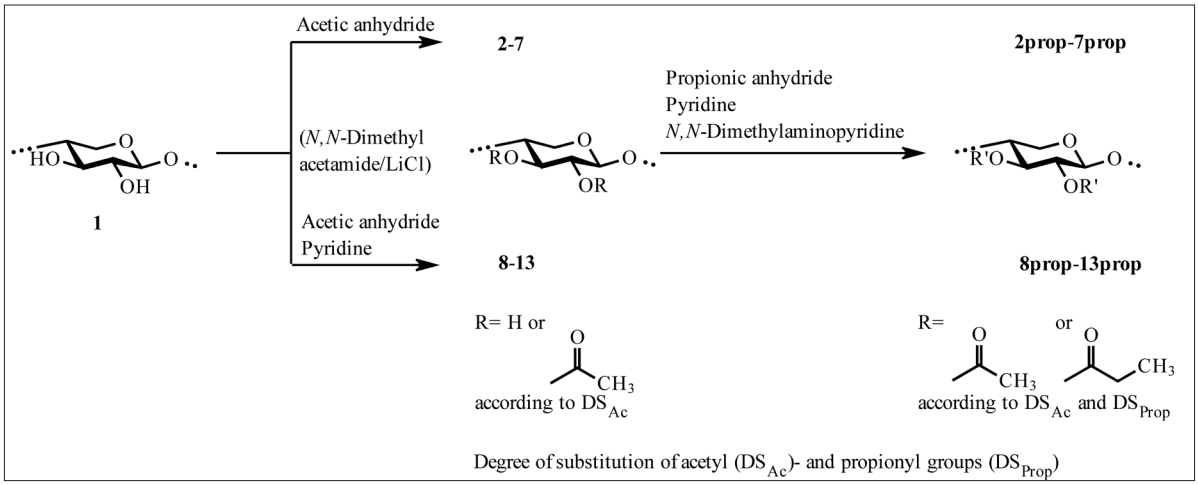

Scheme 1. *Acetylation of xylan **1** with acetic anhydride under homogeneous conditions with acetic anhydride with or without applying pyridine as base and subsequent perpropionylation.*

Table 1. *Conditions for and results of the conversion of xylan **1** dissolved in N,N-dimethyl acetamide/LiCl with 4.0 mol acetic anhydride per mol repeating unit without or in the presence of 4.8 mole pyridine per mole repeating unit at 50°C.*

	Synthesis without pyridine								Synthesis in presence of pyridine							
		Solubility[a]		DS_{Ac}[b] (^{1}H-NMR)		DS_{Ac}[c] (^{13}C-NMR)				Solubility[a]		DS_{Ac}[b] (^{1}H-NMR)		DS_{Ac}[c] (^{13}C-NMR)		
Time (h)	Sample	DMF	$CHCl_3$	Prop.	Ac.	2	3	Σ	Sample	DMF	$CHCl_3$	Prop.	Ac.	2	3	Σ
0.5	**2**	+	-	0.33	0.35	0.10	0.10	0.21	**8**	+	-	0.60	0.54	0.41	0.17	0.58
1.0	**3**	+	-	0.38	0.37	0.28	0.15	0.43	**9**	+	-	0.87	0.71	0.35	0.32	0.67
2.0	**4**	+	-	0.60	0.62	0.35	0.28	0.63	**10**	+	-	1.11	1.13	0.51	0.58	1.09
3.0	**5**	+	-	0.74	0.63	0.41	0.33	0.74	**11**	+	-	1.39	1.32	0.61	0.63	1.24
6.0	**6**	+	-	1.07	0.96	0.54	0.40	0.94	**12**	+	+	1.73	1.63	0.83	1.00	1.83
16.0	**7**	+	-	1.41	1.32	0.69	0.68	1.37	**13**	-	-	2.00	2.00	1.00	1.00	2.00

[a] Solubility in *N,N*-dimethyl formamide (DMF): soluble (+), insoluble (-).

[b] Degree of substitution of acetyl groups determined by ^{1}H-NMR spectroscopy of the perpropionylated samples **2prop-13prop**. Calculation of the DS_{Ac} was carried out using protons of propionyl (prop.) or acetyl (ac) moieties.

[c] Degree of substitution of acetyl groups determined by ^{13}C-NMR spectroscopy of the perpropionylated samples **2prop-13prop**.

Partial DS_{Ac} values at position 2 and 3 as well as the resulting total DS_{Ac} (Σ) are given.

values obtained and accelerated the conversion. All samples, except the completely functionalized sample **13**, are soluble in DMF. In addition, sample **12** (DS_{Ac} 1.73) dissolves in chloroform too. Surprisingly, the completely acetylated sample **13** was neither soluble in DMF nor in chloroform. Most likely, non-polar interactions and perhaps the rigidity cause insolubility due to the very uniform macromolecular structure. This finding is in agreement with previously reported results [14].

Size Exclusion Chromatography

The xylan **1** and xylan acetates **2-13** were subjected to SEC analysis in DMSO (Table 2, Figure 1). In order to exclude the influence of different DS on the molar mass of the polymers, the SEC traces were normalized to the molar mass of the non-functionalized polymer (eq. 2). In case of reaction times from 1 to 2 h, the order of molar mass is xylan, xylan acetate synthesized without pyridine, xylan acetate synthesized in the presence of pyridine. The order is changed at a reaction time of 6 and 16 h, i.e., products synthesized without pyridine possess the highest molecular mass. The SEC traces of the samples synthesized at a reaction time of 16 h exhibited a dominant shoulder at the low-molecular weight flank of the curve. It is assumed that polymer degradation to a certain extent occurred, which is independent of the presence or absence of pyridine.

The number- and weight average degrees of polymerization (DP_n and DP_w) as well as the polydispersity index (PDI) were calculated from the SEC data and the DS_{Ac} values (Table 2). The molar masses respectively the DP values of the xylan acetates are higher as the DP of the initial xylan **1** (DP_n 9, DP_w 25, PDI 2.92). This result was not surprising as the polymer is not fully functionalized and, hence, able to form aggregated structures in

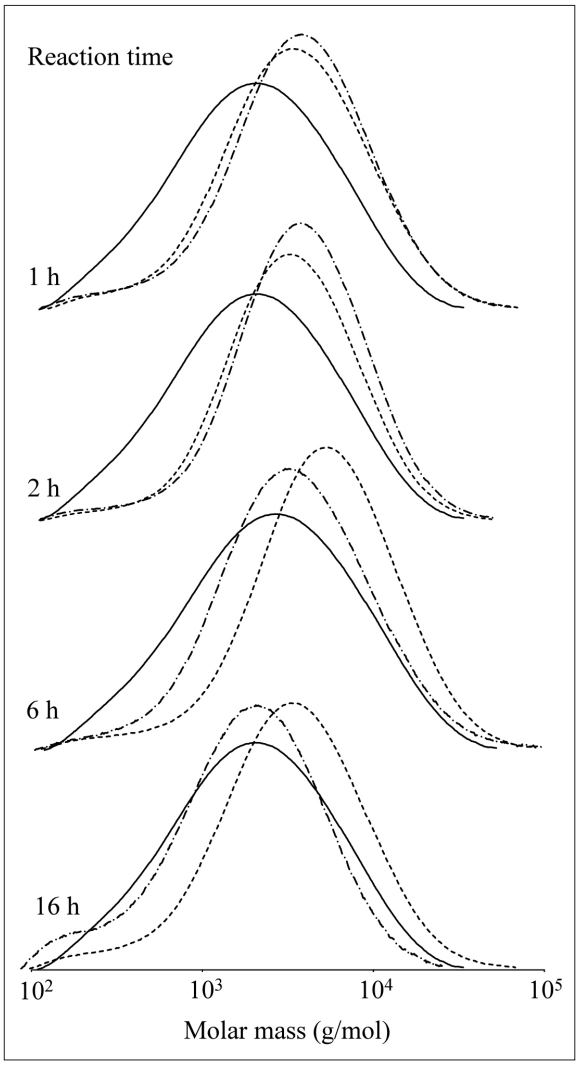

Figure 1. *SEC traces of xylan **1** and xylan acetates prepared in N,N-dimethyl acetamide/LiCl with and without addition of pyridine (see Table 1). The molar masses are normalized to the unmodified repeating unit in order to exclude influence of degree of substitution on molar mass.*

Table 2. *SEC data of xylan acetates obtained by conversion of xylan **1** with acetic anhydride with and without pyridine (see Table 1)*

Synthesized without pyridine						Synthesized in presence of pyridine					
Sample	M_n (g/mol)	M_w (g/mol)	DP_n[a]	DP_w[b]	PDI[c]	Sample	M_n (g/mol)	M_w (g/mol)	DP_n	DP_w	PDI
1	1123	3279	9	25	2.92	**1**	1123	3279	9	25	2.92
3	2221	6036	15	41	2.72	**9**	2558	7050	15	42	2.75
4	2712	6661	17	42	2.46	**10**	2959	7068	17	39	2.39
6	2879	7310	16	41	2.54	**12**	2415	6410	12	31	2.65
7	2594	7414	12	34	2.86	**13**	1642	4582	8	21	2.79

[a] Number average degree of polymerization. [b] Weight average degree of polymerization. [c] Polydispersity.

solution. Moreover, the calibration is influenced by the structure in solution. However, comparison of products obtained by the reactions in DMA/LiCl without and with pyridine lead to the conclusion that the molar mass distribution is not affected by pyridine, e.g., DP_n 15 and DP_w 41 for sample **3** and DP_n 15 and DP_w 42 for sample **9**. The PDI of these samples is 2.72 and 2.75. Obviously, prolonged acetylation of 16 h significantly influences the molar mass distribution (compare samples **7** and **13**). Smaller DP_n values suggest pronounced polymer degradation during the synthesis.

Structure characterization

Exemplary, FTIR spectra of the perpropionylated xylan acetate **10prop** (DS_{Ac} 1.11) and the completely acetylated sample **13** (DS_{Ac} 2.00) are shown in Figure 2. From the absence of the OH band around 3500 cm^{-1} in both spectra, the complete functionalization of the hydroxyl groups could be concluded. Typical signals of the expected structural features of both polymer backbone and the ester groups appear in the spectra: ν(CH, CH_3) at 2941.5 cm^{-1}, ν(C=O) at 1743.1 cm^{-1}, δ(CH_3) at 1375.0 cm^{-1}, ν(C-O-C_{Ester}) at 1240.0 cm^{-1}, ν(C-O-C_{AXU}) at 1051.1 cm^{-1}.

Perpropionylated samples were subjected to ^{1}H- and ^{13}C-NMR spectroscopy (in $CDCl_3$, Figure 3). The signals were assigned in the ^{1}H-NMR spectrum for sample **12prop**: 1.10 ppm H-10 (CH_3, Propyl), 2.02 ppm H-7 (CH_3, Acetyl), 2.29 ppm H-9 (CH_2, Propyl), 3.30 ppm H-5b, 3.76 ppm H-4, 3.90 ppm H-5a, 4.48 ppm H-1, 4.73 ppm H-2, and 5.04 ppm H-3. In the ^{13}C-NMR spectrum, signals were detected at: 9.0 ppm C-10 (CH_3, Propyl), 20.7 ppm C-7 (CH_3, Acetyl), 27.4 ppm C-9 (CH_2, Propyl), 62.5 ppm C-5, 70.8 ppm C-2, 71.8 ppm C-3, 74.7 ppm C-4, 100.1 ppm C-1, 169.3 ppm C-6 (C=O, Acetyl at position 2), 169.8 ppm C-6 (C=O, Acetyl at position 3), 172.7 ppm C-8 (Propionyl at position 2), 173.2 ppm C-8 (Propionyl at position 3).

It is worth to note that in total 4 signals for carbonyl carbon atoms appeared in the ^{13}C-NMR spectrum. This enables the calculation of partial DS_{Ac} values from the integrals of the particular carbonyl peaks in the range from 169 to 174 ppm according to eq. 1 [14]. The resulting partial DS_{Ac} values are summarized in Table 1. It must be pointed out that the values are in good agreement with the DS_{Ac} values determined by ^{1}H-NMR spectroscopy and, hence, those values appear reliable. Obviously, the partial DS_{Ac} values depend on the presence of pyridine as base by the conversion in DMA/LiCl. At short reaction time of 0.5 h, positions 2 and 3 possessed an almost equal partial DS_{Ac} of 0.10 and 0.11 (sample **2**). In case of samples prepared within 1 to 6 h, the partial DS_{Ac} at position 3 was found to be always lower than that at position 2 (samples **3**, **4**, **5**, and **6**). The reactivity of both hydroxyl groups is comparable in case of sample **7**; the partial DS_{Ac} values are almost identical (0.68 at position 3 and 0.69 at position 2). On the contrary, acetylation is more pronounced at position 2 compared with position 3 after 0.5 h acetylation in presence of pyridine (partial DS_{Ac} 0.17 and 0.41 at position 3 and 2, sample **8**). A further increase of

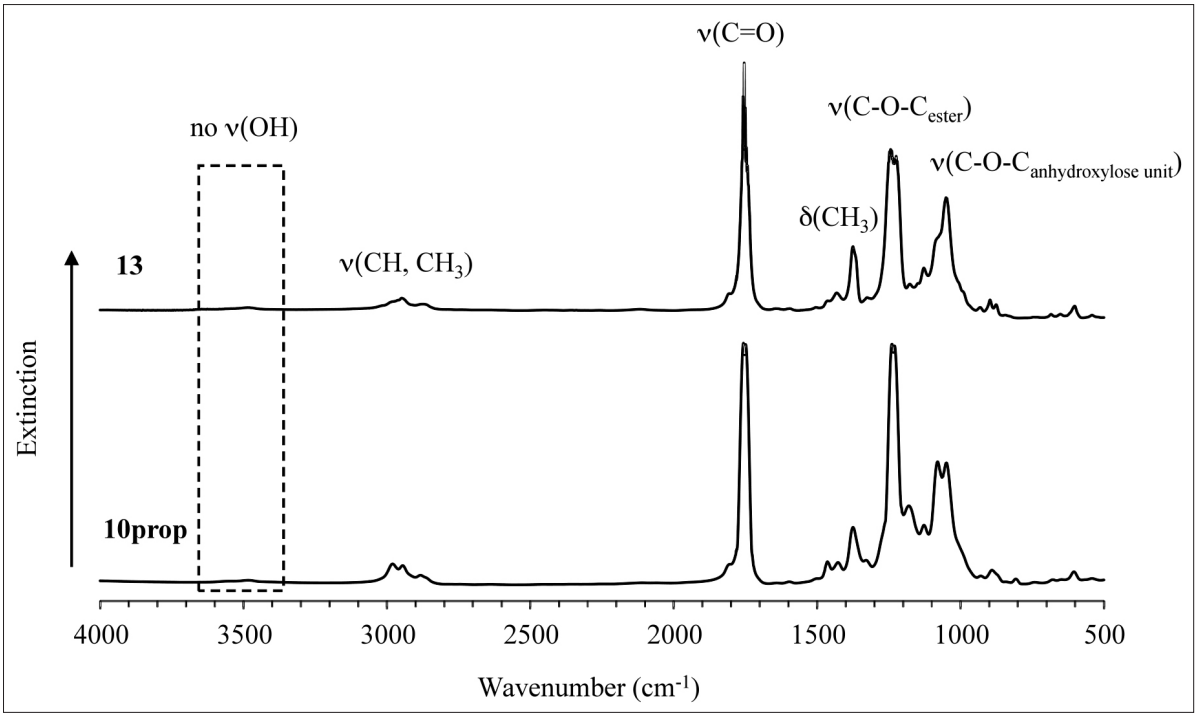

Figure 2. *FTIR spectra of the perpropionylated xylan acetate* ***10prop*** *(DS_{Ac} 1.11, bottom) and the fully acetylated sample* ***13*** *(DS_{Ac} 2.00).*

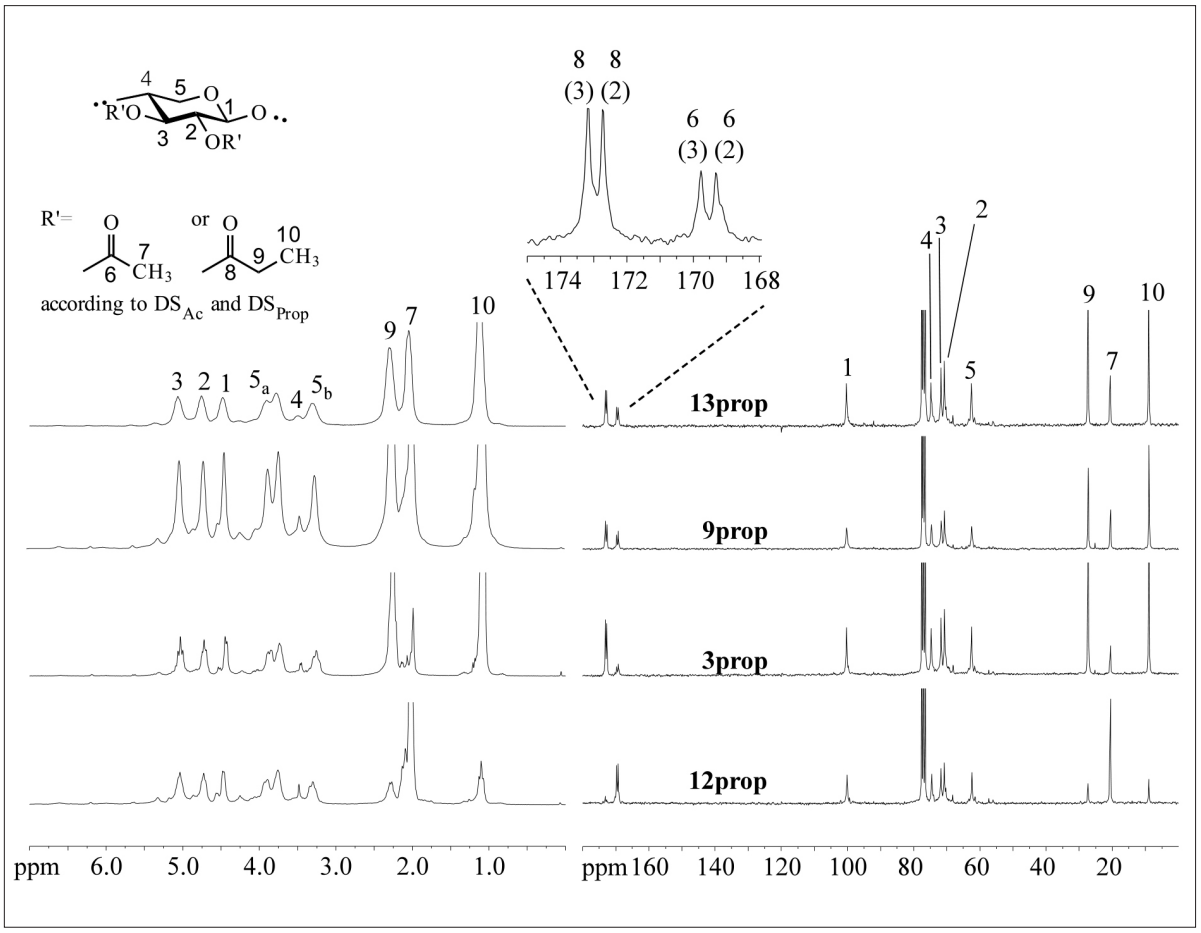

Figure 3. *^{1}H- (left) and ^{13}C-NMR spectra (right) of different xylan acetates recorded after perpropionylation in $CDCl_3$. The numbers in brackets indicate the position of the ester function in the modified anhydroxylose unit.*

the reaction time of up to 3 h afforded products with almost equal distribution of acetyl moieties. The product obtained after 6 h possessed a completely acetylated position 3 and a partial DS_{Ac} at position 2 of 0.83 (sample **12**). However, position 2 appears to react faster in absence of pyridine. Compared to previously published results [14], pyridine obviously equalizes somehow the reactivity of the hydroxyl groups at positions 2 and 3.

Conclusions

Xylan acetates were prepared by conversion of the low-molecular weight material with acetic anhydride under homogeneous reaction conditions in DMA/LiCl. The resulting xylan acetates are soluble in aprotic-dipolar media except a completely functional product. Pyridine, which acts as catalyst and base to trap the acetic acid formed, influences the functionalization pattern of the products. P osition 2 is more reactive than position 3 at total DS_{Ac} below 1 if the reaction is conducted without pyridine. On the contrary, a comparable reactivity is found in presence of pyridine.

Acknowledgements

The generous financial support of bene pharmaChem GmbH & Co. KG, Bayerwaldstraße 7, D-82538 Geretsried, Germany is gratefully acknowledged.

References

[1] A. Ebringerova, T. Heinze, Xylan and xylan derivatives – biopolymers with valuable properties 1. Naturally occurring xylans: structures, isolation, procedure and properties. Macromol. Rapid Commun. 21; 542-556 (2000).

[2] A. Ebringerova, Z. Hromadkova, T. Heinze, Hemicellulose. Adv. Polym. Sci. 186, 1-67 (2005).

[3] T. Heinze, A. Koschella, A. Ebringerova, Chemical functionalization of xylan: a short review. ACS Symp. Ser. 864, 312-325 (2004).

[4] K. Petzold-Welcke, K. Schwikal, S. Daus, Th. Heinze, Xylan derivatives and their application potential – mini-review of own results. Carbohydr. Polym. 100, 80-88 (2014).

[5] Th. Heinze, S. Daus, Xylan and xylan derivatives – basis of functional polymers for the future. RSC Polymer Chemistry Series No. 1, Renewable Resources for Functional Polymers and Biomaterials, Ed. P.A. Williams, Royal Society of Chemistry, 88-129 (2011).

[6] R. Parthasarathi, A. Jayakrishnan, Dextran and pentosan sulfate - clinical applications. In: Biodegradable Polymers in Clinical Use and Clinical Development (Domb, Abraham J.; Kumar, Neeraj; Ezra Aviva, eds.), 185-216, (2011).

[7] S. Daus, K. Petzold-Welcke, M. Kötteritzsch, A. Baumgaertel, U. S. Schubert, T. Heinze, Homogeneous sulfation of xylan from different sources. Macromol. Mater. Eng. 296, 551-561 (2011).

[8] S. Daus, T. Heinze, Xylan-based nanoparticles: prodrugs for ibuprofen release. Macromol. Biosci. 10, 211-220, (2010).

[9] T. Heinze, K. Petzold, S. Hornig, Novel nanoparticles based on xylan. Cellul. Chem. Technol 41, 13-18 (2007).

[10] X.-F. Sun, R.-C. Sun, L. Zhao, J.-X. Sun, Acetylation of sugarcane bagasse hemicelluloses under mild reaction conditions by using NBS as a catalyst. J. Appl. Polym Sci. 92, 53-61 (2004).

[11] N. G. V. Fundador, Y. Enomoto-Rogers, T. Iwata, Syntheses of xylan esters and their application as nucleating agents for PLA. Polym. Prepr. 53, 271-272 (2012).

[12] H Li, D. Li, Y. Lu, Synthesis and characterization of bagasse xylan acetates. Jingxi Huagong 28, 227-231 (2011).

[13] A. Ayoub, R. A. Venditti, J. J. Pawlak, H. Sadeghifar, A. Salam, Development of an acetylation reaction of switchgrass hemicellulose in ionic liquid without catalyst. Ind. Crops Prod. 44, 306-314 (2013).

[14] N. G. V. Fundador, Y. Enomoto-Rogers, A. Takemura, T. Iwata, Acetylation and characterization of xylan from hardwood kraft pulp. Carbohydr. Polym. 87, 170-176 (2012).

[15] A. Eduardo da Silva, H. R. Marcelino, M. C. S. Gomes, E. E. Oliveira, T. Nagashima Jr., E. S. T. Egito, Xylan, a promising hemicellulose for pharmaceutical use. From Products and Applications of Biopolymers, Ed. C. J. R. Verbeek, 61-84 (2012).

Xylan Derivatives Enriched Fibers and their Inherent Properties

Vasken Kabrelian[1*], Sandra Schlader[2], Eva Liftinger[2], Richard Herchl[2], Thomas Röder[2] and Karin Fackler[2]

[1] Kompetenzzentrum Holz GmbH , Altenberger Str.69, 4040 Linz, Austria
[2] Lenzing AG, Werkstraße 2, 4860 Lenzing, Austria
[*] Contact: v.kabrelian@kplus-wood.at

Abstract

In the current study, synthesized xylan derivatives were used as a blend for man-made cellulosic fibers. An inno-vative type of xylan derivatives enriched viscose fiber was developed. The following xylan derivatives were synthesized and used as blends for CV fibers: carboxy methyl xylan (CMX), hydroxyl-propyl-tri-methyl-ammonium xylan (HPTMAX), and 3-butoxy-2-hydroxypropyl xylan ether (BHMEX).
The content of xylan derivatives in the fiber was 4.7% and 9.1%. Water retention values could remarkably be raised due to the CMX content when compared to reference cellulose viscose fibers (CVF) and xylan enriched viscose fibers (XEF). Fiber strength properties showed a comparable level to reference fibers. As performance and comfort are getting more and more important for textiles and non-woven products, the characterization of basic mechanical properties must be completed by methods describing their suitability for sophisticated applications. Inherent properties comprise the special characteristics, originated from the cellulosic fiber itself. These properties are very important, showing a peculiar difference to cotton or to any synthetic fiber. Comparisons between CMX enriched fibers and reference fibers were made for evaluating these new fiber type. The xylan derivatives enriched fibers were evaluated mainly regarding the moisture management and surface properties. Furthermore, thermo-physiological values and mechanical interactions between fibers and skin were analyzed. Overall, this gives a more distinct picture of the benefit for the end-user. The characteristics of the fibers and knitted fibers have been tested with regard to their applicability by carrying out following analyses: sugar-monosaccharides determination (HPLC-Method); scanning electron microscopy SEM; FTIR spectroscopy; Raman spectroscopy; fiber swelling; water retention value (WRV); fiber data (tenacity, elongation); wet abrasion resistance; water vapor absorption; brightness; gravimetric absorbency testing system (GATS); tissue softness analyzer (TSA); adhesive index; drying rate; range of water vapor resistance (Ret), range of thermal resistance (Rct).

Keywords: *Viscose fibers, absorbency, xylan derivatives, fiber properties*

Introduction

In contrast to cellulose, xylans hold a variety of different side groups, such as *O*-methylglucuronic acid residues, *O*-acetyl groups [1,2]. The impact of adsorbed or precipitated xylan on the strength properties of pulps and their shape on the fiber surface is controversially discussed in literature [3,4,5], and new types of fibers were investigated in the last few years to improve the properties of viscose fibers by addition of additives [6]. Therefore, viscose fibers were enriched with xylan as a blend [6,7]. The addition of xylan onto cellulose fibers is a research field of great interest and has been discussed in detail in many works [8,9]. The addition of cationic xylan had a positive effect on the tear resistance and other physical strength properties on various pulp samples, as it acted as a retention aid [10,11], but also increased the refining resistance [12]. Köhnke et al. recognized an improved tensile index of the pulp after a treatment with arabinoxylan compared with the refining intensity [13]. Köhnke et al. also found, that no increase in tensile strength of pulp with additional

xylan could be observed [14]. The influence of additional xylans on physical properties of various pulp samples was studied by Miletzky A, et al [15]. In our previous study we synthesized xylan derivatives from hemi-rich alkaline process lyes in Lenzing AG. In this study we will investigate the influence of these synthesized hydrophilic and hydrophobic xylan derivatives on the viscose fiber properties.

Experimental Materials

Spinning from Different Xylan Derivatives in Viscose (CV)

Xylan and the xylan derivatives carboxymethylxylan (CMX), hydroxyl-propyl-tri-methyl-ammonium xylan (HPTMAX), and 3-butoxy-2-hydroxypropyl xylan ether (BHMEX), were added during the viscose production process to be incorporated into the fiber as a blend like in work from Schild et al. [6]. To avoid intensive degradation and unprofitable losses of the xylan derivatives as well as an excess of CS_2-consumption, the xylan derivatives were added after alkalization and xanthation during the dissolving step to a standard viscose in proportion of about 4.7% on cellulose in lab scale facility.

The chemical and physical fiber properties as well as the inherent properties of fibers and the fabrics were studied according table 1.

Methods

HPLC – Monosaccharide Determinations

HPLC analyses of the cellulosic substrate in DMAC/LiCl were carried out using the following devices: HPLC auxiliary pump (Kontron 420), 2 shock absorber as SSI (Scientific Systems Inc.), Gradient Pump IC-compatible (Dionex GS50), Autosampler (Kontron 460), CarboPac PA10 column (Dionex), PEEK blend Cross, RI- Detector (ERC R1101), and Evaluation software (Wyatt Astra 6.1.1).

Scanning Electron Microscopy (SEM)

The surfaces of the pulp samples were imaged by SEM. Two approaches were taken:

1. sputter coating using gold for conventional SEM and
2. no sputter coating for low-voltage SEM (LVSEM).

Before sputter coating, SKPB hand sheets (with and without additional xylan) were placed in deionized water and mixed in order to separate the fibers from each other. Individual fibers were fixed on carbon tape, and afterwards sputter coating was performed (for 90 s) using gold. A S-4000 (HITACHI) was utilized at an electron energy of 8 keV. for the investigations via LVSEM pieces of SKPB handsheets (with and without additional xylan) were fixed on carbon tape. The same procedure was applied to individual fibers which were first rewetted in deionized water, separated from the hand sheets, and air-dried on the carbon tape. The measurements were performed in an Ultra 55 (Zeiss) at electron energy of 0.7 keV.

FTIR and FT-Raman Spectroscopy

Analyses of FTIR were carried out using these devices:

Bruker Tensor 27 FTIR spectrometer, MCT detector, resolution 2cm-1, 64 scans, and Specac Single Reflection Diamond ATR "Golden Gate". The samples were measured as original ATR spectra without sample preparation (in each case 2 measurements). The spectra were averaged and the mean value spectrum was baseline-corrected (rubber band method).

Analyses of FT-Raman were carried out using these devices:

Bruker Multiram FT-Raman Spectrometer, NdYagLaser 1064 nm excitation wavelength, 500 mW laser power; Resolution 4cm-1, 100 scans.

Table 1. *The studied chemical and physical fiber properties.*

Chemical and Physical properties	Inherent properties Fiber	Inherent properties Fabric
Sugar analysis (total hydrolysis)	Fiber Tenacity conditioned (FTc), Fiber Elongation conditioned (FEc), Fiber Tenacity Wet (FTw), Fiber Elongation wet (FEw)	Absorbency Testing System (ATS)
GPC determination	fiber swelling	
FTIR and Raman spectroscopy	Water Retention Value (WRV)	drying rate
SEM images (cross section, surface cracks)	Wet abrasion resistance (WAR)	
	water vapor absorption	

Table 2. *Sugar analysis results of the CV-F with xylan derivatives and comparison with pure xylan and xylan derivatives.*

Product	Glucan [%]	Xylan [%]	Mannan[%]	sum total[%]
CV Reference	97.3	0.6	0.2	98.0
CV 5.9 % Xylan	91.8	5.9	0.5	98.2
CV 4.7 % CMX	94.8	1.3	0,2	96.3
CV 4.7 % HPTMAX	94.6	1.4	0.3	96.3
CV 4.7 % BHPEX	93.3	1.1	0.3	94.7
CV 9.1 % CMX	93.2	1.6	0.2	95.0
Xylan powder	2.9	82.0	0.1	85.0
CMX deriv.	2.9	23.7	2.3	28.9
HPTMAX deriv.	2.6	31.8	2.9	37.3

The samples were compressed without dilution and measured directly (in each case 2 measurements). The spectra were averaged and the mean value spectrum was baseline-corrected (inverse rubber band method).

Results and Discussion

Table 2 shows the sugar content of xylan and xylan derivatives enriched viscose fibers as well as that of reference viscose fibers (CV). The method of sugar determination is suitable for determining the xylan share in substrates. The method is calibrated on the recovery of xylan and mannan. The glucan value is therefore of limited value. In general, only unsubstituted monomer units are detected. Thus the substituted units remain undetected. This explains the low xylan value for hemi powder (xylan has 85% sugar, 0.5% ash and a dryness fraction of about 95%). The glucuronic side chain is glycosidically bonded, thus hydrolyzed, but cannot be detected via HPL. This the explanation, why about 10% are missing from the 100%. Starting with a degree of substitution of 0.2 (NMR) that would mean that every 5th unit carries a substituent. Thus, an expected xylan value of about 60% would result. The measured values, however, are remarkably lower.

Whereas xylan itself contains about 82% unsubsituted xylan units, the synthesized CMX derivative contains only 23.7% (approx. ¼) unsubstituted xylan units (Table 2). Thus, for the incorporated fiber the real xylan content is higher than the data shows. The proportion of the cellulose is assumed to be constant. In addition, 0.6% of the detected xylan originates from the applied pulp (compare CV reference from table 2). For the sample CMX (CV 9.1%) xylan content is determined with 1.6%. Thereof 0.6% xylan is from the applied pulp, and 1% originates from the CMX derivative. This 1% detected xylan content in the CMX sample is but in fact 4%, as only ¼ is recorded, as explained above. Therefore, the real xylan content is around 4.6%, which is similar to the results with XEF fibers (4.6% vs. 5.9%).

After analyzing the SEM images of cocooned cellulose viscose fiber (CV) as the reference and CV 5.9%, 4.7% CV with CMX, CV 4.7% HPTMAX and CV 9.1% CMX, a smoother surface of the CV fibers with hydrophilic derivatives compared to the reference CV reference could be observed by SEM imaging with the exception of the CV 4.7% BHPEX. The hydrophobic BHPEX didn't show this behaviour due to bad miscibility with viscose solution. In cross-sectional images of the CV-reference and CV with different xylan derivatives, no significant differences could be observed (see figures 1, 2, 3)

Water Retention Value WRV of CV-fiber with Xylan derivatives:

Fibers with spun 4.7% CMX derivatives show a significant increase in the WRV to 108.5%. With a doubled concentration of CMX, no further increase of WRV could be observed. The xylan enriched fiber with 5.9% showed a comparable WRV, while BHPEX- and HPTMAX-blended fibers showed no differences compared to the reference CVF (see table 3).

Moisture Absorption of Cocooned CV-Fiber Xylan Derivatives:

After moisture absorption tests at 55% and 76% relative humidity after 24 hours, we found a remarkable increase in moisture absorption values of cocooned CV-fiber with xylan derivatives compared with CV reference fiber. The highest value observed in CV-fiber was with 9.1% CMX. (Figure 4)

Wet Abrasion Resistance (WAR) of the Spun CV-Fiber With Xylan Derivatives

Wet rub resistance tests of spun CV-fiber with xylan derivatives showed that all values are below the wet

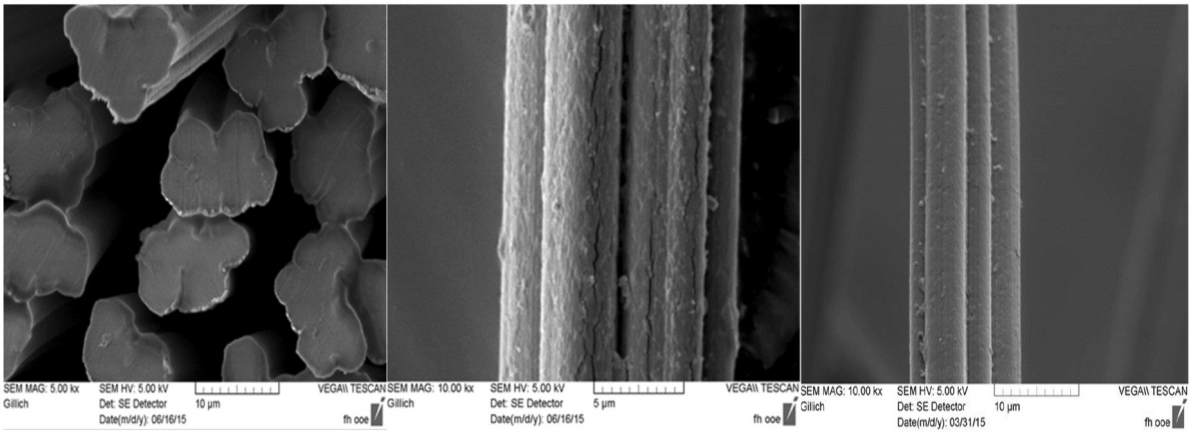

a b c

Figure 1. *SEM- Image of CVF-reference (a,b) and CVF with 5.9% xylan (c).*

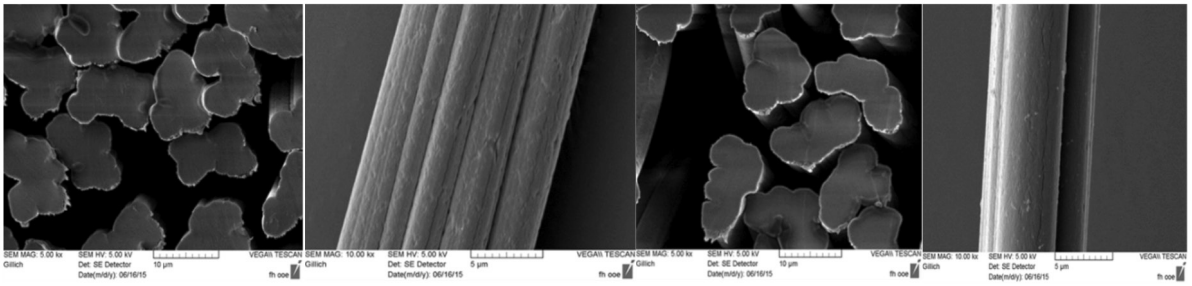

a b c d

Figure 2. *SEM- Image of CVF with 4.7% CMX (a,b) and CVF with 4.7% HPTMAX (c,d).*

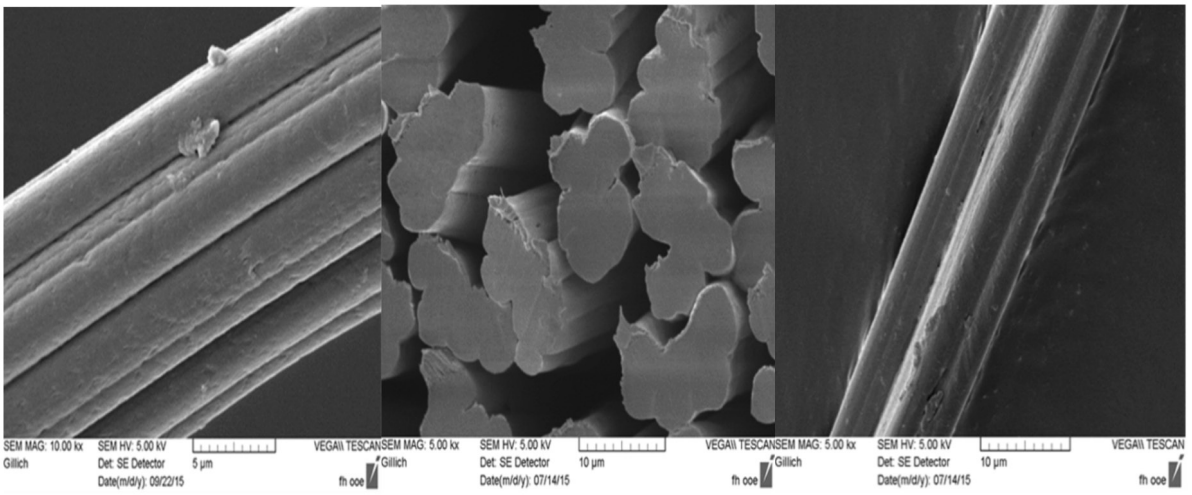

Figure 3. *SEM- Image of CVF with 9.1% CMX (a,b) and CVF with 4.7% BHPE (c).*

rub resistance value of the CV reference sample (except HPTMAX). The lower the number of revolutions, the higher is the tendency to fibrillation. Nevertheless, the differences between the values are very low (see table 4). Summarizing, no significant changes could be found.

Working Capacity (Elongation; Tenacity)

Fiber properties like working capacity and strength showed a comparable level to the reference fibers in exception of BHPEX, while the water retention value could be clearly raised due to addition of 4.7% and 9.1% CMX to the viscose fibers (Figures 5,6,7). It is known, that working capacity is equal to tenacity times elongation.

Table 3. *WRV the CVF with different xylan derivatives.*

CV fiber samples (CVF)	WRV [%]
CVF + 4.7% CM X	108.5
CVF + 9.1% CMX	106.9
CVF + 5.9% xylan	104.5
CVF reference	93.8
CVF + 4.7% BHPEX	89.7
CVF + 4.7% 86.5 HPTMAX	86.5

Table 4. *Wet abrasion resistance of CV-Fiber with xylan derivatives.*

Fiber samples	WAR (U / dtex)	CV (%)
CV Fiber Reference	305	15
CVF + XEF 5.9%	210	25
CVF + 4.7% CMX	286	21
CVF + 4.7% HPTMAX	340	22
CVF + 4.7% BHPEX	266	21
CVF + 9.1% CMX	275	17

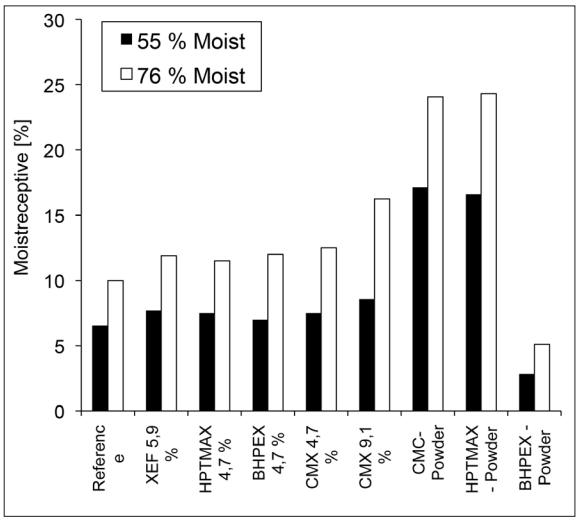

Figure 4. *Moisture absorption of the CVF with xylan derivatives after 24h.*

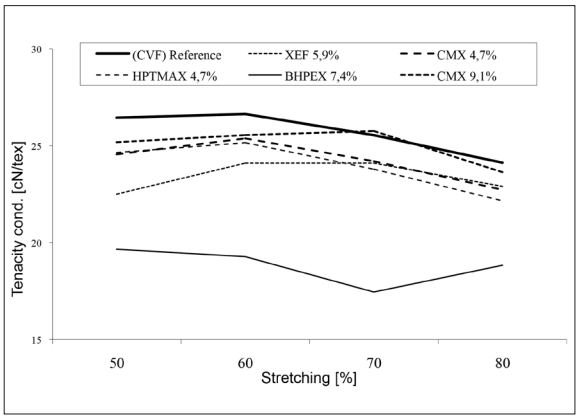

Figure 5. *Tenacity cond. of CVF and CVF with xylan derivatives.*

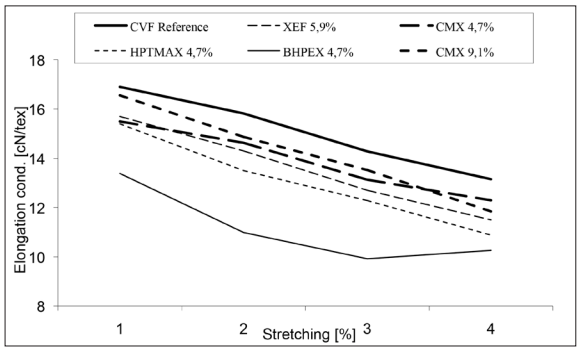

Figure 6. *Elongation cond. of CVF and CVF with xylan derivatives.*

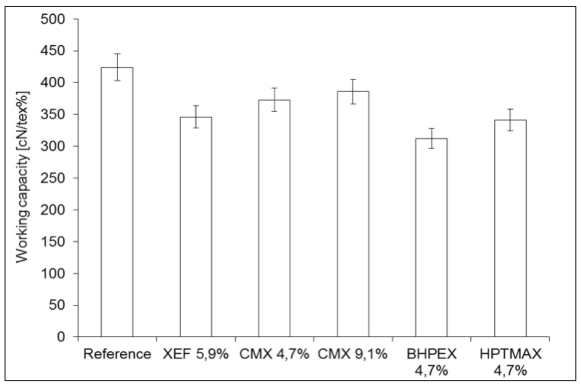

Figure 7. *Working capacity of the CVF with xylan derivatives.*

Drying Rate of Knitted Fibers

The drying rate of the investigated knitted CV fibers with CMX, in comparison with the reference knitted CV fibers and CV fibers with xylan, showed that the knitted CV fibers with CMX have a slower drying rate (Figure 8).

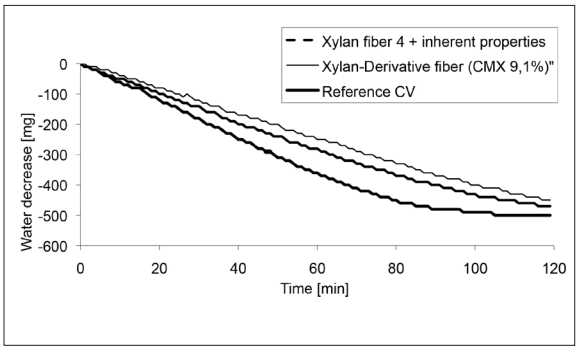

Figure 8. *Drying rate of knitted fibers.*

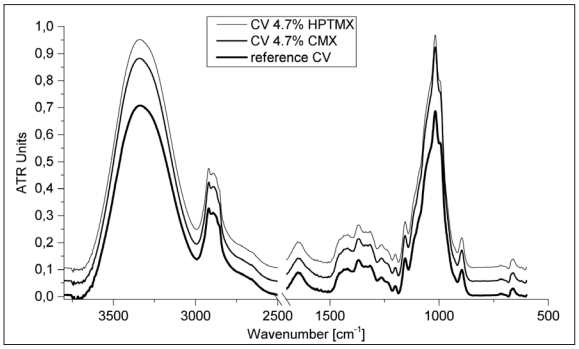

Figure 9. *FTIR spectra (reference CV, CV 4.7% CMX, CV 4.7% HPTMAX).*

FTIR and Raman Studies

In the IR spectra the substitution is not visible, due to the low DS of 0.2, and the low content of derivative in the fiber of less than 10%. Therefore, the IR method is not suitable for this purpose.

Xylan features characteristic peaks at wavelengths of 1.250 and 1.460 cm^{-1} as well as at 1,650 and 1,750 cm^{-1}, resulting from C=O bond stretching vibration at the COOH groups[16,17].

The figure 10 shows the Raman spectra of pure xylan powder, synthesized CMX and CV fiber with 4.7 CMX. The differences between the spectra of pure xylan and synthesized CMX can be detected, at the wavelengths (500 cm^{-1}, 1100 cm^{-1}, 1400 cm^{-1}, 1600 cm^{-1}) could be detected. But as it has been observed in the IR spectra, not much difference could be seen between synthesized CMX and CV 4.7% CMX.

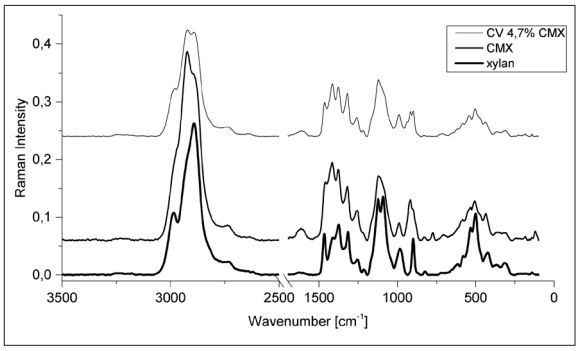

Figure 10. *Raman spectra (Xylan, CMX, CV 4.7% CMX).*

CV-Fiber Impregnation with Xylan Derivatives Solutions

Impregnation method of work: The wet viscose fiber from the final wash box was impregnated in CMX (aqueous solution) and in BHPEX (solved in acetone: water, 50:50) with different liquor ratio and time (Table 5). The impregnated fiber after drying at 30°C was examined by Raman spectroscopy. The reference fiber sample CV was, still wet from the final wash box, was applied with a liquor ratio 1:10.

By Raman studies of the impregnation tests of CV-fibers with CMX / water solutions (Figure 11) the differences can be seen at 1415, 1319, 989 and 503 cm^{-1} and with BHPEX / (water: acetone) solutions (Figure 12) the differences can be seen at 2909, 2874, 1302, 1121, 878 and 840 cm^{-1}.

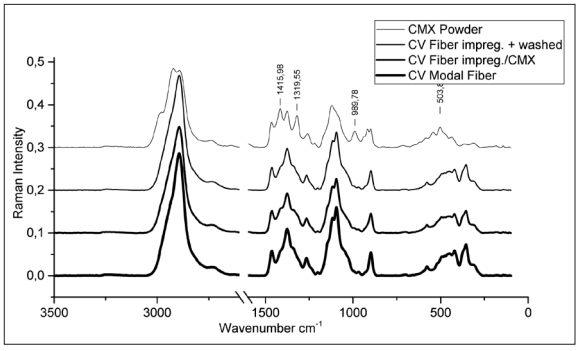

Figure 11. *Impregnation Raman spectra (compared with 10% washed CMX, 60 min).*

Table 5. *Impregnation methods*

Impregnation time	**weight concentration (CMX / water)**		
1 min	2.50%	5%	10%
10 min	2.50%	5%	10%
60 min	2.50%	5%	10%
Impregnation time	**weight concentration (BHPEX / Aceton:Water 50:50)**		
10 min	2.5%	5%	10%

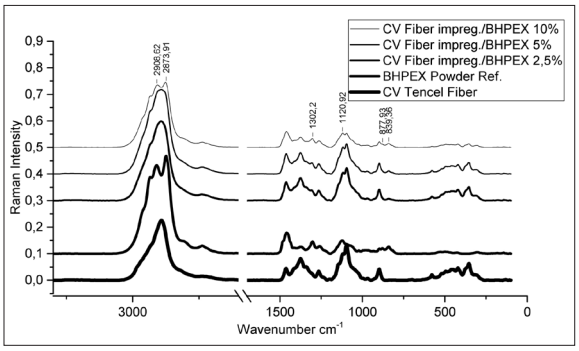

Figure 12. *Impregnation Raman spectra (10 min with different BHPEX content).*

After impregnation and subsequent washing and drying it has been found that approximately 10% of CMX already adhered to the surface of the impregnated fibers.

Conclusion

As a potential application for our newly synthesized xylan derivates, new viscose fibers were spun with 4.7% and 9.1% xylan derivatives in the spinning mass, leading to a content of 3.5% to 4.8% xylan derivatives in the fibers. The physical and chemical properties of the new produced fibers were investigated explicitly. The obtained results from the fiber-property investigation (CV with xylan derivatives) showed that, compared to other xylan derivatives (HPTMAX, BHPEX), the best fiber properties can be obtained by addition of CMX to CVF. The spun CVF with 9.1% CMX showed no significant differences compared to CV with 4.7% CMX.

Fibers with spun CMX showed a significant increase of the WRV from 93.8% to 108.5% and accordingly a slower drying rate compared to standard cellulose viscose fibers. This means, compared to standard cellulose viscose fiber, CMX / CV fiber absorbs faster and larger quantities of water and releases it more slowly during drying. With hydrophobic xylan derivatives the WRV values are below the reference CV values, due to the fact that the hydrophobic materials generally decrease the WRV.

By Raman measurements of the impregnated CV-fibers with CMX (aqueous solution) and with BHPEX (solution in water and acetone) was determined that approximately 10% of CMX already adhered on the surface of the fiber. The same results were also determined for the impregnation with BHPEX. These xylan derivatives were adhered after washing and drying the impregnated fiber to 10%, which was confirmed qualitatively in Raman investigation.

Acknowledgements

Financial support was provided by the Austrian government, the provinces of Lower Austria, Upper Austria and Carinthia as well as by the Lenzing AG. We also express our gratitude to the Johannes Kepler University, Linz, the University of Natural Resources and Applied Life Sciences, Vienna, and the Lenzing AG for their in kind contributions.

References

[1] Ebringerová A, Hrom á dkov á Z, Heinze T. Polysaccharides I Structure, Characterisation and Use. Adv Polym Sci. 2005, 186, 1–67.

[2] Fengel D, Wegener G. Wood chemistry, ultrastructure and reactions. Kessler Verlag, Munchen. 2003

[3] Henriksson A, Gatenholm P. Controlled assembly of glucuronoxylans onto cellulose fibers. Holzforschung. 2001, 55(5), 494–502

[4] Henriksson A, Gatenholm P. Surface properties of CTMP fibers modified with xylans. cellulose. 2002, 9, 55–64

[5] Silva TCF, Colodette JL, Lucia LA, de Oliveira RC, Oliveira FN, Silva LHM Adsorption of chemically modified xylans on eucalyptus pulp and its effect on the pulp physical properties. Ind Eng Chem Res. 2011, 50, 1138–1145

[6] Schild G., Liftinger E. Xylan enriched viscose fibers, Cellulose. 2014, 21: 3031-3039

[7] Wollboldt RP., Weber HK., Sixta H. Deposition of xylan during kraft cooking and O-delignification on pulp and regenerated fibres. In 10th European workshop on lignocellulosics and pulp (EWLP 2008), Stockholm

[8] Treiber E. Einfuß der Hemicellulosen auf die Weiterverarbeitung von Chemifaserzellstoffen. Das Pap. 1983, 37(12), 591-600

[9] Westbye P., Svanberg C., Gatenholm P. The effect of molecular composition of xylan extracted from birch on its assembly onto bleached softwood kraft pulp. Holzforschung . 2006, 60, 143-148

[10] Antal M, Ebringerov á A, Hrom á dkov á Z. Struktur und papiertechnische Eigenschaften von Aminoalkylxylanen. Papier. 1997, 51(5), 223–226

[11] Ren J-L, Peng F, Sun R-C, Kennedy JF. Influence of hemicellulosic derivatives on the sulfate kraft pulp strength. Carbohydr Polym. 2009, 75(2), 338–342

[12] Antal M, Ebringerov á A, Micko MM. Kationisierte Hemicellulosen aus Espenholzmehl und ihr Einsatz in der Papierherstellung. Papier. 1991, 45(5), 232–235
[13] Köhnke T, Pujolras C, Roubroeks JP, Gatenholm P. The effect of barley husk arabinoxylan adsorption on theproperties of cellulose fibres. Cellulose. 2008, 15, 537–546
[14] Köhnke T., Gatenholm P. The effect of controlled glucuronoxylan adsorption on drying-induced strength loss of bleached softwood pulp. Nord Pulp Pap Res J. 2007, 22(4), 508-515
[15] Miletzky A., Punz M., Zankel A., Schlader S., Czibula C., Ganser C., Teichert C., Spirk S., Zöhrer S., Bauer W., Schennach R. Modifying cellulose fibers by adsorption/precipitation of xylan. Cellulose. 2015, 22, 189–201
[16] Kacurakova M, Wellner N, Ebringerova A, Hroma dkova Z, Wilson RH. Characterisaiton of xylan-type polysaccharides and associated cell wall components by FT-IR and FT-Raman spectroscopies. Food Hydrocoll. 1999, 13, 35–41
[17] Fengel D. Möglichkeiten und Grenzen der FTIR-Spektroskopie bei der Charakterisierung von Cellulose. Teil 3. Einfluss von Begleitstoffen auf das IR-Spektrum von Cellulose. Papier. 1992, 1, 7–11

Optimization of the Chemical Process Route to Alkali Blue (Aniline Blue)

Dr. Manfred Hähnke

Manfred Hähnke
D-65779 Kelkheim
email: m.a.haehnke@t-online.de

Abstract

The world market of Alkali Blue (Aniline Blue) pigments, C. I. Pigment Blue 56 and 61, is still very big (12 -14 tsd mt/a). The two established production routes: a) over Pararosaniline and b) over trichlorotrityl-chloroaluminate suffer from a number of limitations, mainly related to technical pathways, chemical complexicity, undesired by-products and their elimination, accessible shade area (from reddish until neutral/greenish blue) and, production costs per unit. A number of connections and the reasons for mentioned trouble have been investigated. Optimized manufacturing processes generating remarkable cost savings are now ready for commercial scale production. Details of commercial scale production plant and controlling devices are commercially available.

Introduction

Alkali Blue (also known as: Aniline Blue, Reflex Blue, Sheetfed Blue) and its higher sulphonated derivatives still have a great significance in the market. After about 150 years there is still high demand e. g. a) in book and newspaper printing (deep black based on carbon black, shaded with Alkali Blue), b) in illustration and advertising papers (just as brilliant blue single shade), c) in flexo print (product labelling and packing), and in higher sulphonated form (as Spirit-, Water- and Ink-Blue).
Worldwide actual consumption of Alkali Blue adds up to 12 – 14 tsd mt p. a. (50 – 70 mio US$ p. a.), partly in paste form (e. g. flush pastes), partly in form of finished powders. Production sites are resp. have been in USA, Germany, India by companies such as BASF, Flint, Microinks, Hoechst, Clariant, Allessa, Sherwin Williams [1, 2].
Chemically, Alkali Blue is a N-phenylated triphenylmethane as its carbonium-cation. A look at the adsorbtion spectrum shows a pretty sharp and high absorbtion peak [3]. The molar colour strength of pure Alkali Blue is extremely high (molar extinction coefficient about 70 000), higher than of most other colorants.

The shade brilliancy of Alkali Blue is extraordinarily high.

Its light fastness is very interesting: Application as single shade (e. g. on paper) leads to a level of just 1 – 2 (Xenotest/blue scale), but as deepblack (carbon black, shaded with Alkali Blue) a level of 6 - 7 can be reached. The reason is that the carbon black absorbs more or less the full irradiation energy of the sunlight, not leaving so much to attack the Alkali Blue. Somewhat surprising is that an application of Alkali Blue on acrylic fibres leads to a lightfastness level of 5 - 6 [4, 5]. However, for the applications on paper the low level fastness is acceptable.
Alkali Blue pigment (mono-sulphonic acid of the triphenylmethane pigment body) is always in a stable amorphous form. This is the reason for its good applications behaviour (rheology, coloristical power, storage stability etc.) [3].
The chemistry of Alkali Blue manufacturing is pretty complex for the very old process using Pararosaniline [6] as well as the one developed after 1970 employing trichlorotrityl-chloroaluminate [7]. Both routes lead more or less to the same final product. But the chemical reactions suffer from a number of problems.

1. Synthesis Route Using Pararosaniline

Target product is a more or less reddish blue.
Brief process description:

Pararosaniline (C. I. Basic Red 9, chloride form) is stirred in an excessive amount of aniline. After addition of catalytic amounts of acetic or benzoic acid a temperature of about 180 °C is maintained for some hours. Under release of NH3 over reddish violet (at 100 - 120 °C) and bluish violet (at 140 – 150 °C) finally a reddish blue (at 180 °C) is formed.

The blue (triphenylated) main product has the following chemical constitution:

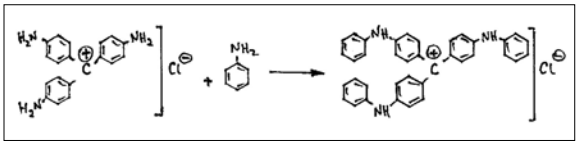

The melt is worked up in aqueous acidic system as chloride and is then isolated by filtration. The raw pigment body contains (depending to a certain extent on the reaction conditions) certain amounts of diphenylated (bluish violet) and monophenylated (reddish violet) byproducts. All other ingredients of the reaction melt go into the filtrate. Aniline is recycled by distillation under alkaline conditions.

The rinsed filter cake is usually dried.

Yield (dry): about 95 – 98% of theory.

The dry stuff is then sulphonated in H_2SO_4 90% at 40 - 60 °C. All coloured components (blue, bluish violet, reddish violet) are transferred to a mix consisting of 80 - 90% monosulphonic acid, 5 - 15% unsulphonated item, 2 - 5% disulphonic acid.

The sulphonation mass is poured onto water/ice and then warmed up to 50 - 60 °C. The precipitating "Raw Blue" is filtered off and rinsed with water untill a weakly acidic pH-value is achieved.

The press cake is treated with aqueous NaOH at a temperature of 80 – 90 °C. All coloured components (including the unsulphonated parts) dissolve into a brownish red colour solution. After an optional clarification filtration, dilute H_2SO_4 is poured in, till a clear mineral acidic pH is reached.

Under defined conditions (time, temperature, pH) "Bronze Blue" pigment is precipitated in amorphous form. It is isolated by filtration and rinsed with water. This filter cake is just ready for flushing with a suitable varnish/resin in a kneader. Flushing means transwetting of the particle surface from aqueous to varnish system. The water separates during kneading and is removed through an overflow valve. The result is an Alkali Blue flushpaste which is now ready to be sold to consumers.

Instead of flushing, another alternative to obtain Alkali Blue in finished powder is to add an alkali-soluble resin to the mentioned alkaline brownish red product-solution. By an acidic precipitation a pigment-suspension results, which may be isolated and immediately spray dried to a finished Alkali Blue powder.

The Problems in Pararosaniline Process

1. The shade area is limited because a real neutral blue can't be obtained. The reasons are: the first reaction step (to reddish violet) happens fast and easily; the second step (to bluish violet) as well. The final reaction step (to neutral blue) needs extremely high temperatures (about 180 °C over long time). This step does not happen quantitatively. Besides the wanted forward reaction, a partial backward reaction also goes on, as diphenylamine splits off.

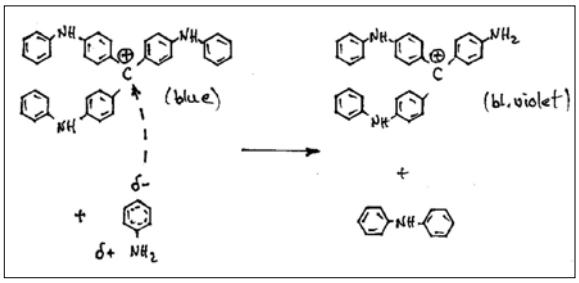

   Therefore, a full neutral blue cannot be reached, neither by higher amounts of catalyst nor by harder reaction conditions.
2. When of working up the reaction melt in aqueous HCl the final pigment body results in the form of a chloride. So during sulphonation gaseous HCl is formed and has to be absorbed by an aqueous wash. An alternative work up of the reaction melt (with H_2SO_4 instead of HCl) is not possible: the resulting diphenylamine-sulfate would not be sufficiently soluble in an aqueous system and the elimination of diphenylamine would fail.
3. Prior to sulphonation the aqueous press cake has to be dried to avoid any influence on H2SO4 concentration. It would be very desirable to get rid of this timely and costly unenjoyable drying step.
4. As mentioned, the sulphonation does lead to a mix consisting of sulphonated and unsulphonated pigment bodies. Only at an optimum average sulphonation rate the target product "Bronze Blue" results with good filtering behaviour and with a relatively low water content. The water content is later decisive for good flushing. A high water content may lead to a slow and unreliable start of transwetting (flushing). As a consequence the flushpaste may suffer from high viscosity and from a loss of coloristical strength.

   It is important to understand why the unsulphonated parts of the pigment body are water soluble

just when mixed with sulphonated parts: sandwich structures (double molecules) are formed, which as a whole are water soluble.

2. Trichlorotrityl-Chloroaluminate Synthesis Route

Target products are a greenish blue as well as a reddish blue. This procedure has been utilized since 1970 [7].
The starting material (4,4‘,4“-trichlorotrityl-tetrchloroaluminate) is produced through Friedel Crafts-reaction: 4-chloro-benzotrichloride reacts in the presence of molar amounts of AlCl3 with excessive amounts of chlorobenzene. Under release of gaseous HCl the Friedel Crafts crystals are produced in good yield.

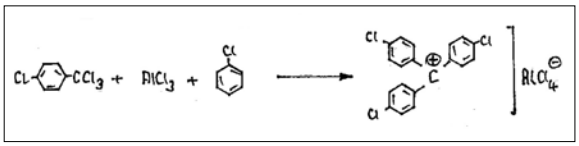

At a temperature below 0 °C these crystals precipitate more or less quantitatively as orange sandy needles. The chlorobenzene mother liquor, containing a few byproducts is removed through filtration. The crystals have to be protected against moisture and are going directly to the next reaction step.
m-Toluidine is poured over the crystals rapidly. So immediately a liquid bordeaux red mass is formed (1. phenylation step). After heating up to 100 – 120 °C the mass becomes green (2. phenylation step) and at about 140 – 150 °C the melt becomes dark blue and bronzing (3. phenylation step). After a few hours the reaction is terminated.
The “Blue Melt” is cooled down to 80 - 90 °C and stirred into an aqueous solution of NaOH. It is important to note that as the mix develops it generates heat and begins to boil. The colour changes to brownish red. After the stirring is stopped the 2 layers are easily separated. The bottom phase is an aqueous solution of excessive NaOH, NaCl and Na_3AlO_3, which is the effluent. The upper layer contains the raw pigment body in the form of free bases (anhydrous base and carbinol base) as well as excessive amounts of m-toluidine.

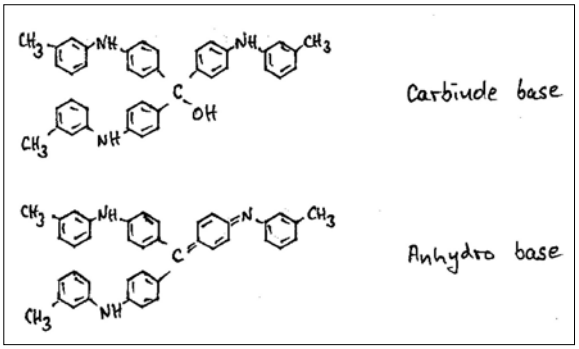

This layer may be dried to flakes by means of a vacuum cylinder dryer. The flakes are just ready for sulphonation, for subsequent pigment precipitation (“Bronze Blue”) and finally for finishing (e. g. flushing) as described earlier.

The Problems in Trichlorotrityl-Chloroaluminate Synthesis Route

The central C-atom shows (in case of Pararosaniline) a reduced chemical reactivity because of the partial delocalisation of the cationic charge to the amino groups. In the case of Friedel Crafts crystals the situation is different: The Cl-atoms cause even a stronger positive charge at the central C-atom, leading to increased chemical reactivity just at this molecular place.

1. Theoretically the Friedel Crafts crystals from the synthesis should give an yield of 92 – 96%. By-products (more or less remaining completely in the mother liquor) can result from low purity of p-chloro-benzotrichloride, from its reaction with chlorobenzene in o-position (instead of p-position), from any over- or under-stoichiometrical amounts of AlCl3 and from any moisture access.
2. In case of a non sufficient rinse of the Friedel Crafts crystals the finally resulting raw pigment would contain certain amounts of green by-products. These would be influencing shade and strength of the Alkali Blue.
3. It is not possible to use aniline instead of m-toluidine for the initial melt reaction [8]. Aniline would just lead to a final product containing large amounts of colourless tetraphenyl-methane derivatives. The reason for this is that the p-position in aniline body must be protected from being chemically attacked by the very reactive trichlorotrityl-cation. This can just be achieved with an aniline with any substitution in p-position to the amino groups or with a stearically demanding substituent in m-position.

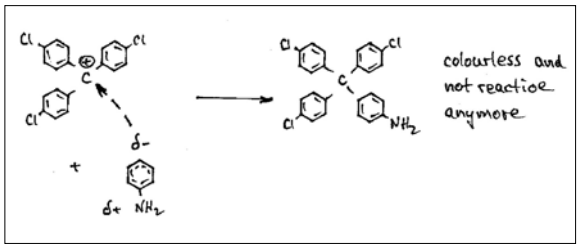

4. In case of an over stoichiometrical amount of AlCl3 in the Friedel Crafts reaction a trichlorotrityl-heptachloro-dialuminate results instead of the wanted tetrachloro-aluminate. This item would anyway be able to react with m-toluidine finally to the same pigment body. But since the hepta-

chloro-dialuminate is soluble in chlorobenzene, it remains in the mother liquor and is lost for conversion to blue pigment.

5. However, starting from trichlorotrityl-tetrachloro-aluminate and m-toluidine it does finally lead to a greenish neutral alkali blue. But the market requires additionally the reddish blue shades.
   Principally, it is possible to get the reddish alkali blue. However, it is pretty complicated: For the 1. phenylation step m-toluidine has to be used. After this reaction is over excessive amounts of aniline are added. The chemical reaction gets over within a few hrs at about 150 °C, leading to the following main components:

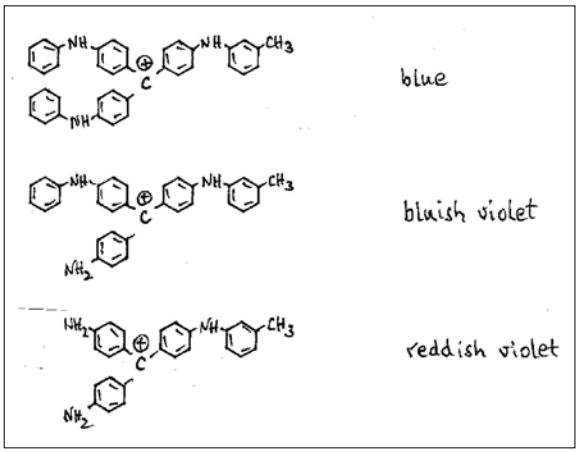

   The diphenylamine, generated as byproduct is usually eliminated as follows: After the reaction melt has been worked up in aqueous NaOH, the upper layer is isolated and diluted with chlorobenzene. Then diluted H_2SO_4 is added and stirred in an amount just to precipitate the whole coloured pigment. The precipitate is then filtered off, leaving the diphenylamine and aniline in the mother liquor. The filter cake is immersed in water and a water steam distillation is carried out until chlorobenzene is completely removed.
   The resulting suspension of raw pigment body (in sulfate form) is filtered off. It has to be dried prior to sulphonation.

This reaction pathway is time-consuming and cost-intensive. But till date it is the only way to get a reddish Alkali Blue, meaning C. I. Pigment Blue 56.
This procedure to reddish type over trichlorotrityl-chloroaluminate is remarkably more expensive than the procedure over Pararosaniline. In case of the greenish neutral Alkali Blue the cost relation is just opposite.

3. Optimized Synthesis Procedures, Based on New Findings

It has been mentioned that the two established synthesis routes do have advantages as well as a number of problems. Meanwhile it is anyway clear that it is possible to combine both routes in a way to enjoy advantages and to get rid of problems. This can be demonstrated in practice. An additional purpose and target is of course to cut down the process costs (equipment, energy, time and personnel) significantly.

Practical Example A

Target product is an Alkali Blue with any desired shade between reddish and greenish brilliant blue.

Reaction Step 1: Friedel Crafts Reaction

Chemical reaction is as mentioned earlier.
28 g of dry AlCl3 is suspended in 100 g water free chlorobenzene. After cooling down to a temperature between -5 and -10 °C, a mixture of 45.6 g p-chlorobenzotrichloride and 45 g chlorobenzene are added under good stirring within 1 hr. For 1 hr the temperature is maintained between at -5 to -10 °C, then allowed to go up within 2 hrs to 20 °C and after additional one hr to 55 - 58 °C. Reaction mass at first becomes yellow orange, later brownish. After 3 - 4 hrs at 55 - 58 °C under constant generation of gaseous HCl the reaction mass is cooled down below 0 °C. An orange brown pulp is formed. After 1 hr at 0 °C the mother liquor is sucked off. The remaining Friedel Crafts crystals are rinsed with little cold chlorobenzene. Any access of moisture must be avoided.
Yield: about 92 - 95% of theory. Immediately the next reaction step follows.

Reaction Step 2: Reaction of Friedel Crafts Crystals With Excessive Amount of m-Toluidine

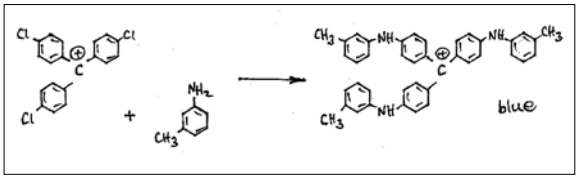

140 g of dry m-toluidine are flooded onto the Friedel Crafts crystals, leading to a temperature increase to 50 - 70 °C. In this exothermic reaction a homogenous liquid mass with dark red colour is formed immediately. Within 2 hrs a temperature of 140 - 145 °C is made and maintained for 3 hrs. During this time the colour changes over green to bronzing dark blue. Residual amounts of chlorobenzene (from Friedel Crafts crystals) are distilled off.

The process described so far finally leads to a greenish neutral Alkali Blue. But this shade is not the real single target. To get finally an Alkali Blue with a shade between reddish and greenish neutral blue the melt has additionally to be treated as follows:

A suspension of Pararosaniline (to choose between 1 and 20 g) in some m-toluidine is added at 140 - 145 °C to the melt. Within 1 - 2 hrs at this temperature the Pararosaniline reacts mainly to bluish violet products with following chemical constitution:

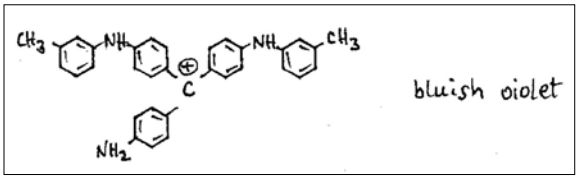

The reaction melt is then cooled down to 90 - 100 °C and stirred to 320 ml of aqueous NaOH 20%, which has been preheated to 50 - 70 °C. Pay attention to the fact that it is an exothermic reaction with rapid temperature increase to the boil. After 30 min of boiling it is cooled down to 60 - 70 °C and the stirrer is switched off. Two liquid layers are formed. The bottom layer, consisting of an aqueous solution of Na_3AlO_3, NaCl and excessive amounts of NaOH is run off. The upper layer contains the brownish red pigment base dissolved in m-toluidine. This layer is rinsed with some warm water. Resulting organic phase then goes to a vacuum thin layer evaporator, where the m-toluidine is distilled off.
The raw pigment base results in the form of brownish flakes giving a yield of 95 – 98% of theory. Residual content of m-toluidine shall below 1 – 3%.

Reaction Step 3: Sulphonation
50 g of the described pigment base flakes are stirred within 30 min at room temperature into 250 g H_2SO_4 92%. After a homogeneous solution is reached a temperature of 40 - 50 °C is made within 45 - 60 min. After 30 min, every 10 min a test of sulphonation rate is carried out by a simple procedure: 3 drops of the sulphonation mass are put into 20 ml of 5% NH_3 in a suitable glass tube. After a short boil a light blue solution shall result which does not release any insoluble parts on a paper filter. Normally sulphonation is terminated after 45 min at 42 - 45 °C. Now immediately the mass is stirred into 250 ml water/ice. After 30 min at 70 – 80 °C the precipitated "Raw Blue" is isolated by filtration and rinsed with water. Yield: nearly quantitative.
The pigment body shall now bear as an average 0.7 – 0.8 sulphonic acid groups per molecule. In case of a higher sulphonation rate an increasingly poorer filtering behaviour would result. Sulphonation conditions have eventually to be adjusted depending on the individual item.

Reaction Step 4: Conversion of "Raw Blue" Into Alkali Blue Pigment

The wet presscake (sulphonated product) is suspended in 500 ml water. At 80 – 85 °C an addition of 45 g NaOH 33% is made. The mixture is heated up to boil, leading to a brownish red solution of the pigment body. In case of residual amounts of undissolved blue particles some more NaOH has to be added. A filtration step is usually not necessary.
Now quickly under heavy stirring 120 ml H_2SO_4 12% is poured in. The target product Alkali Blue precipitates immediately. After 5 min at 98 - 100 °C (alternatively 10 min at 90 - 92 °C) temperature has to be decreased immediately to 70 - 75 °C to ensure an optimal pigment quality. The product is filtered off and rinsed with warm water untill a pH of 3 - 5 is reached.
Yield practically quantitative.
A drying is usually not carried out as the press cake goes for flushing.

Practical Example B

Target product is an Alkali Blue powder product [9, 10] in any shade between reddish blue and greenish neutral blue.

Reaction Step 1: Friedel Crafts Reaction
To follow same procedure as described earlier in this paper resulting in Friedel Crafts crystals.

Reaction Step 2: Reaction of Friedel Crafts Crystals With m-Toluidine Plus Aniline
Reaction with 140 g m-toluidine (as described in method/practical example A) is replaced by the following procedure:
A mix of 30 g m-toluidine and 50 g chlorobenzene is poured over the Friedel Crafts crystals. With the formation of HCl in an exothermic reaction (50 - 60 °C), immediately a dark red liquid reaction mass is formed. The temperature is increased to 120 - 125 °C within 1 hr and maintained for 2 hrs. Then 120 g aniline is added and the melt is stirred for 3 hrs maintaining the temperature between 140 - 145 °C.
A mixture separately prepared as below is then added.
A suspension of 20 g Pararosaniline and 2 g acetic or benzoic acid in 50 g aniline is heated up to 150 - 160 °C. After 1 – 2 hrs the Pararosaniline reacts to a product mix of monophenylated (reddish violet) and diphenylated (bluish violet) derivatives.

This reaction mix is very suitable for shading a greenish neutral blue to reddish. Based on the wanted shade, adequate amount of the mix should be added.
In this procedure practically no diphenylamine formation was observed.

Reaction step 3: Sulphonation
Same procedure as described above.

Reaction Step 4: Convertion of the Shaded Raw Blue to a Shaded Alkali Blue Pigment
After the brownish red alkaline solution of the sulphonated product is prepared, a suitable resin (dissolved in aqueous NaOH) is added. Such resin has to be water soluble at alkaline pH. And it has to be suitable for practical Alkali Blue printing applications. The amount to be added is accordingly selected to render an Alkali Blue with a content of e. g. 85% pigment body [9].
The solution of pigment body and resin is treated (precipitated) as described earlier. After spray drying a finished Alkali Blue powder is produced. Many variations of resin type with varying quantities are possible, based on the planned use.

Conclusions

What are the benefits and advantages of the alternative synthesis routes? It is easy to see that a large constitutional variety of chemicals does finally make the Alkali Blue, depending on the synthesis route itself as well as on the shading operations. Anyway this multiplicity can be controlled with good reproduciblity. Many finished variations are possible, all often lead to high performance Alkali Blue products.

In comparison with the established production procedures a number of improvements are visible:

- The shade area is not limited, reddish until greenish neutral blue can be reached, with high brilliancy.
- During synthesis no remarkable amounts of diphenylamine is produced as an undesired by-product. High expenses for elimination (especially in trichlorotrityl-chloroaluminate route) can be avoided.
- The “Raw Blue” results after work up of the pigment melt in form of the free base(s), not as a chloride (in Pararosaniline route). So a formation of gaseous HCl during sulphonation does not happen.
- The drying of any wet “Raw Blue” press cake is not necessary. This saves operational and energy costs.
- The “right” sulphonation rate leads to an aqueous “Bronze Blue” press cake with excellent filtering behaviour.
- The “right” sulphonation rate is an additional advantage to obtain a fast and complete transwetting from aqueous to varnish system. A flushpaste with minimized viscosity problems (e. g. thixotropic behaviour) results.
- Minimized manufacturing costs can be achieved (utilizing the route over trichlorotrityl-chloroaluminate), if the pigment melt is carried out in a 1 bath-2 step-procedure: starting with m-toluidine and finalizing with aniline. In this way it is possible to avoid generation of diphenylamine. A cost-intensive elimination of diphenylamine (as it is necessary in the trichlorotrityl-chloroaluminate route for manufacture of reddish Alkali Blue shades) is not necessary.
- Generally, the described procedures lead to Alkali Blue items with the same high brilliancy and colour strength as those made over established procedures.
- The discussed and demonstrated alternatives are ready for further development and for trying out on pilot plant scale.
- Technical details concerning production equipment as well as measuring and controlling devices are commercially available.

References

[1] Project report on micro inks (2014), Ekta Vekariya
[2] Standard Ultramarine and Color Company, www.colorantshistory.org
[3] Industrielle Organische Pigmente (1995), Herbst and Hunger
[4] Patent DE 2359466 (1976), Hoechst
[5] Patent DE 2413299 (1978), Hoechst
[6] Polytechnisches Journal, Ueber Anilinblau (1878)
[7] Patent DE 1098652 (1961), Farbwerke Hoechst
[8] Patent DE 1644619 (1972), Farbwerke Hoechst
[9] Patent FR 2017958 (1970), Farbwerke Hoechst
[10] Offenlegung DE 2914299 (1979), Hoechst

Correlation of Substantivity and Chemical Constitution of Cellulose Dyestuffs

Dr. Manfred Hähnke

Manfred Hähnke
D-65779 Kelkheim
email: m.a.haehnke@t-online.de

Abstract

All water soluble dyestuffs (textile and paper) possess a specific substantivity to cellulosic material. This is of course right for Direct Dyes and it is even right for Reactive Dyes prior to chemical fixation at alkaline pH, of Vat and Sulphur Dyes prior to reoxidation and of Naphtol AS products before being coupled to the colored pigment.
Substantivity is a decisive value for selection of an exhaust or a continuous application method.
Specific substantivity value of every cellulose dye (under defined conditions) is depending on the size of conjugated π electron system and on hydrophilic substituents within the dyestuff molecule.
A special new algorithm has now been developed to calculate the substantivity (relative adsorption Ads_{rel}) values possible, based on molecular dyestuff constitution.
An acceptable correlation of calculated versus experimental data of substantivity values was reached.

Introduction

The large majority of all cellulose dyestuffs are water soluble and possess a more or less pronounced substantivity to cellulosic substrate.
Pigment preparations make an exception: The originally water insoluble colour body has to be ground to a microcrystalline aqueous dispersion. By means of a suitable “binder” the pigment particles are then fixed/sticked on the substrate (cellulosic fibres as well as synthetic fibres, polymer foils, paper, metal, glass).
Back to cellulosics. It is well known that a big variety of different dyestuff types can be applied from aqueous solution. These dye classes differ from each other remarkably in colour strength, brilliancy, light fastness etc. Their substantivity from aqueous bath to cellulosic material is decisive for selection of technical application method. And substantivity is finally responsible for resulting stability of the colouration under wet conditions.
Acid Dyes (low molecular weight) are only weakly substantive. Therefore they are not at all utilized for cellulosic textiles, anyway they are used to a small extent for paper (dry end use).
Reactive Dyes (low up to high molecular weight, at the end high wet fastness properties) have to be adsorbed substantively/physically on cellulose, before they are fixed chemically in a second step or simultaneously at alkaline pH. Their substantivity is extremely product- and range-specific.
Direct Dyes (high molecular weight) show a high substantivity to cellulose, therefore they just lead to an acceptable wet fastness level.
Basic Dyes behave similar as Acid Dyes as far as substantivity is concerned.
Vat and Suphur Dyes both become water soluble just in presense of reducing chemicals and alkali, in this stage showing medium up to high substantivity.

Physical Nature of Substantivity

As already mentioned, all water soluble dyes show a more or less pronounced substantivity to cellulose. Always an equilibrium (dye concentration in aqueous solution respectively adsorbed on cellulose) is formed. Such equilibria follow special physical/mathematical rules [1]. Langmuir adsorption isotherme e. g. is describing the situation at equilibrium [2]:

$$C_{Dye}^{ads} = \frac{K \cdot C_{Dye}^{ads\ max} \cdot C_{Dye}^{lös}}{1 + C_{Dye}^{lös}}$$

with C_{Dye}^{ads} = dye concentration on cellulose

$C_{Dye}^{ads\ max}$ = maximum dye concentration on cellulose (saturation)

$C_{Dye}^{lös}$ = dissolved/unadsorbed dye concentration

K = Langmuir adsorption coefficient (product-specific constant)

Different dyestuff classes and items possess (under standardized conditions) a large variety of k values. On top of that adsorption is of course always depending on salt concentration and salt type (NaCl, Na2SO4, KCl etc.), temperature, pH value, cellulose type, total dye amount (depth target), dye combinations, time exposure (diffusion rate and speed) [3,4,5].

Physical/Chemical Fundamentals Concerning Dyestuff Substantivity

Every organic dyestuff is possessing a π electron cloud based on its molecular binding system, half of that cloud situated above and the other half below molecular plane.

Precondition for the existance of a π electron cloud is a molecular structure characterized by alternation of single and double bonds throughout the chromophores, named conjugation. Free, non binding electron pairs of –O- and –N- bridges behave like double bonds as well. Another general precondition for conjugation and a π electron cloud is that the colour part (the chromophore) is planar.

Under these conditions double bonds resp. free electron pairs are delocalized to the mentioned π electron cloud. Regarding e. g. following simple azo-pyrazolon dye formula (b) describes the real situation better than formula (a), because the π electron cloud is more obvious:

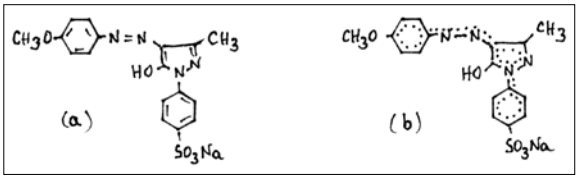

Totally 10 π electron pairs are conjugated, in detail:

- 7 -C=C- double bonds
- 1 -C=N- double bonds
- 1 -N=N- double bonds
- 1 non binding free electron pair (at pyrazolon-N)

At any place(s) of the conjugated π electron system dyestuff molecules may bear a certain number of substituents (-CH_3, -OCH_3, -Cl etc.). Depending on specific ± I (inductive) effects and ± M (mesomeric) effects of these substituents the π electron density of the whole conjugated system is boosted or reduced. The ± I and ± M effects of the substituents may be opposite, their real effectivity is resulting additively.

The finally developed π electron cloud is able to accept H-bridges from the HO-groups of cellulose. Physical/chemical binding power of this H-bridge is depending from size and strength of the individual π electron cloud. So it is obvious that every dyestuff behaves differently, in other words: The molecular attraction (substantivity) must be dye-specific.

Other parts in molecular dye structure are also playing an important role: Solubilizing (hydrophilic) substituents like –SO_3H, -COOH, -NR_3 + etc.

The water solubility of a dye is resulting from the development of a hydrate shell around the hydrophilic groups. In case of an ionized –SO_3H group a shell e. g. of 6 H_2O is formed. On top of the 1st hydrate shell other hydrate layers are following (with reduced binding power). Very important for the solubilizing effect is anyway, whether or not any sterical hinderance influences the size of the hydrate shell, e. g. in case of large substituents in direct neighbourhoud.

Non ionizing hydrophilic substituents in the dye molecule e. g. –OH groups also form hydrate shells, but with smaller size, binding power and solubilizing effect.

Taking both into consideration , attraction on cellulose by means of a π electron cloud and the dissolution over hydrophilic groups in a dye do lead to an adsorption equilibrium. Most decisive is whether the equilibrium lies more on the left or on the right hand side of that equilibrium Dye^{ads} Dye^{sol}.

Calculation of Relative Adsorption Value Ads_{rel}

Basic idea:

The molecular structure respectively its influence on the adsorption behaviour of water soluble cellulose dyes have been pointed out. So it should be possible to develop an algorithm for determination of a relative adsorption value Adsrel if chemical constitution is known [6,7].

Finally, the calculated Adsrel values should correlate with the experimentally determined substantivity values of the dyes.

Experimental Determination of Substantivity:

a) Usually adsorption behaviour (substantivity) is measured under standardized conditions (dyestuff-, water- and salt-amount, salt-type, temperature and T-programme, pH value) after reaching the adsorption

equilibrium. Specific adsorption values for any dye item respectively for any range or class may be obtained.

b) The specific adsorption behaviour can also be determined chromatographically (solid phase: cellulose; mobile phase: aqueous NaCl solution). Resulting RF values indicate individual substantivity of every dye item.

New Calculation Algorithm:

$$Ads_{rel} = \frac{(a + m_1 \cdot b_1 + m_2 \cdot b_2 + \dots)^x}{n_1 \cdot c_1 \cdot f_1 + n_2 \cdot c_2 \cdot f_2 + \dots}$$

A relatively simple algorithm for the determination of substantivity/adsorption has been developed, which is leading to Adsrel values of dyestuff items:

With the meaning of

number of double bonds (quinoide CO groups included) and free –O- and -N- electron pairs within a conjugated molecular system (whole-number)

number m of substituents with ± I / ± M effect (added), located in the conjugated system, with values of (b) between 0.2 and 0.6, depending on the type of substituent

conjugation exponent, with values between 1.9 and 2.1, depending on chromophore size

number n of hydrophilic substituents in the whole molecule, with values of (c) between 0.2 and 3, depending on type of substituent

correction factor in case of a sterically hindered hydrate shell, with values between 0.4 and 1, depending on direct neighbour substituents

Comparison of Calculated Adsrel Values With Experimentally Determined Substantivity Values

For the evaluation of the utilized algorithm it makes sense to plot the calculated Adsrel values of the dye items against their experimentally determined substantivity values.

An interesting curve is received (see Graph 1). All of about 50 considered dyestuff items are positioned (with little deviations) along 1 line, independent from dyestuff item and class.

This is a strong indication that the worked out and utilized algorithm is indeed suitable to determine/describe substantivity/adsorption behaviour of cellulose dyes.

The deviations above and below the curve line may be depending on the influence of the substituent positions along the basic molecular structure or probably just on measuring inaccuracies.

It must be clear anyway that the developed algorithm is just suitable for comparison of substantivity/adsorption of dye items under standardized conditions. The dependence of substantivity values from salt concentration and salt type, temperature, pH value, cellulose type as well as from dyestuff combinations and color depth has to be considered separately respectively on top.

Examples

Selection of		Substantivity*		Ads_{rel} **	
VS Reactive Dyes	C. I. Reactive	Ester-	Vinyl-	Ester-	Vinyl-Form
Remazol ® :					
Golden Yellow RNL	Or 107	4	10	11	24
Brilliant Red 3BS	Re 239	24	38	48	75
Brilliant Blue R spec.	Bl 19	13	24	36	65
Black B	Bla 5	10	25	24	62
Sumifix ® :					
Supra Red 3BF	Re 195	13	29	35	70
Supra Blue BRF	Bl 221	11	19	30	55
Supra Navy BF	Bl 222	17	31	48	72

* Experimentally determined: dyeing with 0.5% dye, Co mercerized, liquor ratio 1:20, temperature 60 °C, 10 g/l commun salt

** Calculated over described algorithm

It can be seen that and how the commercial ester form (anchor $–SO_2-CH_2-CH_2-SO_3Na$) differs from its applicationally (at alkaline pH) reactive vinyl form (anchor $–SO_2-CH=CH_2$).

It is somewhat surprising that there do exist such big Ads_{rel} value differences from item to item within a single commercial sales range.

Selection of other Reactive Dyes		Reactive (Anchor)		Substantivity*	Ads_{rel}**
Procion ®	Orange PX-RN	(MCT)		15	30
	Black PX-N	Bla 8	(MCT)	8	10
	Red H-E3B	Re 120	(MCT/MCT)	80	180
	Navy H-ER	Bl 171	(MCT/MCT)	60	135
Lanasol ®	Orange 2G	Or 29	(Bromoacryl)	17	33
	Red 2G	Re 84	(Bromoacryl)	25	48

* Experimentally determined: dyeing with 0.5% dye, Co mercerized, liquor ratio 1:20, temperature 60 °C, 10 g/l commun salt

** Calculated over described algorithm

Selection of other Dyestuff Classes	C. I.	Substantivity*	Ads_{rel}**
Acid Dyes:			
Tartrazine	Ac Ye 23	4	18
Orange II	Ac Or 7	19	35
Telon ® Blue CD-FG	Ac Bl 145	11	36
Basic Dyes:			
Astrazon ® Yellow GL	Bas Ye 28	25	61
Red F2BL	Bas Re 46	17	47
Blue FGGL	Bas Bl 41	28	64
Direct Dyes:			
Sirius ® Black S-VSF	Dir Bla 22	***	230
Cotonerol ® A	Dir Bla 19	***	190
Cotonerol B	Dir Bla 32	***	200
Vat Dyes (vatted):			
Indanthren ® Yellow 5GF	Vat Ye 46	40	89
Brilliant Pink RB	Vat Re 1	10	21
Blue RS	Vat Bl 4	25	54
Dark Blue BOA	Vat Bl 20	30	62

* Experimentally determined: dyeing with 0.5% dye, Co mercerized, liquor ratio 1:20, temperature 60 °C, 10 g/l commun salt

** Calculated over described algorithm

*** Not determined

As mentioned before, the plot of calculated adsorption values Adsrel against experimentally determined substantivity values shows a most interesting curve (Graph 1). All dyes are located with little deviations only on that curve, not depending on dyestuff type/class, molecular basic structure type or molecular weight. This indicates that the developed algorithm is pretty suitable indeed to calculate substantivity/adsorption of water soluble cellulose dyestuffs, if the chemical constitution is known. Anyway it must be mentioned once again that the algorithm is just suitable to compare dye items with each other under standardized conditions. Concerning the dependency from salt concentration and salt type, temperature, pH value, cellulose type and in case of different dyeing depths and dye combinations additional studies are useful.

Benefit of the Calculatoric Substantivity Determination for Research

Dyestuff research people get an option to predict/evaluate any requested cellulose substantivity over the algorithm in a simple way just over a tailor made change of molecular constitution, without the necessity of large lab trials.

a) Substantivity of a dyestuff can be increased (mainly for exhaust application) or deminished (mainly for continuous application) just by a variation of hydrophilic substituents.

Example:

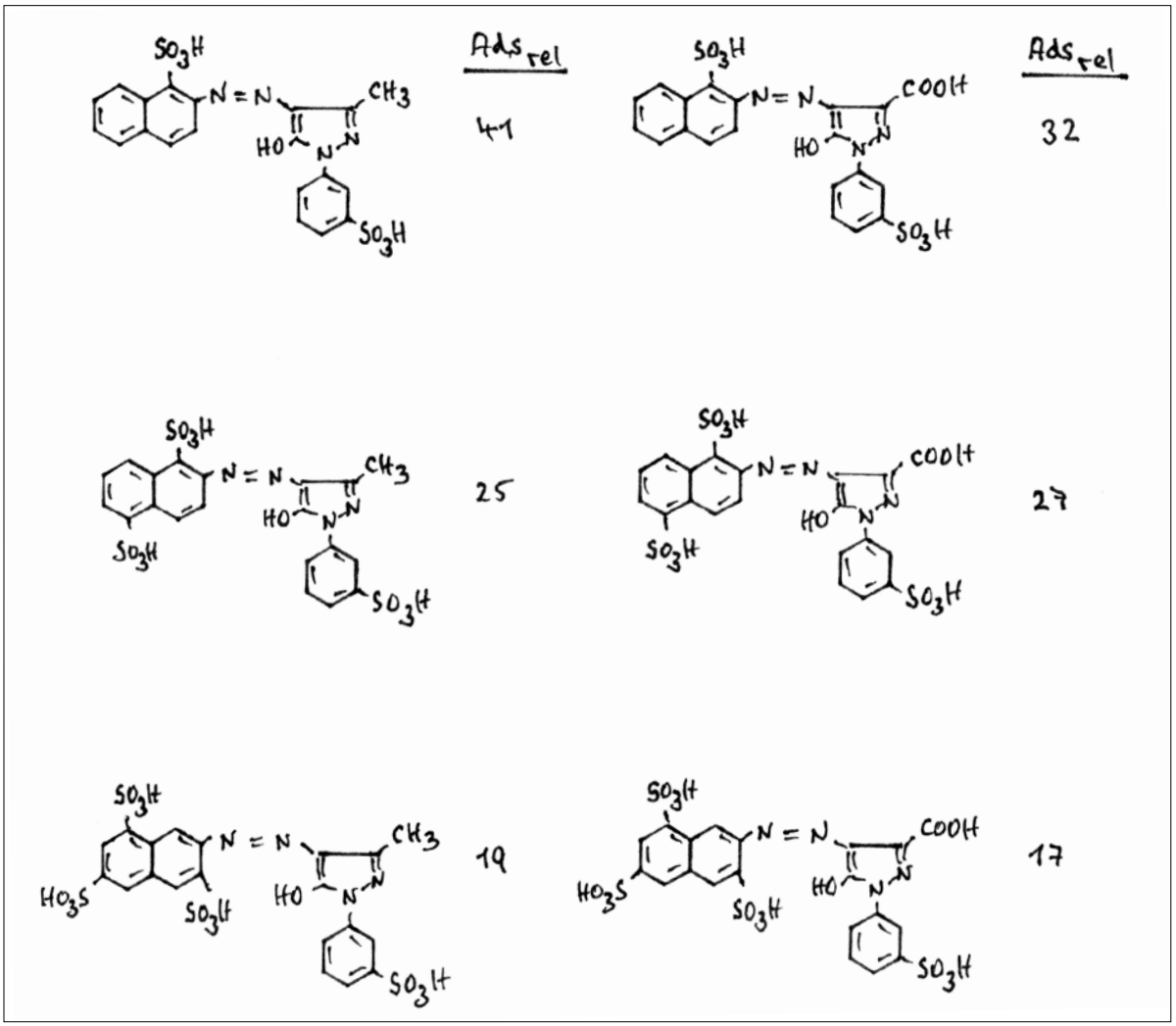

b) Another optional target can be calculated/predicted as well: Any sterically caused twisting within a dyestuff chromophor is leading to a diminished cellulose substantivity, because a disturbed planarity is influencing π electron cloud/density.

Example:

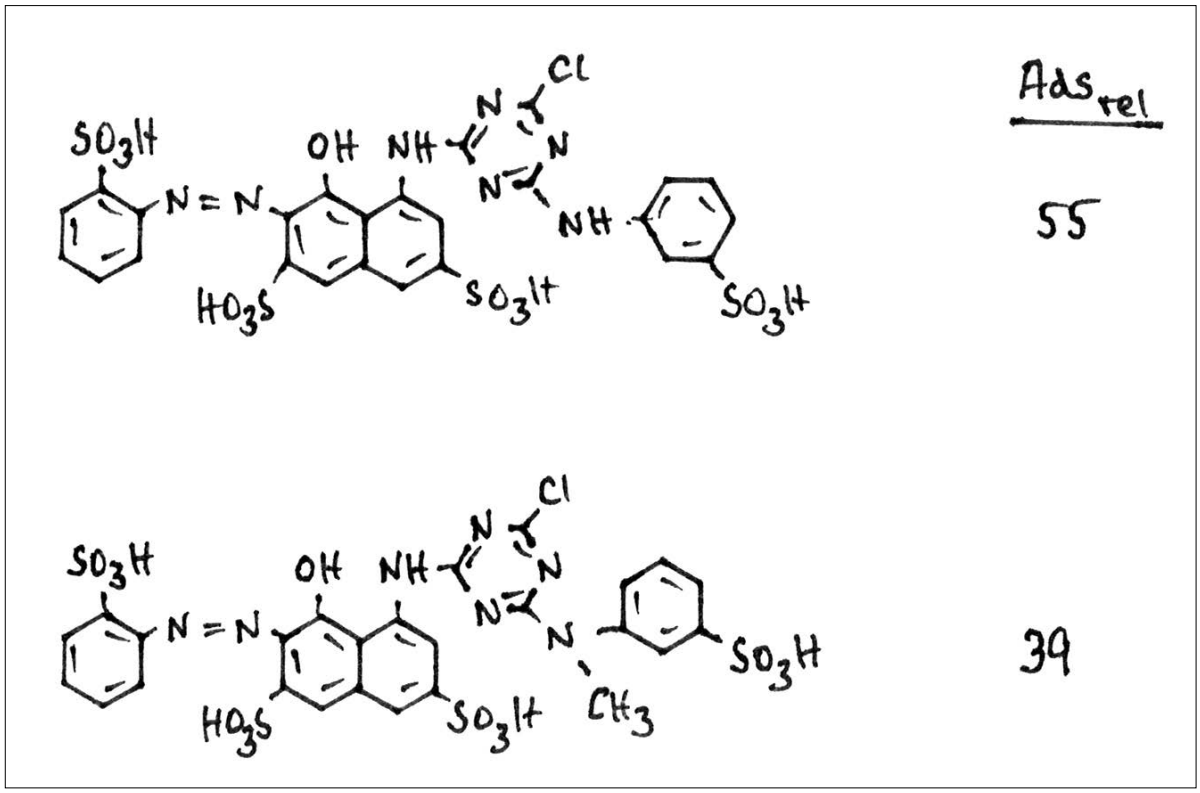

c) In case the dye molecule is bearing 2 separate (not fully conjugated) chromophores, substantivity is remarkably decreased. In such a non-planare molecule the π electron cloud at the "left hand side" and at the "right hand side" has to be calculated separately and then summed up. Anyway the hydrophilic substituents have always to be taken into account for the complete molecule (left plus right hand side).

Example:

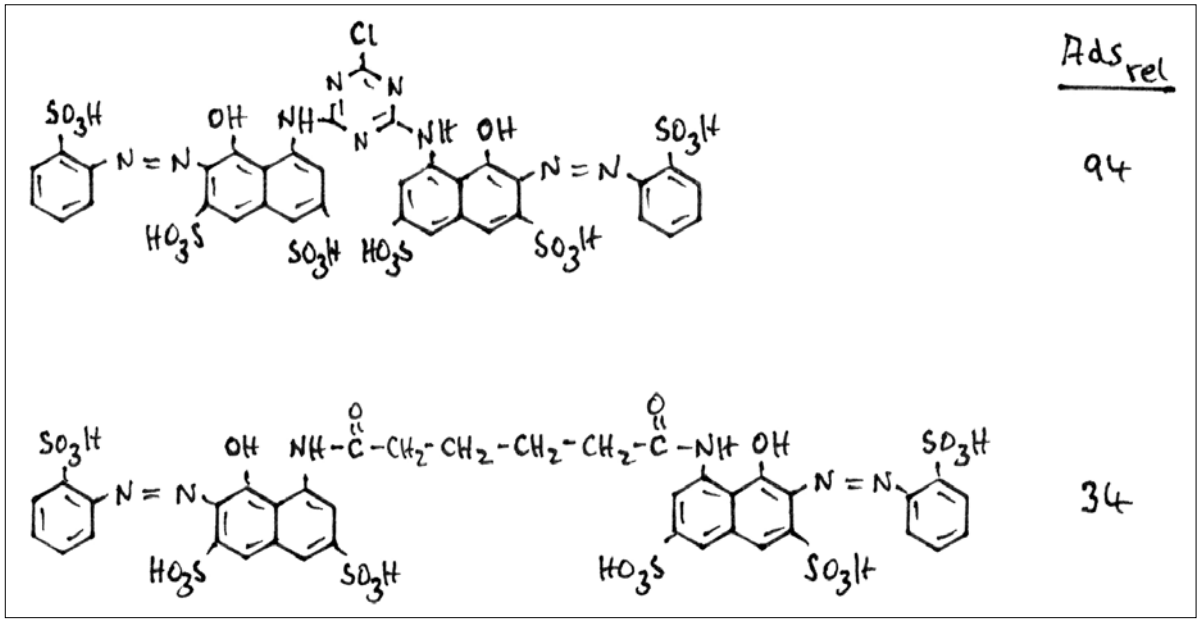

Benefit of a Calculatoric Substantivity Determination for Applicational Practise

It has already been mentionned, that the discussed Adsrel values are only suitable for the comparison from dye item to dye item under standardized conditions.

Of course dyeing practise offers and utilizes a number of options to make substantivity level of all dyes according to applicational necessities, e. g. through salt concentration in dyeing bath or temperature etc.

From a physical-chemical viewpoint the salt impact makes that easily clear: In aqueous solution of a dye a dissociation according to following equation exists:

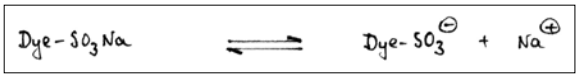

Without salt (NaCl, Na_2SO_4 etc.) the equilibrium lays on the right hand side. As a consequence, substantivity to cellulose is diminished very much. Contrarily an increased salt concentration pushes the equilibrium to the left hand side and consequently to a higher substantivity.

This is of course common knowhow, here just as an example. The influence of salt concentration, salt type, temperature, pH value, cellulose type, dyestuff amount (depth target), dye combinations, time program (diffusion behaviour) has to be considered on top respectively separate.

In practice the large majority of textile dyes are carried out as combinations, even trichromatic ones. The combination partners are adsorbed substantively in amount relation of basic dyeing recipe only in case, they possess all (nearly) same molecular substantivity. If this is not the case, stronger adsorbing dye(s) do/does occupy cellulose preferentially, the weaker adsorbing dye(s) is/are suppressed. In exhaust procedure light shades are not really sensitive in this sense. But medium and deep shades may suffer extremely from described problem. In continuous dyeing (padding) non-optimal combinations may lead to a non-acceptable shade tailing.

A real wish directed to dyestuff suppliers would be an indication of calculated or experimentally determined substantivity values for every dye should be published in commercial shade cards for to take conclusions and to avoid the described problems.

It's interesting to observe that since a few years dye mixtures are offered in the market, which consist of components with nearly same cellulose substantivity/ Adsrel values.

Example: A Dark Blue consisting of C. I. Reactive Blue 19 and Black 5, both having an Adsrel value of about 60.

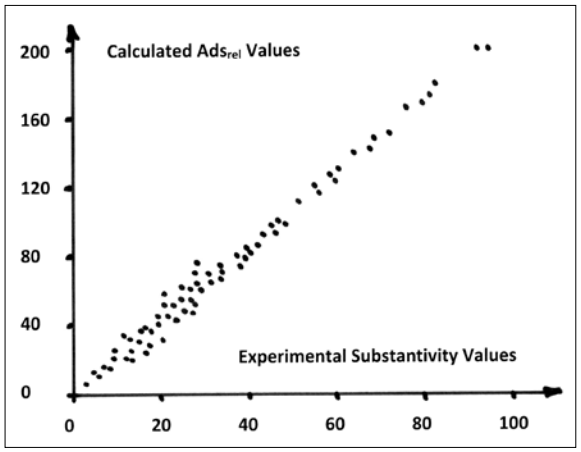

Graph 1: *Correlation of calculated Ads_{rel} values with experimentally determined substantivity values for more than 50 dyestuff items (different dye classes)*

Conclusions

The developed algorithm for calculation of relative, dye-specific adsorption of water-soluble cellulose dyes releases in a sufficiently precise way Adsrel values, close to experimental substantivity findings. This is not really a surprise if cause and molecular interdependences are considered.

References

[1] P. W. Atkins, Phys. Chemistry (1998)
[2] I. Langmuir, Surface Chemistry (1932)
[3] H. Sumner, J. Society of Dyers and Colourists (1986), 102 (10), 301-305
[4] Bae Sook Hoe et al, Dyes and Pigments (1997), 34 (1), 37-55
[5] S. Timofei et al, Dyes and Pigments (2000), 47 (1-2), 5-16
[6] M. Haehnke, Melliand Textilberichte (2009), 1-2, 42-45
[7] M. Haehnke, Lenzinger Berichte (2013), 91, 23-29

Possibilities for Efficiency Improvement of the Lyocell Process – Effects of Molecular Mass and Molecular Mass Distribution

Birgit Kosan, Frank Meister and Katrin Römhild

Thüringisches Institut für Textil- und Kunststoff-Forschung e.V., Breitscheidstr. 97
D-07407 Rudolstadt, Germany
Phone: (+49) 3672 379 220, Fax: (+49) 3672 379 379, e-mail: kosan@titk.de

Abstract

The effects of the average degree of polymerisation and of the molecular weight distribution of pulps on Lyocell process parameter were studied. These pulp properties delimit applicable cellulose concentrations, especially with regard to the dissolution and shaping steps.
In the case of polymer solution processes, the applicable polymer concentration is the decisive factor for the economic efficiency of the whole process. Other than in melt spinning processes, significant lower space-time yields are strongly dependent on the used polymer concentration in the case of solution spinning processes.
The rheological characteristics of cellulose dopes are an important criterion both in the dissolution and the shaping step, respectively. Especially the dopes viscosity level is a significant factor because of the necessary temperature limits at the use of NMMO. Different Lyocell pulp grades were tested at initial state and after DP-reduction by acid degradation, grinding processes as well as pulp mixtures with respect to applicable cellulose concentrations and achievable fibre properties. The investigations demonstrated, that a reduction of the DP level of the initial pulps by 80 units permitted an improvement of the dope concentration for 2% at comparable zero shear viscosities, whereby a secure shaping into cellulose fibres with stable fibre properties was possible applying usual spinning conditions.
The results of the investigations demonstrate that a moderate DP reduction by acidic pulp pre-treatment or grinding permits the use of increased cellulose concentration in the dissolution and in the spinning step but without any improvement of the mechanical fibre properties.

Introduction

The direct dissolution process using N-methylmorpholine-N-oxide monohydrate (NMMO) is a technology for dissolution and shaping of cellulose, established in the market.[1] The solvent is non-toxic and nearly completely recyclable.[2] But in the case of the application of polymer solution processes, the applicable polymer concentration is the decisive factor for the efficiency of the whole process. Compared to melt spinning processes, only significant lower space-time yields are possible in the case of solution spinning processes depending on the suitable polymer concentration.

At cellulose shaping in NMMO, applicable polymer concentrations are significantly influenced by the molecular mass and the molecular mass distribution of the pulp used. Currently the Lyocell process for the production of cellulosic staple fibres normally applies pulps that average degrees of polymerisation (DP) lies in the range of 500 to 650. Because of the rheological properties of the polymer dopes and the restricted shaping temperatures, the suitable polymer concentration today is limited to about 12 up to 15 wt-%.[3]
An improvement of cellulose concentrations could significantly permit to increase the efficiency of the Lyocell

Table 1: *Conditions of acid treatment and DP_{Cuoxam} of the treated pulp samples.*

Pulp sample	Treatment conditions	DP_{Cuoxam} after acid treatment
M-584	60 min at 60°C	415
S-510	60 min at 60°C	421
S-510	60 min at 60°C	437
S-510	120 min at 65°C	361
S-510	120 min at 80°C	250

process. For that reason, the influence of a decrease of the average DP of pulps for dissolution and shaping in NMMO on applicable cellulose concentrations, the producible solution states and the spinning conditions as well as the attainable fibre properties should be determined.

Materials and Methods

The investigations were carried out using dissolving eucalyptus pulp (S-510), cotton linters pulp (M-584) as well as microcrystalline cellulose (Avicel-173). The determined analytical data of the pulp are listed in table 2.
N-Methylmorpholine-N-oxide (NMMO) was used as 50 wt-% aqueous solution, manufactured and supplied by BASF, without any further pre-treatment.
All other used chemicals were obtained in analytical grade and HPLC-grade for SEC measurements, respectively and were used without any further pre-treatment.

Applied Methods for DP Reduction of the Used Pulps

DP reduction of the used pulps was carried out by acidolysis using sulphuric acid. For that purpose, the pulp samples were disintegrated using Ultra-Turrax tool and then treated with 5% sulphuric acid at liquor ratio of 1:20 over 60 minutes at 60°C and over 120 minutes at 65 and 80°C, respectively. The used treatment conditions and determined DP-values are listed in table 1.
Also grinding processes were used for DP reduction. The pulp sample S-510 was ground using a FRITSCH planetary ball mill Pulverisette-5 with zirconium oxide balls. Grinding times were 75 min at 200 revolutions per minute. The DP_{Cuoxam} of the ground samples was decreased to 401 and 421, respectively.
Furthermore a DP reduction of the used pulp for the dope preparation was generated by mixing of pulp samples S-510 and M-584 with different amounts of low DP-cellulose Avicel-173.

Preparation of Cellulose Dopes

The preparation of cellulose dopes was carried out using a special vertical kneader system, linked with a RHEOCORD 9000 (HAAKE). Temperature, torque moment and revolutions per minute (rpm) vs. time were recorded on-line. The dopes were prepared, starting from an aqueous suspension of the pulp in 50 wt.-% aqueous NMMO, by removal of the excess water at elevated temperatures, higher shearing stress and low pressure during the dissolution processes (80 - 95°C mass temperature, 800 - 40 mbar pressure, 5 - 20 rpm). 0.5 wt-% propylgallate, with regard to cellulose, were used for stabilisation of the NMMO solutions. After the finishing of water removal (achieving a NMMO monohydrate state), an after-dissolution step (60 min, 90°C mass temperature, 250 mbar) followed for homogenisation of the prepared dope.

Table 2. *Selected data of cellulose characterisation by capillary viscosity (DP_{Cuoxam}) and SEC (M_w, M_n and M_w/M_n).*

Cellulose	Sample	DP_{Cuoxam}	M_w	M_n	M_w/M_n
Virgin cellulose samples:					
Eucalyptus	S-510	510	169,248	54,199	3.1
Cotton linters	M-584	584	219,915	74,715	2.9
Microcrystalline cellulose	Avicel-173	173	40,683	16,748	2.4
Eucalyptus pulp S-510 after DP reduction by:					
H_2SO_4 degradation	S(H_2SO_4)-361	361	123,650	37,635	3.3
Ground by ball-mill	S(ground)-421	421	146,563	41,085	3.6

Spinning Trials

Spinning trials were carried out by dry-wet spinning experiments for preparation of staple fibres of about 1.7 dtex fineness using a laboratory piston spinning equipment, which is described in former publication.[4] Spinning nozzles, containing 30 holes with capillary diameters of 100 μm were used for all spinning experiments. The spinning temperatures were selected in each case according to the rheological properties of the used cellulose dope.

Cellulose Characterisation

The virgin and DP reduced pulp samples as well as the cellulose samples regenerated from the dopes and from the spinning tests were characterised by capillary viscosity for determination of the average degree of polymerisation (DP_{Cuoxam}) and by size exclusion chromatography (SEC) for the investigation of the molecular weight distribution (MWD). The details of this cellulose characterisation were described in former publication.[5]
The results of cellulose characterisation of the virgin pulps and selected DP reduced samples are pictured in table 2 and figures 1 and 2.

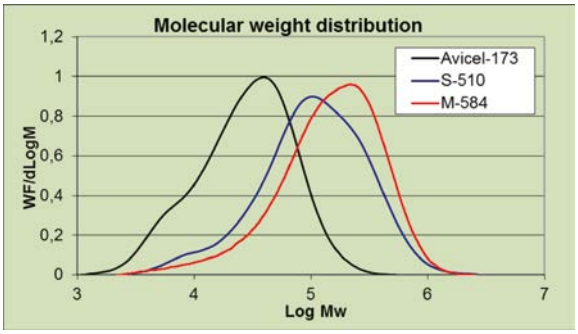

Figure 1. *Molecular weight distributions (MWD) of the virgin samples.*

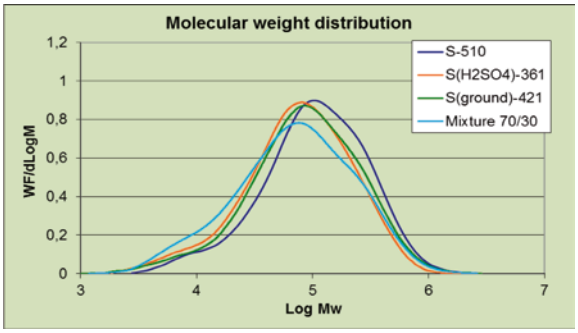

Figure 2. *MWD of DP-reduced samples using pulp S-510 (H_2SO_4 degraded sample, ground sample as well as mixture between S-510 / Avicel-173 (70/30)* compared with the virgin sample S-510.*

* The MWD of the blended sample is calculated from the SEC-measurements of the virgin cellulose samples.

Analytical Characterisation of Cellulose Solutions

Optical characterisation of cellulose solutions was carried out by means of polarisation microscopy (ZEISS Axiolab). The rheological measurements were realised as described following. The determination of the solids contents in the solutions was performed by means of weighing precipitated films, after exhaustive solvent extraction and drying.

Rheological Characterisation

The rheological characterisation of cellulose solutions was performed using a rheometer HAAKE MARS with cone / plate measuring system (4° angle geometry) and electrically heated cone & plate unit with active cone heater.
Zero shear viscosities were calculated from creep attempts in the rotation mode at shear stress of 90 Pa. The determined cellulose solutions showed significant viscoelastic behaviour. A characterisation of the viscoelastic properties was realised in the oscillation mode. Oscillation tests were carried out as frequency sweeps (0.046 – 14.7 Hz, deformation: 0.07) at different temperatures (60 / 85 / 110°C). WLF-transformation was used for calculation of master curves and relaxation spectra at 85°C reference temperature. This method permits an interpolation of the frequency / angular rate range over several decades and is an evaluated method for the determination of viscoelastic properties of polymer solutions. Details of the rheological dope characterisation had been described in former publications.[6,7,8,9]

Fibre Characterisation

The textile-physical fibre parameters were determined according to the following methods:

- fineness according to DIN EN ISO 1973,
- tensile strength and elongation according to DIN EN ISO 5079 and
- loop tenacity according to DIN 53843, part 2.

Results and Discussion

In a first study the effect of molecular mass and MWD of the pulps on applicable dope concentrations, achievable dope properties and their spinning behaviour as well as attainable fibre properties were determined. For this purpose, cellulose dopes with different cellulose concentrations were prepared using virgin pulp samples S-510 and M-584 as well as pulp samples which DP's were reduced by acid treatment, grinding and blending with Avicel-173. Figure 3 demonstrates zero shear viscosities of prepared cellulose dopes depending on pulp properties and the cellulose

concentrations. The pictured graph results from dopes which were prepared by using virgin pulp sample S-510 and DP-reduced samples from this pulp. The sample names containing "(H2SO4)" are acid treated samples. The numbers at the end stand for the DP of the treated pulp samples. The blend of S-510 and Avicel was used with a mass ratio 70/30. The calculated DP of the mixture sample results in 410.

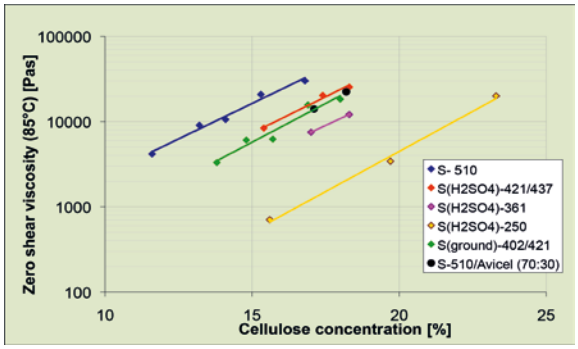

Figure 3. *Zero shear viscosities of cellulose dopes at 85°C.*

The zero shear viscosities of dopes using the virgin pulp S-510 have values between 4,000 and 30,000 Pas at cellulose concentrations from 11.6 up to 16.8 wt-%, respectively. In logarithmic scale, the zero shear viscosities show nearly linear dependence from the pulp concentration used. DP-reduction of about 90 units from 510 to around 420 in the pulp causes lower zero shear viscosities of the dopes independent from the used method for DP-reduction. About 2 to 3% higher pulp amounts could be used in dopes, if the shear viscosities would be keeping constant. A stronger reduction of the DP leads to further shifting of the curves to higher cellulose concentrations.

The master curves (Fig. 4) and weighted relaxation time spectra (Fig. 5) illustrate the influence of the DP-reduction of about 90 units on further rheological dope properties compared with a 3% lower concentrated dope of the virgin pulp. The data of complex viscosities as well as the storage and loss moduli of the dopes using DP-reduced pulps with cellulose concentrations of around 18 wt-% are very compatible with the values of 15.3 wt-% dope from the virgin pulp samples. Small differences exist especially at high angular velocities.

The same trend occurs also for the weighted relaxation time spectra. Small differences show the dope using ground pulp sample, which are justified also in the lowest dope concentration of 18.0 wt-% and the lowest starting DP of the pulp sample of 402. The determined DP-values of the precipitated cellulose directly after the dissolution process were 482 in the case of the virgin pulp, 422 for the H_2SO_4-precipitated pulp sample, 388 for the dope using ground pulp and 391 for the mixture of S-510 / Avicel.

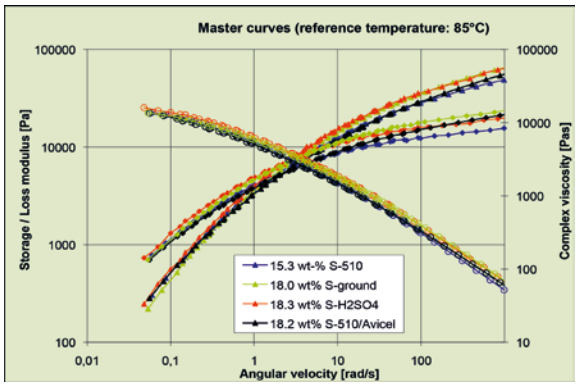

Figure 4. *Master curves of dopes from DP-reduced pulp (starting DP between 402 and 437) compared with a lower concentrated dope from the virgin pulp.*

Triangles: Storage moduli
Squares: Loss moduli
Open circles: Complex viscosities

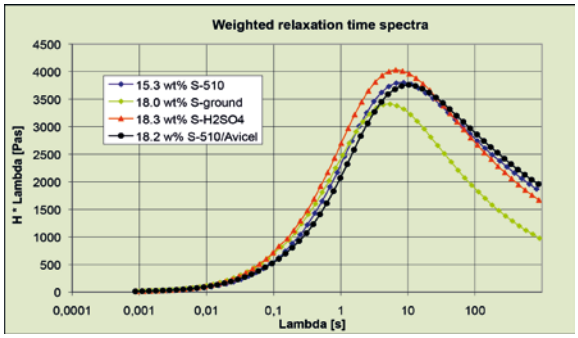

Figure 5. *Weighted relaxation time spectra of dopes from DP-reduced pulp (starting DP between 402 and 437) compared with a lower concentrated dope from the virgin pulp.*

A dry-wet spinning of the dopes, prepared from DP-reduced pulp samples, was possible with good spinning stabilities and was very comparable to the spinning behaviour of dopes using virgin pulp samples using lower cellulose concentrations. The trends in achieved fibre properties are pictured in figure 6. They are diagrammed depending on the used pulp and the cellulose concentrations.

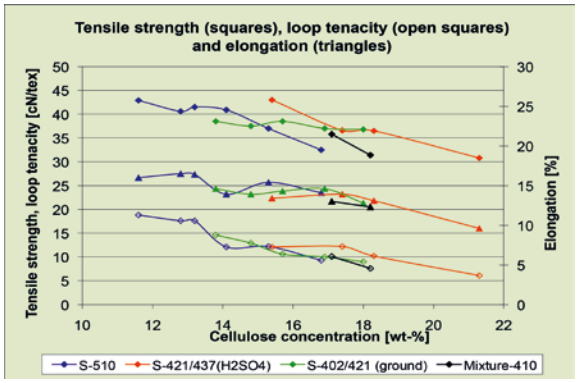

Figure 6. *Fibre properties depending on the used pulp and the cellulose concentration of the dope.*

Table 3. *Selected data of fibre characterisation by capillary viscosity (Fibre-DP) and SEC (M_w, M_n and M_w/M_n).*

Fibre sample from shaping of:	Fibre-DP	M_w	M_n	M_w/M_n
12.8 wt-% S-510	465	194,122	62,725	3.1
17.4 wt-% S (H_2SO_4)-421	405	112,378	46,866	2.4
16.9 wt-% S (ground)-421	404	124,645	44,219	2.8
17.1 wt-% S-510/Avicel	392	172,037	38,881	4.4

The virgin pulp S-510 permitted the preparation of staple fibres with tensile strengths of 42.9 – 40.6 cN/tex, fibre elongations of 16.5 - 13.9% and loop tenacities of 18.8 – 12.1 cN/tex using cellulose concentrations between 11.6 and 14.1 wt-%. A further increase of the cellulose concentration resulted in a decrease of the fibre properties, in particular in the case of tensile strength.

A reduction of the DP-level of the used pulp of about 420 by acidic degradation or grinding processes allowed the preparation of staple fibres with comparable fibre properties using cellulose concentrations up to 18.3 wt-%. The usage of pulp blends (S-510 / Avicel) with resulting comparable DP leaded to slightly lower values of fibre properties, especially at the tested higher cellulose concentration of 18.2 wt-%.

However, when using of the pulp mixture, the DP of the available fibres was comparable to the fibres, prepared from the pulp samples, degraded by acidic treatment or grinding processes, but the MWD of the fibres differed significantly (table 3).

The effect of a further DP-degradation of the used pulps on the resulting fibre properties was further studied by acidic degradation of the virgin pulp S-510 decreasing to DP-levels of 360 and 250 (figure 7).

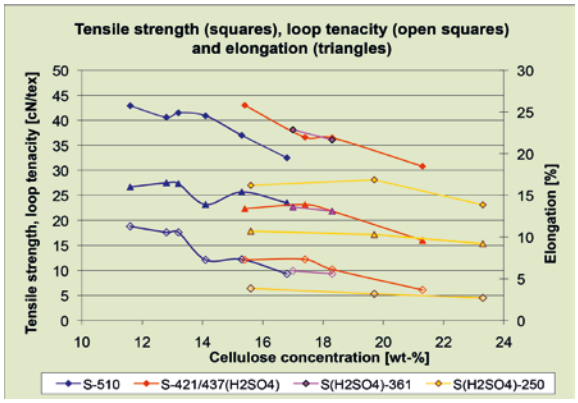

Figure 7. *Fibre properties depending on the DP-level of the pulp and the cellulose concentration of the dope.*

The obtained fibre properties illustrate, that the strong pulp degradation to DP of 250 permitted a further increase in cellulose concentration for shaping, but resulting in a significant degrease of the obtainable fibre properties at all cellulose concentrations determined.

Comparable investigations were also carried out using virgin cotton linters pulp sample M-584. The virgin pulp was shaped at cellulose concentrations between 11.8 and 14.9 wt-% (figure 8). The fibres showed high tensile strengths, especially using cellulose concentrations of 11.8 and 13.8 wt-%. A further increase of cellulose concentration to 14.9 wt-% caused a slight decrease of the fibre properties. Also, the viscosity level of the dope increased significantly. The zero shear viscosities of the dopes (measuring at temperatures of 85°C) are illustrated in figure 8 at x_2-axis. An acid DP-reduction of the pulp to DP value of 415 permitted the shaping of a dope with increased cellulose concentration (16.9 wt-%) but significantly lower zero shear viscosity and resulted into fibres with comparable or slightly reduced mechanical properties.

The use of a pulp mixture of the virgin pulp M-584 and Avicel-173 for adjustment of a comparable DP-level of 415 provides fibres with further reduced mechanical properties.

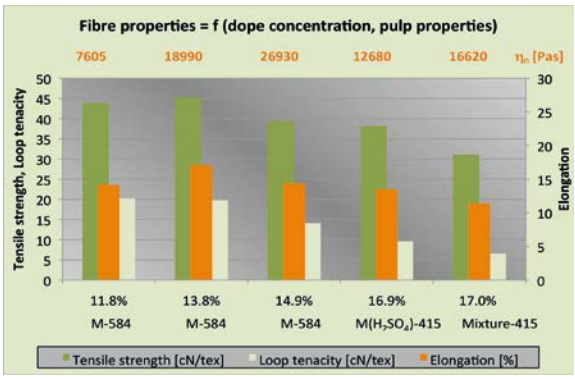

Figure 8. *Properties of fibres, prepared from cotton linters pulp samples with different DP.*

Conclusions

The studies could demonstrate that applicable cellulose concentrations for the dissolution and shaping of cellulose in NMMO are limited by the DP and MWD of the used pulps because of resulting rheological dope

characteristics and the in maximum attainable fibre properties. The exceedance of an optimal dope concentration causes a decrease of the fibre properties at dry-wet spinning process. This should be caused by worse dissolution states at enhanced concentration on the one hand and insufficient mobility of the polymer chains when shaping at increased polymer concentration on the other.

The carried out investigations provided the experience, that a DP-reduction of the pulp by about 80 units permits an improvement of the cellulose concentration for about 2% at comparable zero shear viscosities of the dopes. The shaping by dry-wet spinning using such pulps with moderate reduced DP provided fibres with comparable tensile strengths and only slightly reduced elongations and loop tenacities at 2% higher cellulose concentrations.

The used kind of the DP reduction (acidic degradation, milling) didn't show significant differences.

However, a blending by low molecular pulp samples is unfavourable because of a lower dope quality (undissolved particles) and higher amounts of short-chain polymer segments.

Nevertheless, the results of the investigations demonstrated, that a moderate DP reduction permits an increase of the cellulose concentration in the dissolution and in the spinning step for the improvement of the whole process efficiency.

Acknowledgements

These works were financially supported by the German Federal Ministry of Economics and Energy (BMWi No. MF100038). The authors thanks for the granted support.

References

[1] H. Harms, Potentiale einer neuen Fasergeneration, Lenzinger Berichte 81 (2002) 27-34

[2] W. Kalt, B. Zauner, Das Lenzing Lyocell Projekt – Start in ein neues Zeitalter der großtechnischen Zellulosefaserherstellung in Europa, Lenzinger Berichte, 80 (2001) 10-12

[3] C. Michels, B. Kosan, Das Lyocell-Verfahren – gegenwärtige Leistungsgrenzen aus stofflicher und technologischer Sicht, Lenzinger Berichte, 80 (2001) 13-21

[4] B. Kosan, C. Michels, F. Meister, Cellulose, 15 (2008) 59-66

[5] B. Kosan, K. Schwikal, F. Meister, Effects of pre-treatment and dissolution conditions for improved solution and processing properties of cellulose in ionic liquids, Lenzinger Berichte, 90 (2012) 76-84

[6] C. Michels, Das Papier, 1 (1998) 3-8

[7] C. Michels, B. Kosan, Chemical Fibers Int., 50 (2000) 561–566

[8] C. Michels, B. Kosan, Lenzinger Berichte, 82 (2003) 128–135

[9] C. Michels, B. Kosan, Lenzinger Berichte, 84 (2005) 62–70

Comfort Meets Functionality: Skin-Friendly Solutions for Adult Incontinence

Martin Haeubl[1], Gerlinde Holzleithner[1], Shayda Rahbaran[1], Jutta Klinger[1], Elisabeth Stanger[1], Christine Wolf[2] and Michaela Dvorzak[3]

[1] Lenzing AG, Werkstrasse 2, 4860 Lenzing, Austria
Phone: +43 7672 701 3488; Email: m.haeubl@lenzing.com
[2] Hy-Tec Hygiene-Technologie GmbH, Schillerstraße 14, 42781 Haan, Germany
[3] Joanneum Research Forschungsgesellschaft mbH, Leonhardstraße 59, A-8010 Graz, Austria

Abstract

Product performance, sustainability and skin friendliness are important aspects in almost all segments of the hygiene market. Offering a unique combination of all of these functions is the foundation, based on which TENCEL® fibers already have a proven track record in the baby wipes market in the US. In this study Lenzing AG will present the latest developments regarding the performance of modified TENCEL® fibers in hygiene applications.
Therefore the beneficial properties of TENCEL® fibers within the hygiene market were systematically studied and new fields of interest were screened. Comfort and skin friendliness were specified as essential properties in the segment of pads for adult incontinence. Within this segment it turned out that the topsheet could be improved by the use of TENCEL® fibers. Due to the fact that topsheets are in direct contact with the skin, they are representing one of the critical factors for wearing comfort. This is the case because consumers associate the total product wearability with softness and touch of a pad surface.
Today the majority of topsheets is made from crude-oil based polymer materials (e.g. PP). Whereas these materials undoubtedly offer adequate liquid management options, there are clear indications that fabrics based on cellulosic fibers offer improved skin comfort. Additionally, nonwoven fabrics based on TENCEL® fibers offer consumers a discrete, textile-like product appearance and skin-feel, which is especially important if they conduct an active life style.

Introduction

Since 1967, PP 100% spunbond started to become the dominating material in topsheets of female hygiene and adult incontinence products and currently there are hardly any alternatives to this kind of products, which show similar performance. Topsheet materials containing cellulosic fibers have nearly been completely substituted by PP since that time although cellulosic fibers can offer improved comfort features next to a more textile like appearance of a pad's surface. Nevertheless, most cellulosic fibers have a higher wetback than PP and therefore a lower performance. As a consequence, the modified spunlaced TENCEL® fiber, a more hydr phobic cellulosic fiber, was invented to overcome this drawback. Due to the fact that this fiber combines the performance of PP 100% with the comfort of a cellulosic fiber, it is possible to use this kind of fibers in topsheet applications again. The consumer trial described in detail below was conducted to measure comfort and performance of this new product in comparison to a state of the art PP 100% spunbond topsheet.

Aims

The comfort and performance of disposable adult incontinence insert pads with an identical pad design, but two different topsheets were tested on women living in the community with stable moderate/heavy urinary incontinence.

Design and Methods

We conducted a double blinded, randomized, crossover trial comparing the performance and comfort of two different topsheets (PP 100% 14 g/m^2 spunbond vs. TENCEL® : modified TENCEL® 50:50 mixture 30 g/m^2 spunlaced) on an identical pad design (similar to TENA Lady Extra 4 droplets (SCA)). For better readability TENCEL® : modified TENCEL® 50:50 mixture 30 g/m^2 spunlaced is referred to as Lyocell* within the rest of this paper.

Figure 1. *Picture of the tested insert pad product; category Extra, 4 droplets (similar to TENA Lady Extra, 4 droplets)*

Recruitment of Participants

The inclusion and exclusion criteria for participants are shown in Table 1. The aim was to recruit participants who were already using products for moderate to heavy incontinence and had stable incontinence symptoms. In this trial, only women were included due to the fact that the chosen insert pad design was only optimized for this gender.

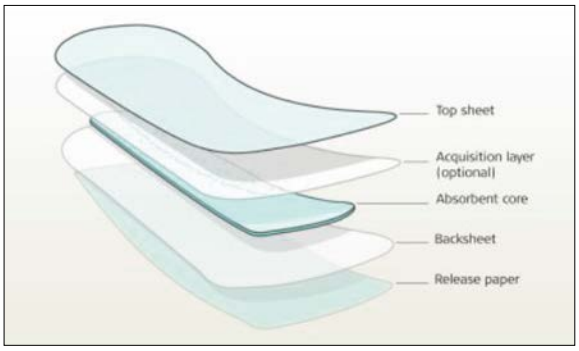

Figure 2. *Scheme of the design of the tested adult incontinence insert pad (ref. to: EDANA (European Disposables and Nonwovens Association, http://www.edana.org/images/default-source/default-album/maandverband2.jpg)*

Participants were recruited in the following ways:

1. According to a database from Hy-Tec GmbH potential testers were contacted in Germany, who have already participated in previous incontinence trials and who were using a specific pad design with a specific absorbency. These candidates were contacted by phone and an invitation letter.
2. Further recruitment was done by Hy-Tec GmbH via contacting adult incontinence support groups and advertisements in newspapers.

Study Process

After the potential participants had received the invitation letter and had signed the informed consent they had to fill in a questionnaire containing demographic data (age, size, weight, and waist), the brand and absorption range of their currently used insert pad and the amount of these pads used per day / night. The subjects

Table 1. *Inclusion and exclusion criteria.*

Inclusion criteria	Exclusion criteria
Adult women (>18 years)	Fecal incontinence
Able to manage everyday life situations	Terminal phase of an illness
Urinary incontinence	Resident in a home for elderly people or a community with professional care
Currently using absorbent products for moderate/heavy urinary incontinence	Prior (within last 4 month) or concomitant chemo- or radiotherapy
Willing to comply to study procedures	Dementia
Able to complete self-report questionnaires	Other trial or panel
Signed informed consent	

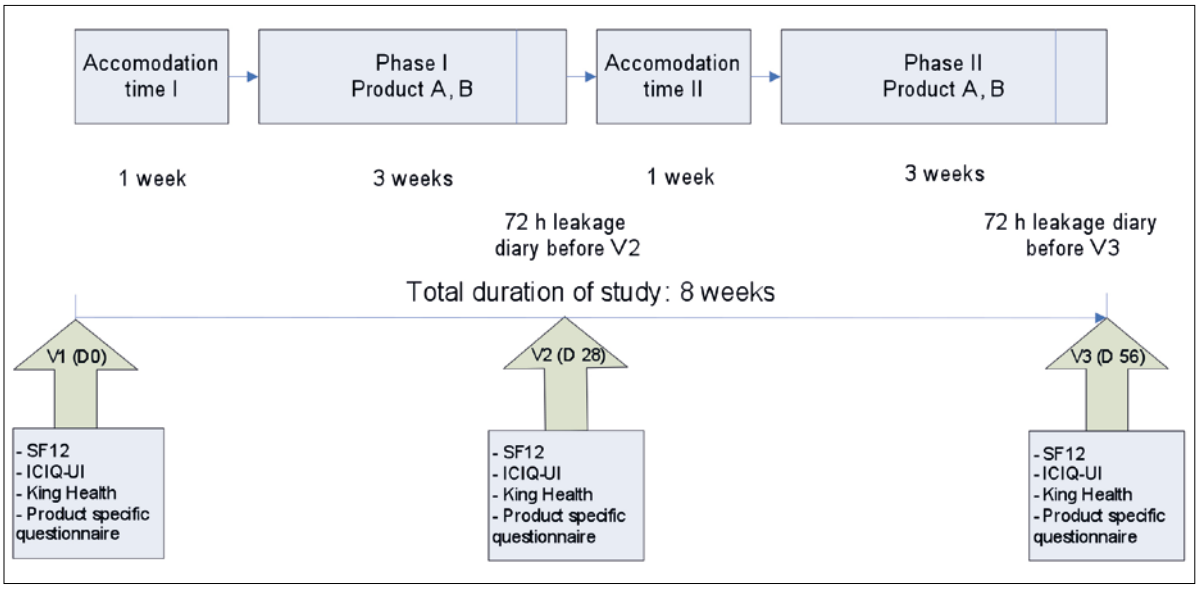

Figure 3. *Study scheme (adapted from the study designs described in [1], [2], [3], [6]); D = trial days.*

received the test pads in DEC-2013 and each individual started the trial on 12-JAN-2014. During the study the participants tested two kinds of insert pads, which had an identical design but differed regarding their topsheets. Both pad types were tested for 4 weeks each. Data was not collected during the first week of testing to avoid effects and bias that are only caused due to product change. Therefore only in week 2 - 4 and 6 - 8 the participants recorded the number of pads used per day / night and the fact whether or not leakage occurred (day / night). During the last 72 hours of each testing period the participants had to record the weight of each pad (g), the exact wearing time of each pad and whether or not leakage occurred (per each pad used). Next to that, quality of life (QoL) questionnaires were handed out to the participants at V1, V2 and V3 (Figure 3). The following questionnaires were used in this trial: SF-12, ICIQ-UI SF [4], and the King Health QoL [5] questionnaire.

Participant Monitoring and Data Management

All participants were monitored by Hy-Tec GmbH (Christine Wolf). Hy-Tec contacted all participants by email and telephone on a regular basis. This was also the procedure how queries were resolved. After all data was entered, all queries were resolved and source data verification was completed, the database was locked and the trial was unblinded for further statistical evaluation.

Analysis

Data were entered into Microsoft Excel and checked for accurate entry. The statistical analysis was conducted by Joanneum Research Forschungsgesellschaft mbH, Austria (Michaela Dvorzak) using the statistical software program R (www.r-project.org).

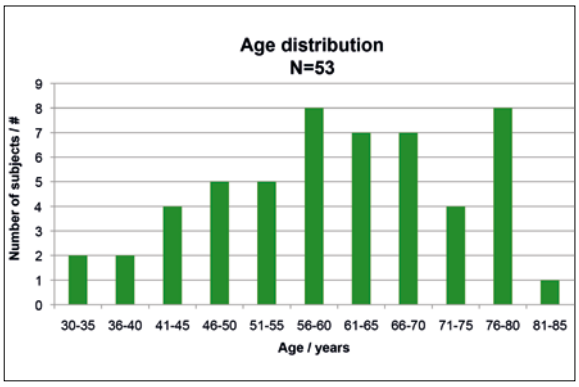

Figure 4. *Age distribution of participants*

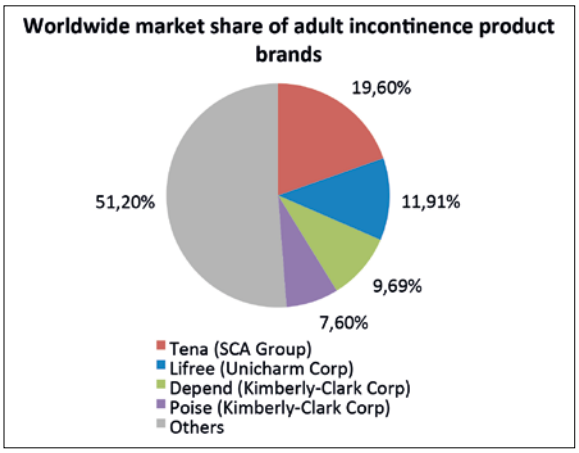

Figure 5. *Worldwide market share of adult incontinence product brands (ref. to Euromonitor 08_2014).*

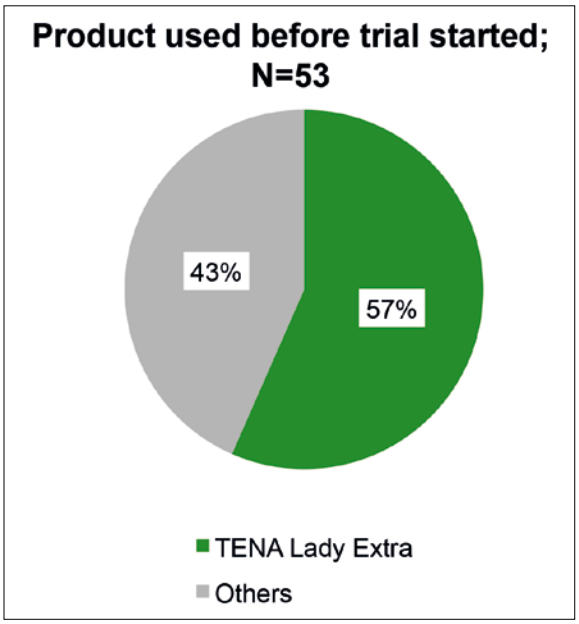

Figure 6. *Products used by participants before they entered the study.*

Results and Discussion

Participants' Characteristics

53 participants met the inclusion and exclusion criteria to start the product tests. All of these 53 participants were recruited in Germany by Hy-Tec GmbH and all of them were able to complete the trial.

Figure 4 displays the age distribution of the testers, whose mean age was 59.4 years. In addition to that, most of the participants (57%) used an insert pad from the brand TENA (SCA) which is the current worldwide leader concerning market share (Figure 5, Figure 6). Therefore it was possible to compare our test product with the adult incontinence insert pad that is currently mainly demanded by customers and is offering state of the art design and performance.

Evaluation of the Study Results

Before the trial started, the participants were asked to fill in the ICIQ-UI SF [4] questionnaire (V1) in order to evaluate the situations in which they were leaking urine. All incontinence related symptoms and their occurrence are shown in Figure 7. Multiple answers were possible. The outcome of the trial showed that the majority of participants had been suffering from leakage before they were able to reach the toilet, as well as incontinence induced by coughing or sneezing. Nocturnal incontinence as well as incontinence induced by physical exercising was among the top 5 as well. In addition to that, a high amount of participants was showing incontinence symptoms where no specific reason or trigger could be identified.

In Figure 8 and Figure 9, the mean number of products used per day and night is shown. It can be seen that more PP 100% pads were used in the 3 weeks testing period (3.9 pads per day) than with the Lyocell* mixture in the same time period (3.7 pads per day). The difference seen here is quite small. However, pairwise comparisons (based on Wilcoxon signed rank tests) confirmed that the number of used products during the day was significantly smaller for TENCEL®* compared to PP 100% (V=313.5, p=0.017). The same holds for the consumption of night products where significantly fewer products were used with Lyocell* compared to PP 100% (V=173, p=0.004). This is a clear indicator that the wearing time of pads with a Lyocell* topsheet was longer compared to a PP 100% topsheet. The reason for the lower consumption of the former product is based on the fact that all participants have been using their product since months or years and their pad consumption has already been optimized. Next to that they developed a feeling of trust and security while wearing this product and knew exactly, when they had to change it to avoid any leakage or discomfort. Another

reason for a lower consumption could be design specific difference between the former pad and the test pads.

Figure 10 and Figure 11 clearly show that the amount of urine, which was absorbed per pad at the time when it was exchanged, was definitely higher for the

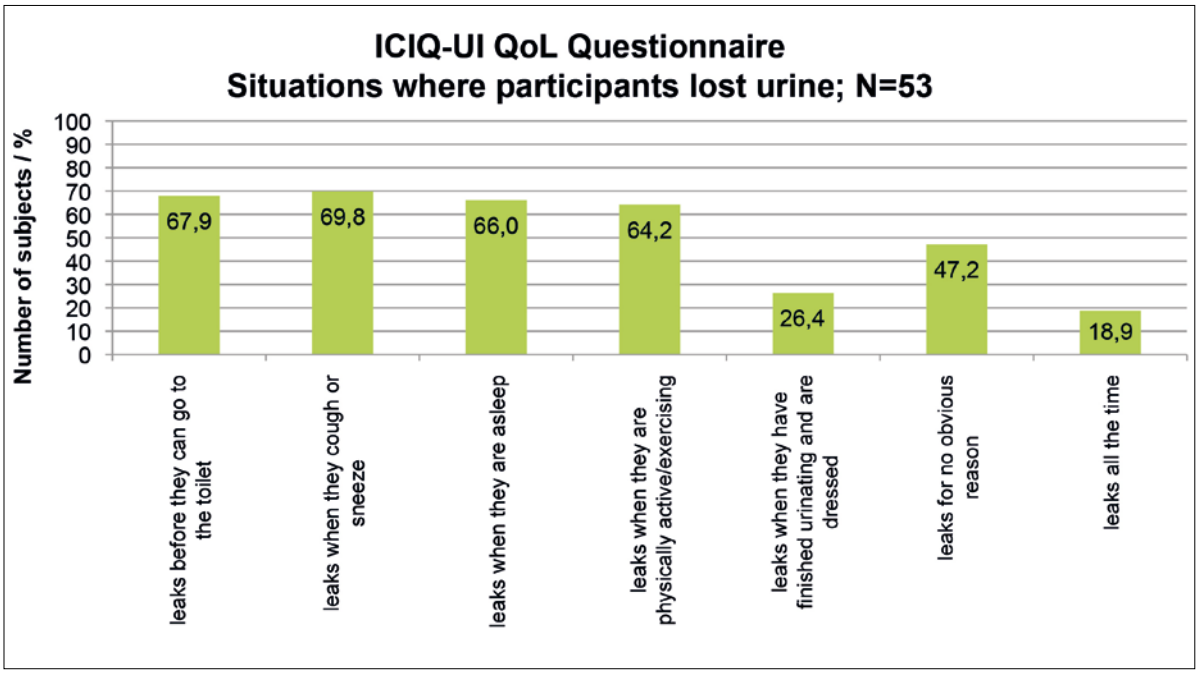

Figure 7. *Situations where subjects lost urine (ICIQ-UI QoL questionnaire).*

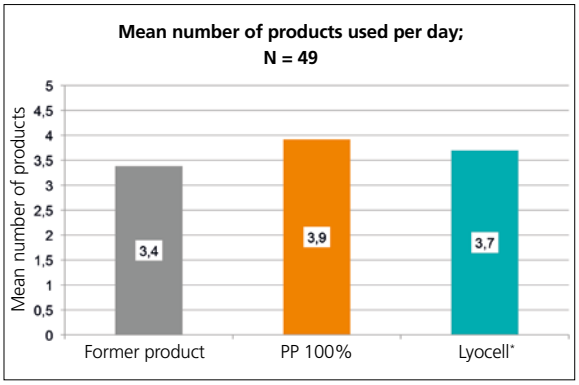

Figure 8. *Mean number of products used during daytime (4 subjects had to be removed due to incomplete data).*

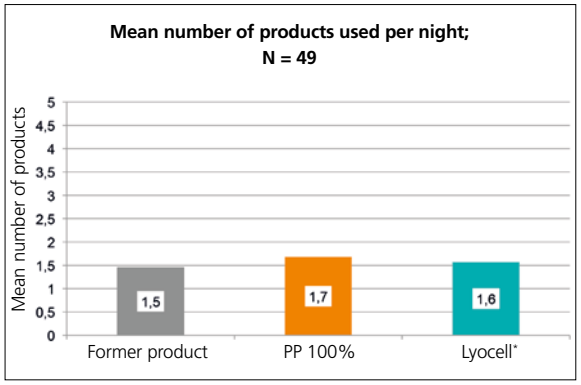

Figure 9. *Mean number of products used during nighttime (4 subjects had to be removed due to incomplete data).*

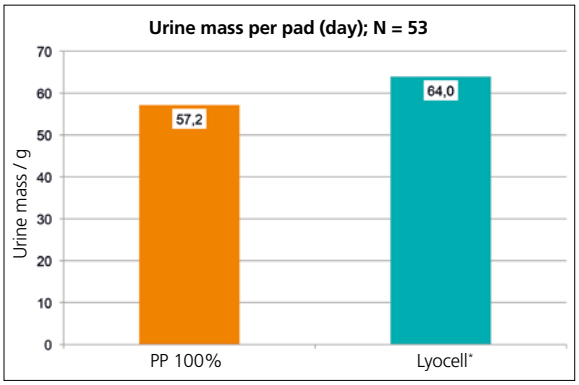

Figure 10. *Median urine mass per pad during daytime.*

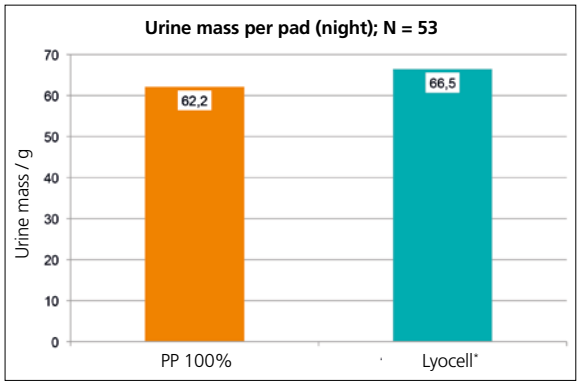

Figure 11. *Median urine mass per pad during nighttime.*

Lyocell* mixture than for PP 100%. The reason for that is the increased wearing time, which is shown in Figure 12 and Figure 13. The longer a pad is worn the more urine is absorbed. Figure 12 points out that the wearing time during daytime of a single pad is shifted from shorter time intervals (100 - 200 min per pad) to longer ones (225 - 275 min per pad). So the question has to be asked why the participants were wearing the pad with the Lyocell* mixture for a longer time than that with PP 100%. One hypothesis could be improved

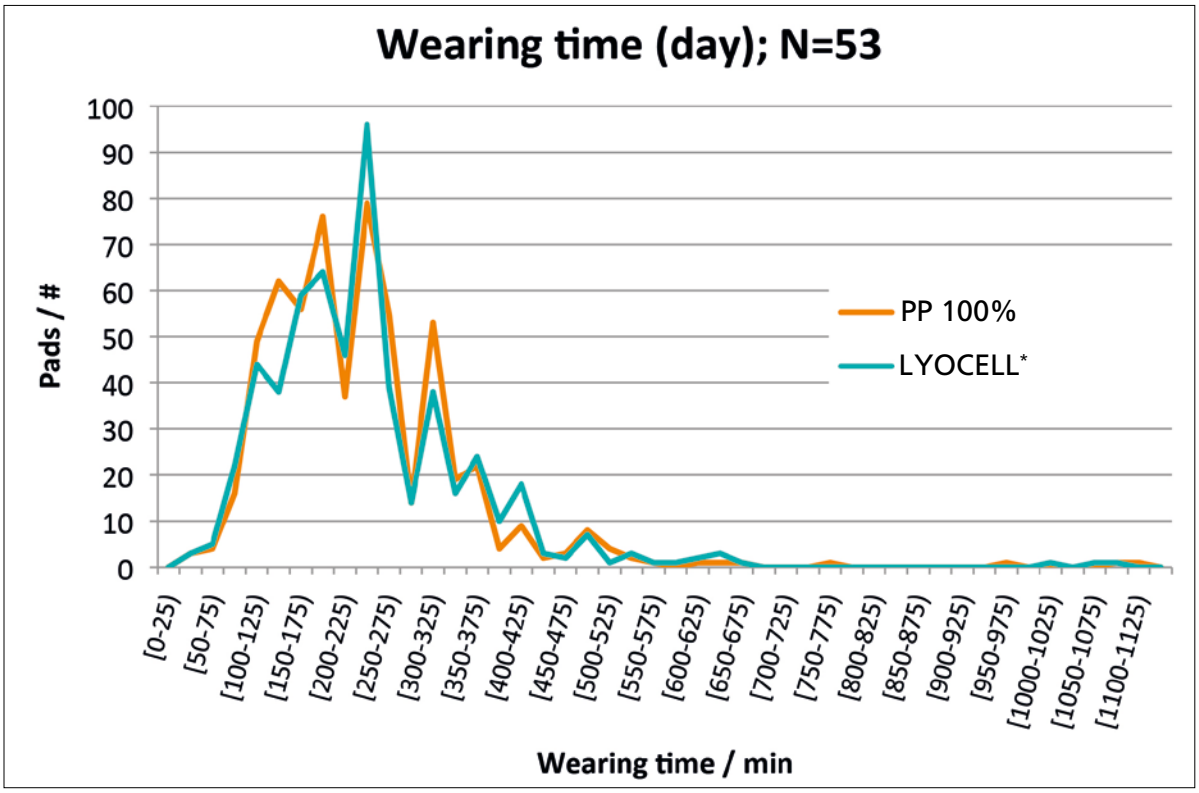

Figure 12. *Wearing time of pads during daytime.*

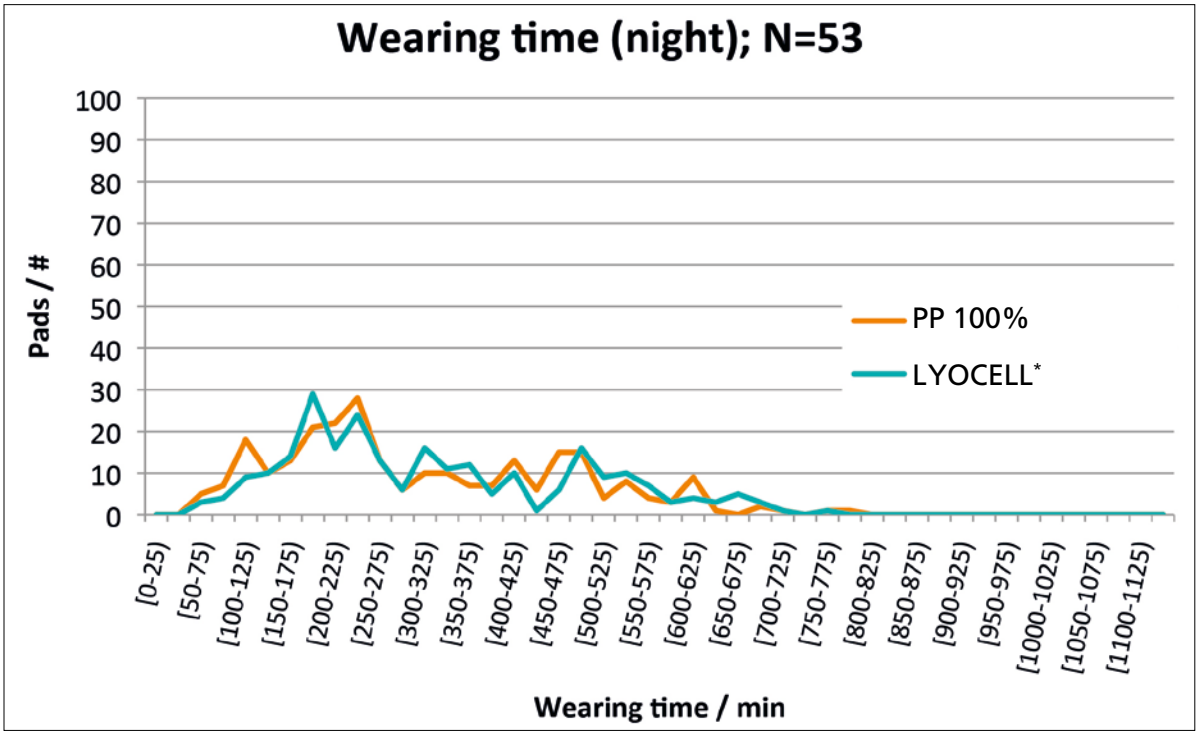

Figure 13. *Wearing time of pads during nighttime.*

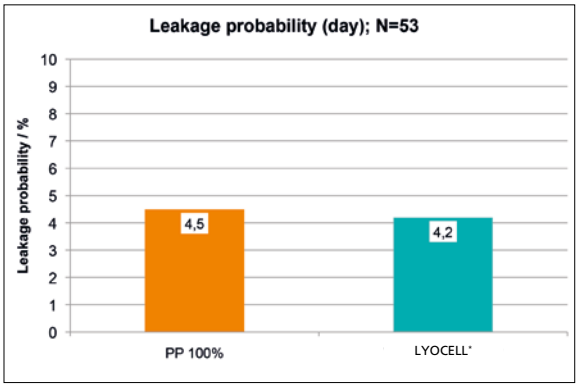

Figure 14. *Leakage probability of pads during daytime.*

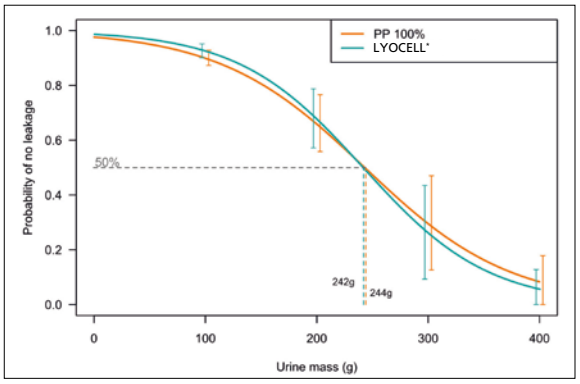

Figure 15. *Probability of no leakage of pads vs. urine mass during daytime.*

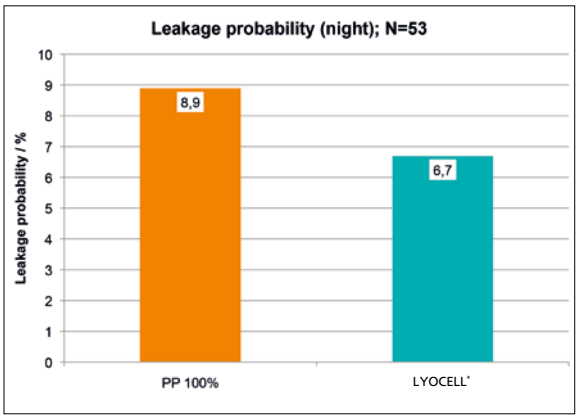

Figure 16. *Leakage probability of pads during nighttime.*

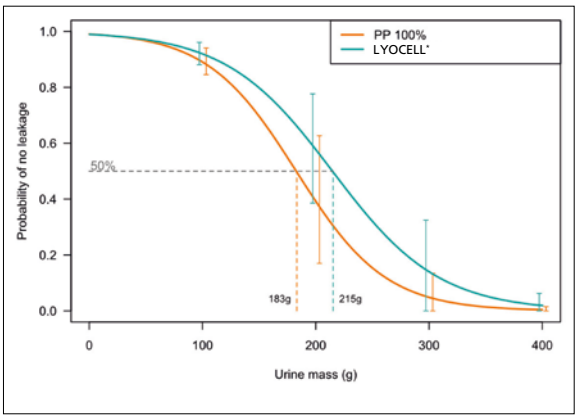

Figure 17. *Probability of no leakage of pads vs. urine mass during nighttime.*

wearing comfort or trust in the product, next to higher feeling of security. The participants were asked questions regarding these attributes in the product specific questionnaire, which are discussed later on.

After having a look at the wearing time of a single product, we will now have a closer look at the performance of the two different topsheets. The main performance indicator for an adult incontinence pad is leakage, because this is the main reason why an insert pad is worn.

Therefore all participants recorded leakage of each individual pad during the 72 h leakage diary (Figure 3) at the end of each 4 weeks trial phase.

In Figure 14 - 17 one can see the leakage data which has been obtained during the trial. During daytime (Figure 14) it can be deduced that there is hardly any difference between the pads equipped with PP 100% and those with Lyocell* topsheets. This can also be pointed out in the leakage curves (daytime) shown in Figure 15.

In contrast to that, the results at nighttimes draw a different picture. Figure 16 shows that there is a clear difference between the pads equipped with PP 100% and those with the Lyocell* mixture. This difference can also be seen in the leakage curve (nighttime) shown in Figure 17. One hypothesis is that at night urine is absorbed faster by the Lyocell* mixture because of the different position of the body. Another hypothesis is that the Lyocell* topsheet distributes the liquid more equally so that local oversaturation of the super absorber-fluff pulp mixture is avoided, which finally leads to less product leakage.

One of the major outcomes of the trial is shown in Figure 18. There the median proportion of nights without changing the products is shown per subject. This item is equal to the amount of undisturbed sleep per partici-

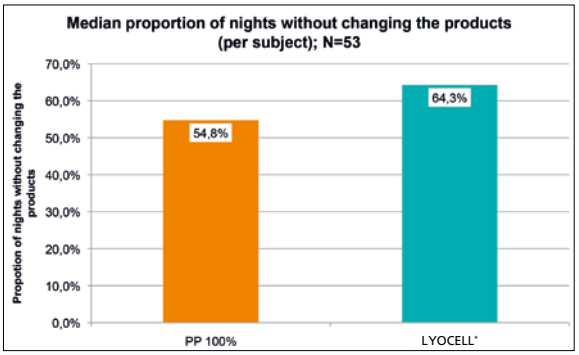

Figure 18. *Percentage of undisturbed sleep.*

pant. Currently a lot of people suffering from adult incontinence have to get up at least once or even twice a night to change their pad because it leaks or feels uncomfortable. In case of using a pad equipped with a Lyocell* topsheet participants could enjoy a 10% higher amount of undisturbed sleep (nights without changing the pad). The reason for that could be that the pad did not feel uncomfortable and/or did not leak. A 10% higher amount of undisturbed sleep at nights has a great impact on the quality of life of the participants. This means that stress which is generated with respect to the adult incontinence symptoms can be dramatically reduced by just changing the topsheet of an adult incontinence pad.

At the end of the 8 weeks test period containing two test phases with the two topsheets, the participants were asked which kind of product they would prefer. The results are shown in Figure 19. More than 52% of the participants rated the pad containing the Lyocell* topsheet as superior product. 10% of the subjects thought that both products where quite equal while 37% preferred the PP 100% topsheet. This means that the majority of the participants preferred the pads with the Lyocell* topsheet.

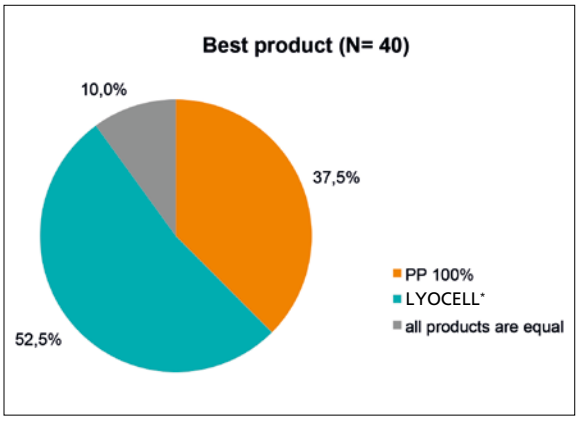

Figure 19. *Percentage of participants who have rated a specific test product as superior.*

As already mentioned previously, the participants had to fill in a product specific questionnaire. This questionnaire was adopted from an incontinence specific trial, having a closer look at pad designs, which has been conducted by M. Fader and A. Cottenden in the UK [2]. For a more specific evaluation of the topsheet relevant topics further questions were added. The participants rated each topsheet according to all the items mentioned in this questionnaire, which was answered at V1, V2 and V3 (see Figure 3). Each of the items listed in the survey had to be evaluated by all subjects using a 1 - 10 scale. 1 was the worst rating while 10 was the best one. Due to the fact that ratings with respect to comfort and trust are very individual and subject specific feelings, it was decided to evaluate these questions by a pairwise comparison per subject. This means that the product scores of each individual subject for product A and B have been compared. As a consequence the number of people who rated a specific product as best regarding one item of the questionnaire was counted and then these numbers were plotted in the item specific axis of the radar diagrams which can be seen in Figure 20 - 22. In the first radar plot (Figure 20) people rated the Lyocell* topsheet as significantly better than the PP topsheet concerning the items "overall performance", "rustling while wearing the pad" and "itching while wearing the pad". With regard to the item "stickiness to the skin while wearing the pad", Lyocell* was only slightly better than PP and in the rating focusing on "sensation of heat while wearing the pad" both topsheets showed quite equal results.

As shown in Figure 21, no differences can be deduced regarding the items of the product specific questionnaire, which evaluated design specific differences (i.e. "fit" and "pad stays in place"). The most important points in this radar diagram are those that focus on comfort (i.e. "wet comfort" and "dry comfort"). The figure clearly shows that both topsheets were performing equally with respect to wet comfort. The main reason for that is the fact that urine as well as water acts as a softener for cellulosic fibers. Products for adult incontinence are wet most of the wearing time and therefore comfort of the Lyocell* mixture is as good as that for PP. In comparison to wet comfort, the evaluation of the item "dry comfort" showed a difference between Lyocell* and PP. Due to its textile like touch the Lyocell* topsheet was rougher than the waxy and very smooth PP one with its permanent hydrophilic finish. A hypothesis why people feel this difference is the fact that subjects suffering from adult incontinence are getting used to the very smooth and waxy surface of PP and therefore are not used to the textile wearing comfort of normal underwear anymore.

The evaluation of the items "ability to absorb urine without leakage" and "ability to neutralize odor" shown in Figure 21, showed hardly any differences concerning performance of the two topsheets. In comparison to these items the evaluation of the element "ability to keep skin dry" showed a slightly better performance for PP. The reason for that could be the inherent property of cellulosic fibers to absorb all kind of liquids. Due to the fact that the Lyocell* mixture contains 50% (w/w) TENCEL® standard fiber and 50% (w/w) modified TENCEL® fiber with its hydrophobic properties, there is a small chance that the wetback of this topsheet is slightly higher for the Lyocell* mixture, although lab tests had shown that both topsheets performed quite equally.

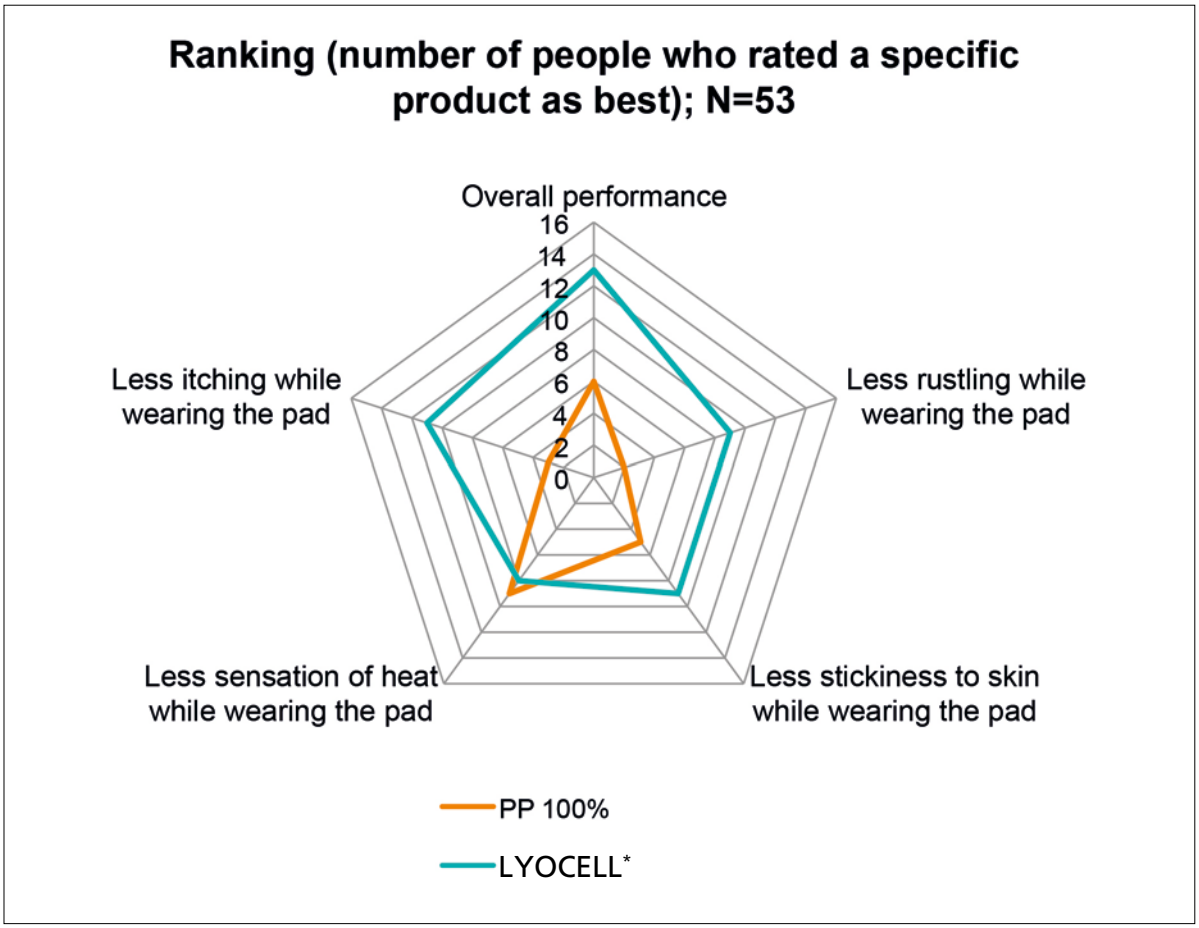

Figure 20. *Radar diagram of product specific questionnaire.*

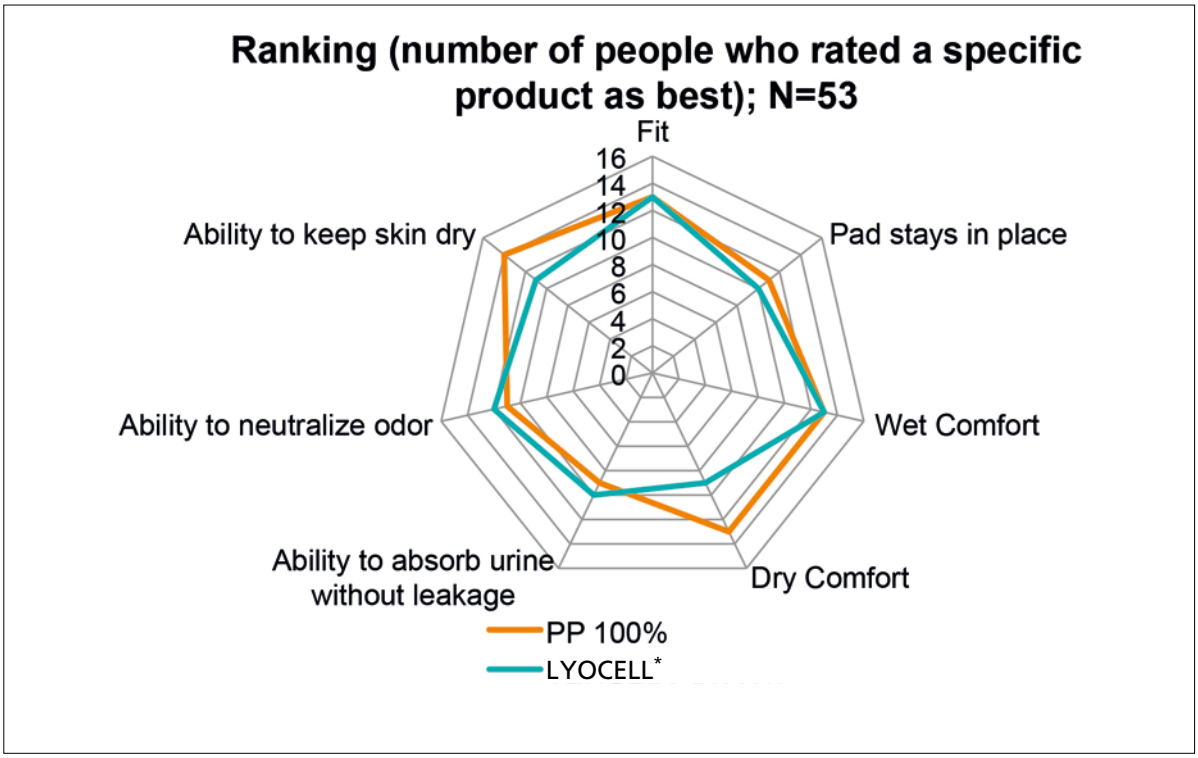

Figure 21. *Radar diagram of product specific questionnaire. Questions adapted from [1], [2].*

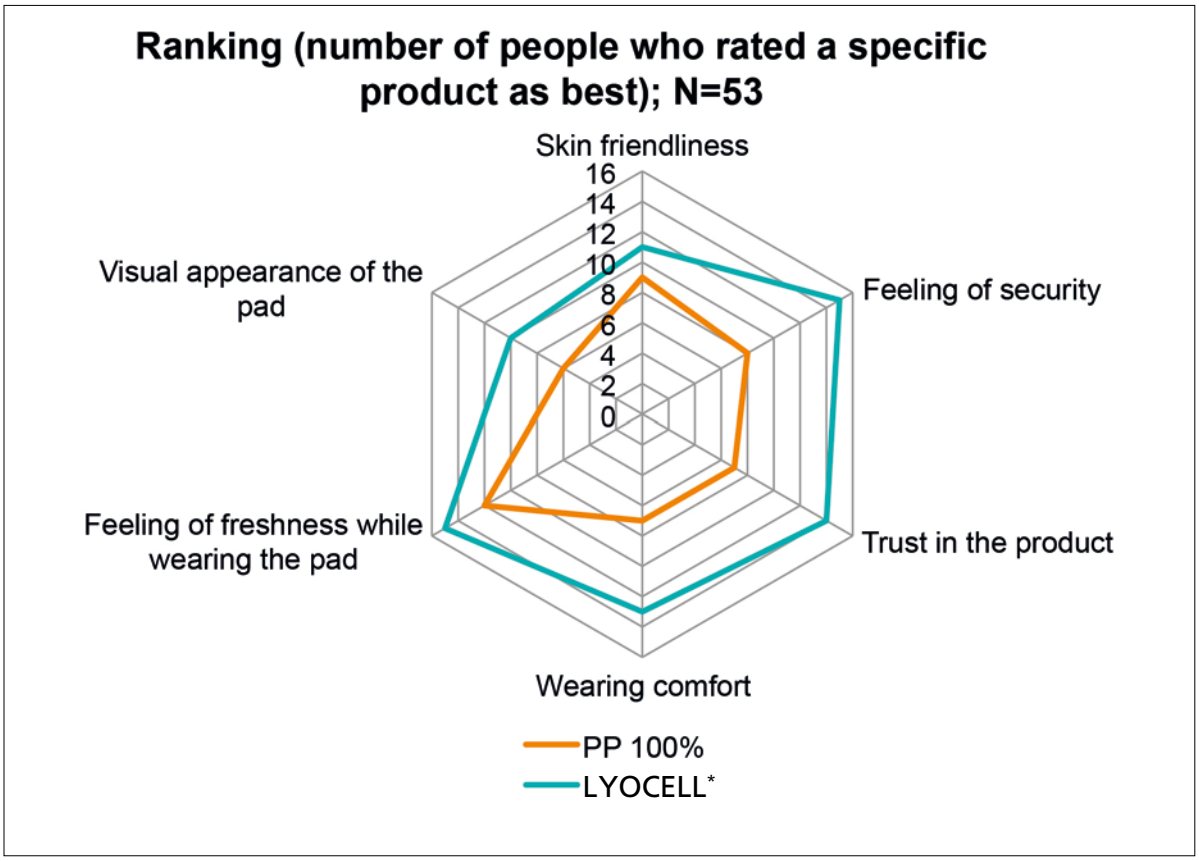

Figure 22. *Radar diagram of product specific questionnaire. Questions adapted from [1], [2].*

The major reasons why people who are suffering from adult incontinence decide to buy a new or different product are the items "feeling of security" and "trust in the product". In both cases the Lyocell* topsheet is significantly better than the PP one. Lyocell* is also slightly better regarding the items "feeling of freshness while wearing the pad", "visual appearance of the pad" and "skin friendliness". A hypothesis why Lyocell* performed better regarding visual appearance in the consumer perception is the more textile look and feel. Finally, Lyocell* also showed significantly better performance regarding the wearing comfort of the product, which proves that topsheets containing cellulosic fibers are definitely adding comfort with respect to wearability.

Conclusions

The outcome of the trial was that people using the Lyocell* topsheet had higher trust in the product and a higher feeling of security, leading to longer wearing times of each single pad and less pad consumption. Next to that, discreetness of the pads could be improved by the fact that the Lyocell* topsheet showed better performance with respect to leakage and reduced noise generation. In addition to that, participants reported better wearing comfort for pads with the Lyocell* topsheet. One major part of this improved wearing comfort is the fact that the subjects experienced reduced itching, when using the Lyocell* topsheet.

The most important result of this trial is the fact that participants who were testing pads equipped with the Lyocell* topsheet enjoyed a 10% higher amount of undisturbed sleep, which is supposed to dramatically improve the quality of life of people suffering from adult incontinence. The sum of all those advantages explains why participants rate the Lyocell* topsheet as best product with the best overall performance.

References

[1] Chartier-Kastler, E., Ballanger, P., Petit, J., Fourmarier, M., Bart, S., Ragni-Ghazarossian, E., Ruffion, A., Le Normand, L. and Costa, P. (2010). Randomized, crossover study evaluating patient preference and the impact on quality of life of urisheaths vs absorbent products in incontinent men. BJU International, 108, 241 – 247.

[2] Fader, M., Cottenden, A., Getliffe, K., Gage, H., Clarke-O'Neill, S., Jamieson, K., Green, N., Williams, P., Brooks, R. and Malone-Lee, J. (2008). Absorbent products for urinary/faecal incontinence: a comparative evaluation of key product designs. Health Technology Assessment, Vol. 12, No. 29.

[3] Hartung, J. and Elpelt, B. (1986). Multivariante Statistik – Lehr- und Handbuch der angewandten Statistik. Oldenbourg Verlag, 2. Auflage.

[4] Kelleher, C. J., Cardozo, L. D., Khullar, V. and Salvatore, S. (1997). A new questionnaire to assess the quality of life of urinary incontinent women. British Journal of Obstetrics and Gynaecology, Vol. 104, pp. 1374 – 1379.

[5] Mapi Research Trust (2011). Scaling and Scoring of the KHQ Version 1.0. Lyon, France.

[6] Schumacher, M. and Schulgen, G. (2007). Methodik klinischer Studien – Methodische Grundlagen der Planung, Durchführung und Auswertung. Springer, 2. Auflage.

[7] Morfeld, M., Kirchberger I., Bullinger M., SF-12 QoL questionnaire (4 weeks), 2nd extended and revised edition, Hogrefe Verlag, Göttingen

How Nonwoven Properties are Influenced by Moisture

Isabell Pape

Hochschule Reutlingen, Fakultät Textil & Design
Alteburgstraße 150, D-72762 Reutlingen
Email: isabell.pape@student.reutlingen-university.com

Abstract

Cellulosic fibres such as viscose or TENCEL®[1] differ in their moisture management properties compared to synthetic fibres like polyester. These properties highly influence the fabric touch. In order to obtain further information about the impact of moisture, nonwovens manufactured from viscose, TENCEL® and polyester were tested. The results obtained during the research show, that the moisture management properties of fibres already affect the spunlace process. The resulting structural differences and the specific moisture management cause a significant impact on the thermal and haptic properties. Among others the moisture uptake from air differs remarkably in between the samples. Therefore the moisture influence on the test results differs in those stages. This confirms that, in particular, nonwovens, which are used in a wet stage, need to be tested in wet moisture stages too.

Introduction

When it comes to the use of fibres in applications which are in contact with the skin, such as wipes or facials [1], thermal absorption and surface properties regarding fabric characteristics are of particular importance. Therefore it is necessary to have optimal thermal and haptic properties. Those are influenced by moisture and can differ depending on the moisture uptake. The properties of viscose and TENCEL® are especially influenced by water. For example, water reduces the tenacity of cellulose based fibres [2], which turns into a softening effect. Due to the different properties of polyester and cellulosic fibres, it is recommended to mix these fibres in order to receive a wider range of properties. Moreover it impacts the moisture management and therefore it is important to evaluate this impact and the resulting characteristics.
The current study analyses nonwovens at different moisture stages to receive first impressions on how the properties change due to the increase of moisture in the material. To compare different nonwovens, samples made of TENCEL®, viscose and polyester are used, as well as fibre mixes, to get a wider range of properties. During the tests a stable standard atmosphere is held. Moreover, many of the applications of nonwovens are in a wet stage. This must be considered problematic, because some testing methods are designed only for dry materials. Therefore, some methods need to be adopted for measurements in a wet stage, in order to get test results which reflect the properties during the usage.

Materials and Methods

Materials

The materials used are spunlaced nonwovens with a specific weight of 50 g/m². They are made of 100% TENCEL®, viscose or polyester as well as 50/50% and 30/70% mixtures of TENCEL® or viscose (50% and 30%) with polyester. In addition, all nonwovens are made under the same production conditions using fibres with a titer of 1.7 dtex, a length of 38 mm and from the same batch. The viscose and TENCEL® fibres were provided by Lenzing AG, Austria.

Methods

Three testing methods were used to get a first impression of the moisture influence on haptic and thermal properties of the nonwovens. The preparation of the

samples was standardized. To evaluate the dry mass the nonwovens were stored for 24 hours in the vacuum oven. For the absorbency from the air they were stored 24 hours in standard atmosphere or in a climate box with 98% relative humidity. For the wetted samples 2.5 times the amount of water by dry mass was added.

Absorbency Testing System (ATS)

The ATS is used to measure the absorbency of fabrics without any additional force. It measures the volume of the liquid which is absorbed by the sample and converts it into mass to calculate the absorbed liquid. This test gives information about the absorbency capacity as well as the absorbency speed. At the beginning of every test, the machine gives an impulse to start the absorbency. After the impulse is given, it is ensured that the fabric absorbs the liquid without external influence. [3]

Tissue Softness Analyzer (TSA)

The TSA is a testing system, which is well established for tissues, but quite new for nonwovens. It measures surface properties of tissues, regarding softness, smoothness and roughness, as well as stiffness. With this parameters it is able to calculate the "handfeel" (HF), a parameter which is equal to an initiated impression of the human skin. [4] The method differs to established testing systems like the ring method [5]. A sound spectrum is recorded by the motion of several blades moving over the samples surface with specific speed and pressure. The peaks used for evaluation can be correlated to two different vibration types, caused by different surface properties. This research focuses on the results of the TS 7 and TS 750 parameters which give information about the softness and roughness of the samples.

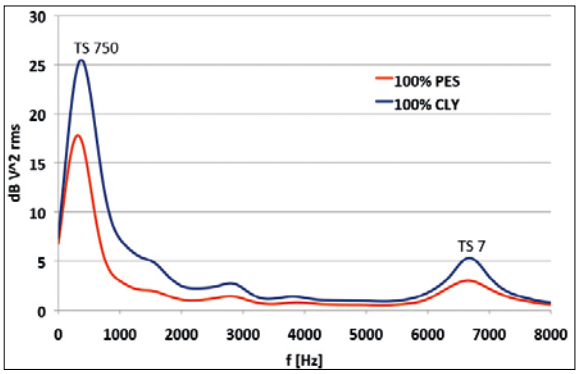

Figure 1. *Frequency of TS 750 and TS 7 [4]: The two main peaks within the sound spectrum, which was generated by the TSA, refer to the surface geometry and the structure of the sample (in case of TS 750), and to the properties of single fibres, like stiffness or bending length in case of TS 7.*

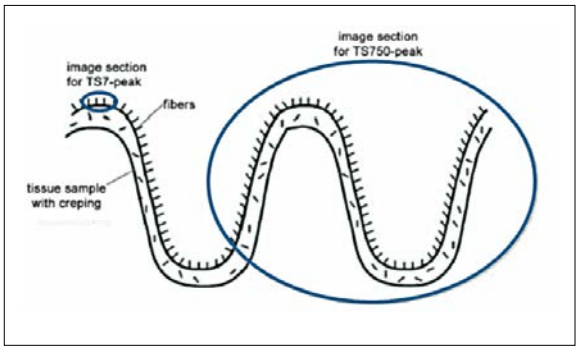

Figure 2. *Fabric sections of TS 750 and TS7 [4]: The cross-sectional view of a sample shows the origin of the two relevant peaks for softness measurement.*

The TS 750 is based on surface geometry and structure of the sample, as seen in figure 2. The structure causes a vertical vibration of the sample. The frequency of this vibration is about 750 Hz (Figure 1). The bigger the structural differences the higher the peak. The TS 7 is based on the stiffness of single fibres, fibre bending length and internal structure, as seen in Figure 2. Stiff fibres cause a horizontal vibration of the blade itself. This vibration has a special resonance frequency which shows up around 7000 Hz (Figure 1). The shown frequency spectrums are converted into bar charts to get a better comparison between the fibres in the different moisture stages. [4] [6]

Alambeta

The Alambeta measuring device gives information about the warm-cool feeling of a fabric, while it is shortly touched. It measures the heat flow between the device and the fabric in order to calculate the thermal absorptivity [W m-2 s1/2 K]. Therefore, the measuring head is heated to 32°C to simulate the human skin while the fabric has standard atmosphere. The temperature difference of 10°C initiates the heat flow while the surface structures and other specific fibre properties influence the amount of heat flow. To compare the test results two facts need to be mentioned. First, differences of a thermal absorptivity rate less than 30 are measurable but not noticeable for the human skin. Second, the higher the measured thermal absorptivity, the cooler the touch of the fabric is perceived. [7]

Results and Discussion

The influence of the different moisture properties already starts at the spunlace process. The impact of hydroentanglement depends on fibre properties such as Young's modulus, density and hydrophilicity. To entangle fibres with a low wet modulus less power is needed. Moreover a uniform wetting causes a more uniform entanglement. [8]. As a result the bonding of hydrophilic fibres and fibres with a low wet modulus is

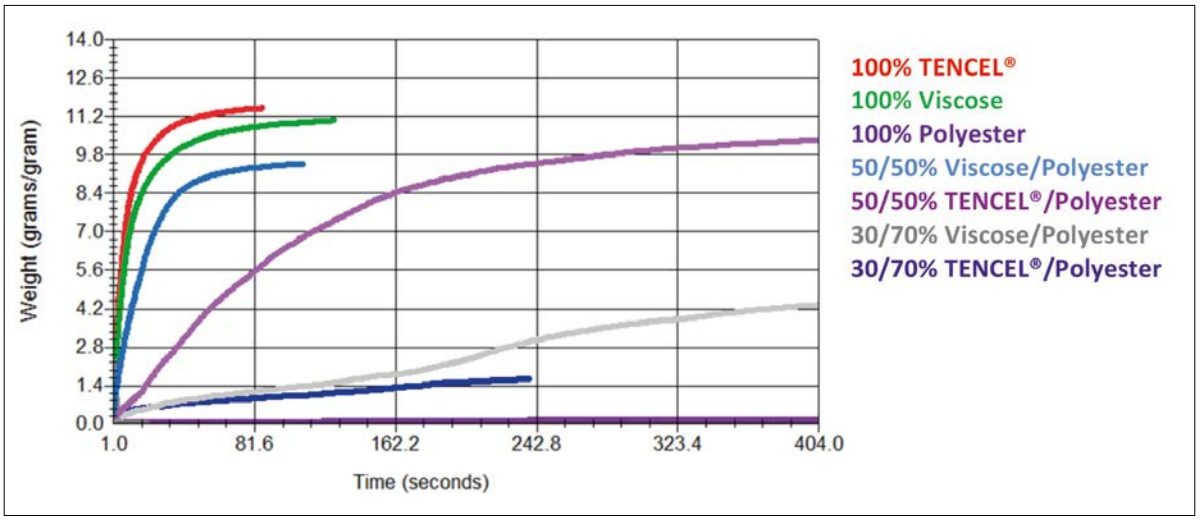

Figure 3. *ATS results: The volume and rate of liquid water uptake varied depending on the samples moisture management properties. The graph illustrates that the absorbency capacity as well as the absorbency speed was the highest with TENCEL®.*

stronger and there is less void space, if they are all made under the same production conditions. Therefore the structure of polyester is looser and the thickness higher than of TENCEL® and viscose, although they all have a specific weight of 50g/m^2. [9] In addition the entanglement of the viscose samples is the tightest because it has the lowest wet modulus. [2, 10] This also intensifies the difference between the tested samples. Moreover the capillary pressure is an important factor for the absorbency of nonwovens because it is the main factor for the moisture transportation after a fabric has absorbed a liquid. [11] Therefore many small void areas are promoting a higher liquid flow better than a few big void areas. However, characteristics of nonwovens are the diffuse arrangement of fibres and the high porosity. These properties are responsible for the low absorbency of polyester nonwovens. Due to the hydrophobic properties of polyester, water uptake is only possible through capillary transport. The randomly arranged fibres and higher void space of the used polyester nonwovens inhibit this wicking effect. As a consequence, the absorptivity and moisture transport decrease with the increase of polyester. [11, 12]

The tests confirm that the higher the air humidity, the higher the moisture uptake. While Figure 3 shows the absorbency of the liquid moisture, Figure 4 points out the moisture increase during different humidity states in the air. Furthermore, a decrease of the moisture absorption is caused by an increasing polyester content in the nonwovens. The absorbency results shown in Figure 3 reveal that TENCEL® has the highest absorbency rate, even better than Viscose. According to Figure 3 polyester affects TENCEL® in the absorbency rate and speed more than it affects viscose. The absorbency speed and the absorbency capacity of the 50/50% TENCEL®/polyester mix decreases a lot while the viscose/polyester mix just loses absorbency capacity. Moreover Figure 3 shows that a share of 30% cellulose fibres is not enough to keep the good absorbency properties. One reason for the different impact is that the TENCEL®/polyester nonwoven has a looser structure than the viscose/polyester sample. This inhibits the wicking effect and hence the absorbency speed is slowed down.

Different moisture management affects the amount of absorbed liquid from air humidity. Therefore the possible influence of water varies between the tested nonwovens as seen in Figure 4. The difference is especially important for cellulose fibres, because moisture influences the fibre softness and stiffness. For the interpretation and analysis it is essential to keep in mind that if there is defined air humidity, the moisture amount of the tested nonwovens differs as seen in Figure 4. In a 2.5 times wetted state the moisture amount of each nonwoven is defined and the same. Therefore the moisture influence and the moisture storage differ significant. While TENCEL® and viscose are able to swell, polyester is not able to do so. This difference influences the thermal and haptic properties. Moreover to increase the moisture content of a polyester nonwoven effectively, it is necessary to add water directly onto the nonwoven.

TSA

The TSA results also confirm that water has a massive influence on the surface properties of nonwovens. As a result there is the assumption that some differences may not be as strong in reality as the graphs signalize. According to the TS 7 test results, the polyester nonwoven shows the highest softness in dry state compared to viscose, which has the hardest feel. In the wet

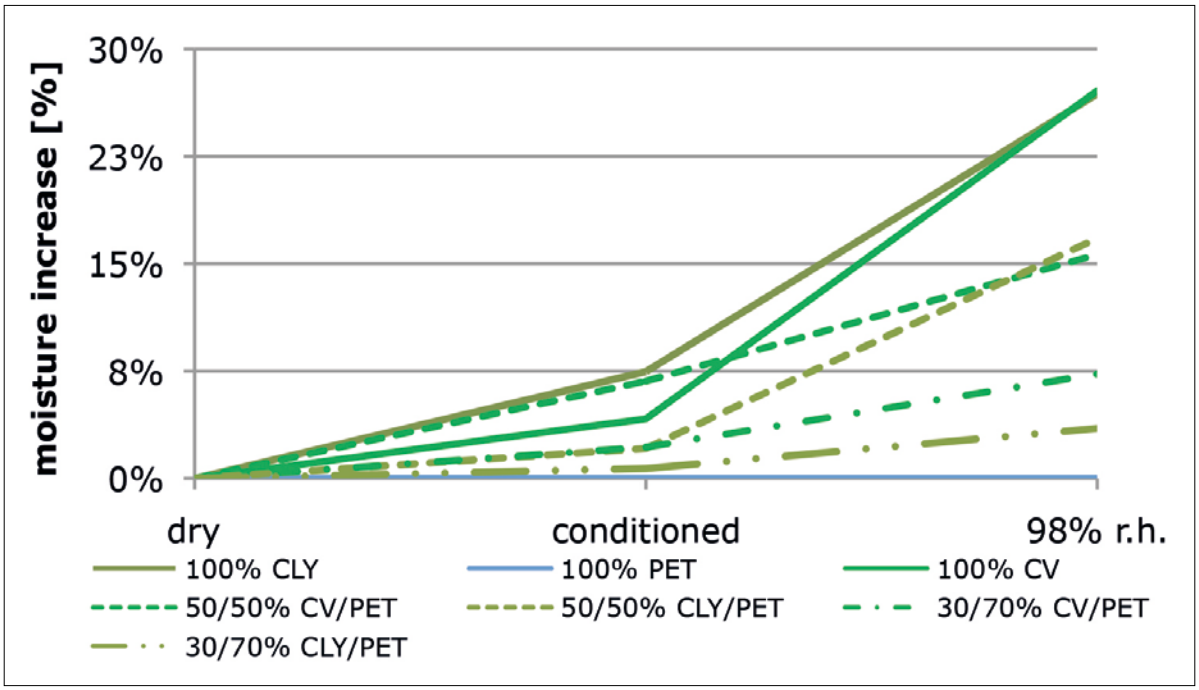

Figure 4. *Moisture increase: Differences in moisture management were shown by analyzing three different humidity stages. Moisture absorption decreased, the higher the polyester amount in the samples was. TENCEL® and viscose showed the highest absorbency rates.*

stages, when the moisture percentage of cellulose fibres rises, the nonwovens become softer. This effect intensifies with moisture increase and it causes the nonwovens with a high percentage of cellulose fibres to change the most. Moreover, the softness of the viscose samples changes the most. This is attributed to the fact that water reduces the tenacity of viscose more than of TENCEL®. [2] [10] Furthermore the roughness seen in Figure 6 of viscose and viscose-mixtures is higher than of the other samples. One reason could be the high fibre friction, which causes a higher resistance. This can result in stronger vibrations. The fact that viscose is swelling a lot and polyester stays rather dry also intensifies the increase of the roughness. This is also causing that the TS 750 test results of the fibre mixes are higher than the 100% viscose and polyester samples.

Moreover the experiment concludes in two unexpected results. The first one is that the 2.5 times wetted nonwovens shows a higher TS 750 peak than the nonwovens which are stored at 98% room humidity. According to emtec Electronic GmbH[2] it is possible that the filled space between the fibers causes a higher reflection of the soundwaves and thus, the microphone records a louder sound. With this test it is shown that a direct comparison between the 2.5 times wetted state and the conditioned state is impossible. Furthermore, the irregular increase of sound from the polyester is the highest. The fact that polyester is not swelling can be one reason for this. All the moisture is stored in the void areas and in the inner layer of the nonwovens, which can increase the reflection of the soundwaves. Secondly, in relation to the test results shown in Figure 4, the change between the conditioned stage and the 98% room humidity from the polyester sample is higher than it should be. The high standard deviation can cause these irregularities. The test results also show, in comparison to the other samples in that stage, the 30/70% TENCEL®/polyester sample is unusual low in the last moisture stage. To verify this result it is necessary to perform more tests to reduce the standard deviation and confirm the results.

Alambeta

The influence of water on the thermal absorptivity depends on the structure and the moisture properties of the fibres. This is due to the fact that the heat flow moves faster through the fibre than through the air [11]. As a result fabrics with high porosity keep the heat better than smooth fabrics with a high fibre volume fraction. Moreover, water has a cooling effect because it fills up the space between the fibres and has a higher thermal conductivity than air. [13] Moisture, which is stored on the surface, intensives the cooling effect, because of the vaporization coldness. Therefore the cool feeling of the nonwovens is bigger, the higher the moisture percentage gets. The test results confirm this assumption. First it is shown that the higher the polyester amount is, the lower the thermal absorptivity of the nonwovens gets. Second the cool feeling increases with higher moisture percentage as seen in Figure 7 and Figure 8.

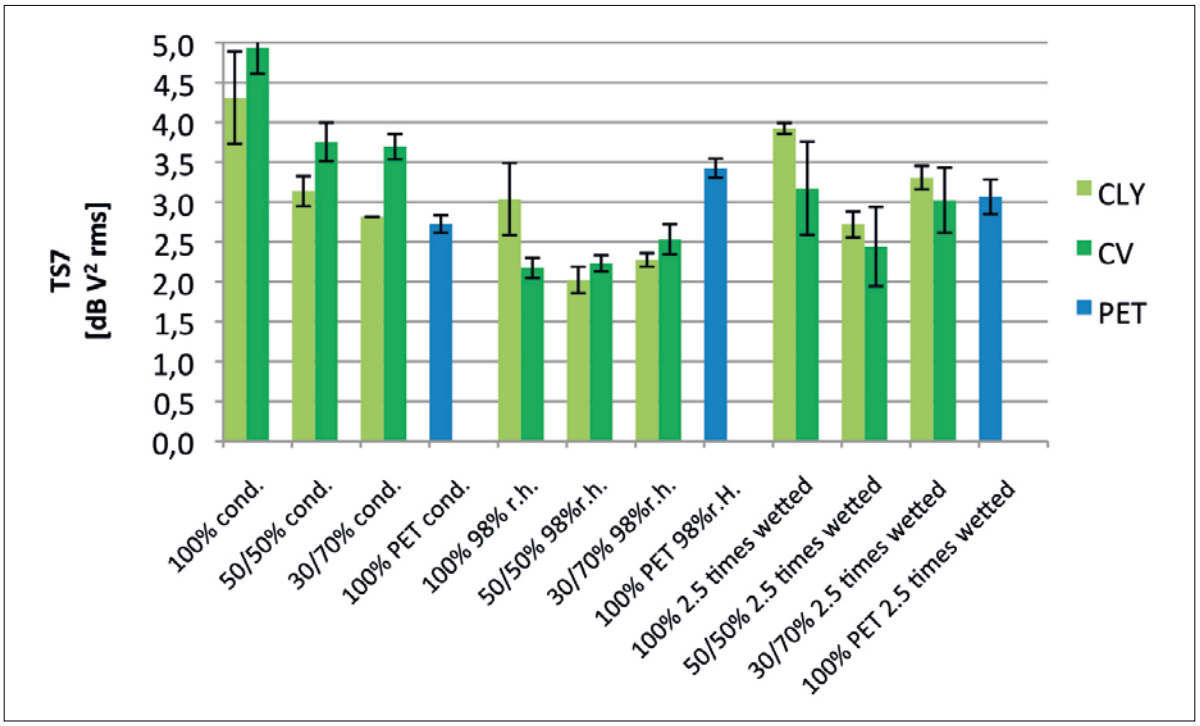

Figure 5. *TS 7 results: Vibrations at a frequency of around 7000 Hz (TS 7) give information on the properties of single fibres. High values refer to stiff fibres or high bending length for example. Water acts as a softener for cellulosic fibres, therefore values are usually lower in wet state.*

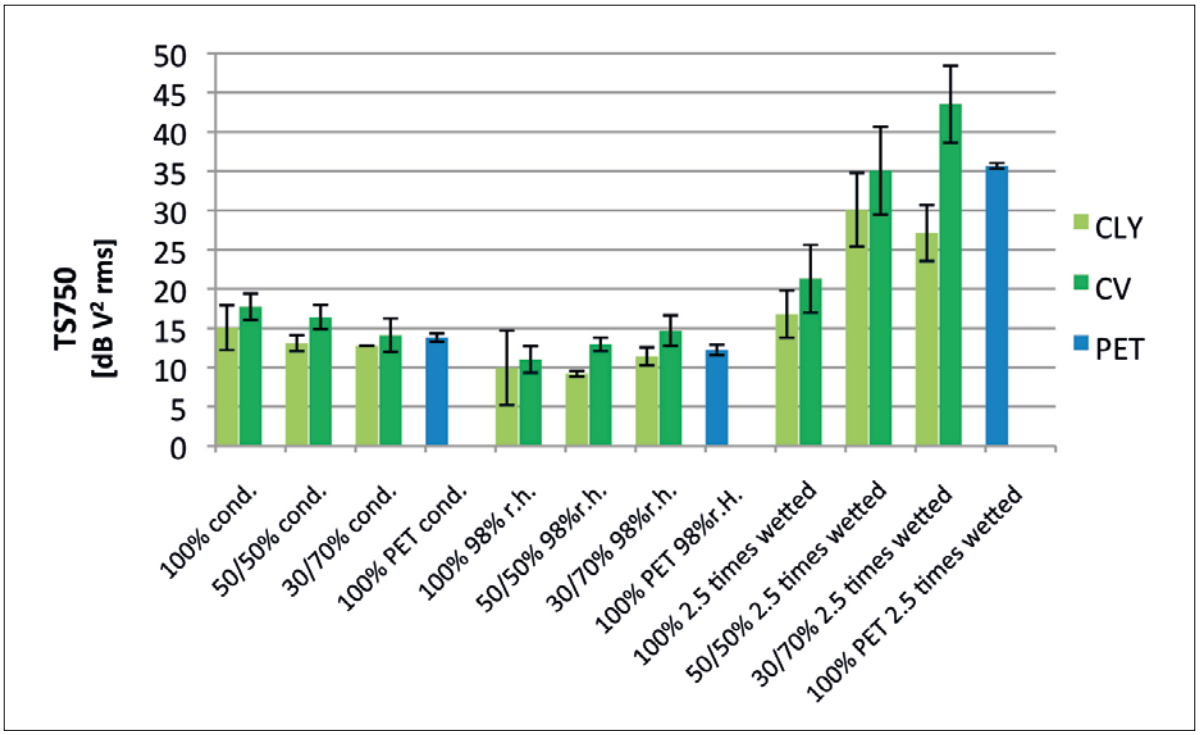

Figure 6. *TSA 750 results: Vibrations at 750 Hz (TS 750) refer to the surface structure and geometry of the samples. The higher the values, the rougher the surface is. In wet state the amount of water seemed to overlay all surface effects, therefore a direct comparison to the conditioned samples was not possible.*

The viscose sample, as shown in Figure 7, has the strongest thermal absorptivity in all moisture stages, which means it has the coolest touch. Furthermore, water has the most influence on it. Moreover, polyester influences TENCEL® more than viscose, because the thermal properties are similar to each other and the structure of the 100% TENCEL® nonwoven is already more loose than the viscose sample. The moisture

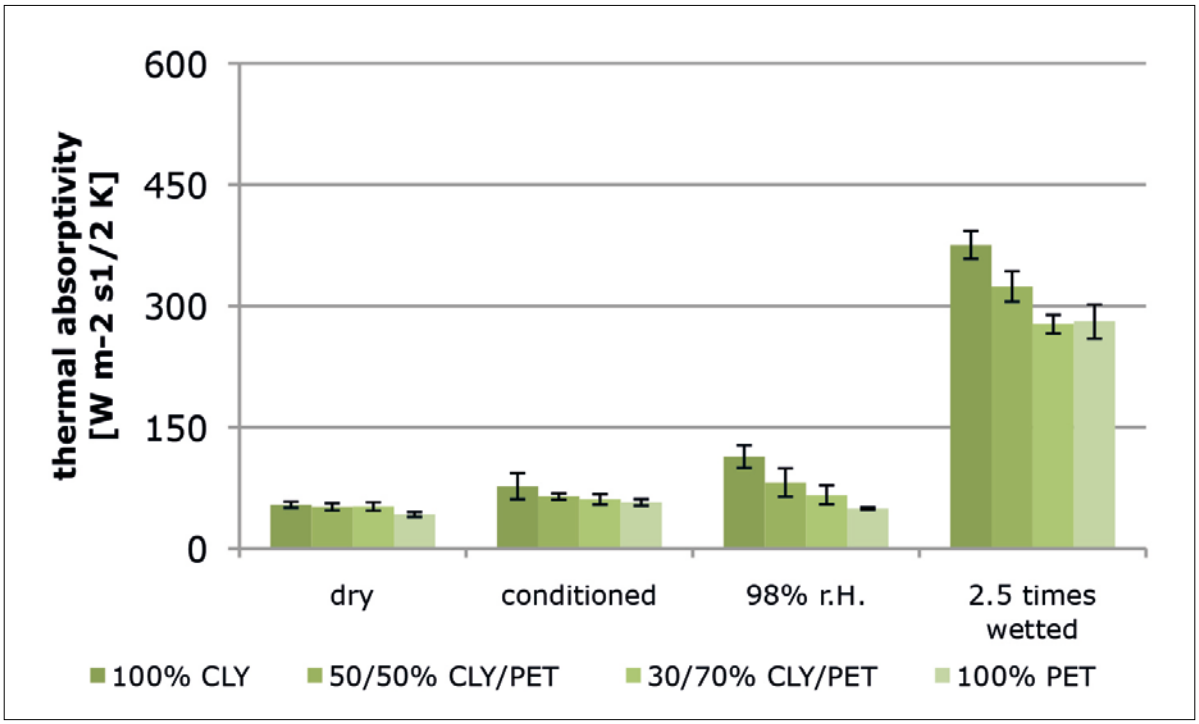

Figure 7. *Alambeta results TENCEL®: The Alambeta measuring device, which gives information about the warm-cool feeling of a fabric while it is shortly touched, showed, that water has a big influence on the thermal absorptivity. With cellulosic samples water seemed to increase the thermal activity constantly, while with polyester only high amounts of water caused an effect. However, at this high humidity stage the effect was already overlayed by the thermal activity of the water itself.*

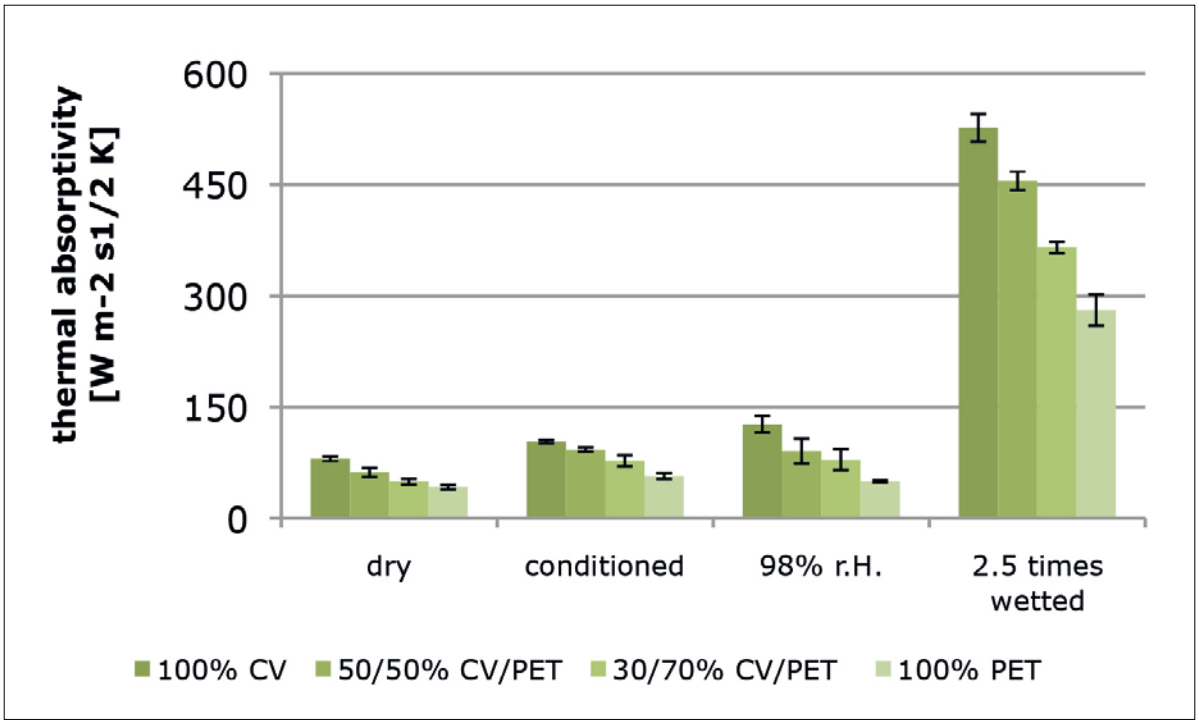

Figure 8. *Alambeta results viscose: As seen in Figure 7, the cool feeling increased with higher moisture percentage. The viscose sample had the highest thermal absorptivity in all stages, which means that it had the coolest touch.*

influence becomes stronger, depending on the increase of the moisture percentage. The high fibre volume fraction of the viscose nonwovens causes a stronger influence of liquids, because there is less space to store the liquid and the swollen fibres on the surface intensify the effect. The test also displays that the different moisture intake from air is not affecting the tendency between the nonwovens.

Conclusions

This series shows that moisture has a high impact on the properties of nonwovens. The different responses to moisture already affect the hydroentanglement and therefore the structure of the nonwovens. In addition, the thermal properties in particular change enormously. The random fibre location and high void space impede the uniform moisture intake particularly for samples with mixed fibre content. Especially the moisture absorption from air differs remarkably in between the fibres. Therefore the moisture percentage varies hence the influence differs, whereby it is not intense. Moreover, to compare fabrics with diverse high moisture percentages it is necessary to adapt the TSA test. As "free" water inside the nonwovens influences the signal a direct comparison between dry (and moderate moist) samples and wet ones is not possible. However, samples under the same conditions can be compared and here the results show the softening effect of water on cellulose, which leads to softer nonwovens in the wet state, which is the common usage, as well. Not only are the final product properties influenced by the different response to moisture of various fibres, but already the production itself too. It was shown that identical spunlace conditions can lead to different nonwovens structures depending on the used fibres. This has to be taken into consideration, when comparing the properties of the products.

Acknowledgments

The work and results described in this paper are part of a bachelor thesis, which was conducted from October 2015 to March 2016 at Lenzing AG. The author thanks Eva Liftinger, M.Sc. and Dr. Josef Innerlohinger (both Lenzing AG) and Prof. Dr. Ing. Volker Jehle (Reutlingen University) for intensive support. Furthermore the author thanks Lenzing AG for providing the laboratory facilities and financial support.

References

[1] A. Wilson, "Development of the nonwoven industry," in Handbook of Nonwovens, 2007, pp. 1-15.

[2] W. Albrecht, M. Reintjes and B. Wulfhorst, "Lyocell-Fasern," Faserstoff-Tabellen nach P.-A Koch, 1997.

[3] Sherwood Instruments, Absorbency Testing System, Locksley, 2006.

[4] Emtec: Grüner, Giselher, TSA Tissue Softeness Analyzer, Emtec, 2013.

[5] Y. E. Mogahzy, F. Kilinc and M. Hassan, "Developments in measurement and evaluation of fabric hand," in Effect ofmechanical and physical properties on fabric hand, Camridge England, Woodhead publishing Limited, 2005.

[6] U. Schloßer, T. Bahners, E. Schollmeyer, J. Gutmann and G. Grüner, "Griffbeurteilung von Textilien mittels Schallanalyse," Melliand Textilberichte, pp. 43-45, 2012.

[7] L. Hes, ALAMBETA textile measuring instrument simulating human skin, 2003.

[8] S. J. Russell, S. Anand und D. Brunnschweiler, "Mechanical bonding," in Handbook of Nonwovens, 2007, pp. 255-266.

[9] I. Pape, Ermittlung der inhärenten Eigenschaften von Vliesen in Abhängigkeit von Fasermischungen und deren Feuchtigkeit, Lenzing: Bachelorarbeit, 2016.

[10] D. K. Götze, Chemiefasern nach dem Viskoseverfahren, Springer Verlag, 1967.

[11] D. Brojeswari et al., "Moisture Transmission through textiles Part I: Processes involved in moisture transmission and the factors at play," AUTEX Research journal, pp. 100-110, 06 2007.

[12] P. Kaethik, H. Arunukumar and D. S.Sugumar, "Moisture Management Study in Inner and Outer Layer Blended Fleece Fabric," IJERT, pp. 1-13, September 2012.

[13] P. Kurzweil, B. Frenzel and F. Gebhard, Physik Formelsammlung, Vieweg + Teubner, 2009, p. 143.

Wood Based Fibers for Industrial Applications

Marina Crnoja-Cosic, Berndt Köll, Martin Marsche and Robert Malinowsky

LENZING AG, Werkstrasse 2, 4860 Lenzing, Austria

Abstract

Cellulose, the most abundant polymer on this planet, plays a key role in the global fiber market.
Austria headquartered Lenzing AG developed a process to transform wood based precursor material into a fiber with multiple end-uses. Innovation has always played an important role in its corporate history. The invention of Lenzing Modal® was followed by the development of a producer dyed color pigmented modal fiber with outstanding fastness properties. Many years of intense research resulted in a fibre production process only using a physical cellulose dissolving mechanism known by its generic name Lyocell. Lenzing AG is selling Lyocell products under its brand-name TENCEL®.
Historically used only for global apparel and home textiles its unique inherent properties the fibers are applicable for technical end-application as described hereafter.

Lenzing Modal® Color as an Alternative for Plastic Nets

Lenzing fiber products are part of the natural cellulose cycle. Outstanding trait of them are, that they are from renewable source and naturally compostable.
The wood pulp used for man-made cellulose fiber products stems from sustainably managed sources. The origins of the forests and plantations and their methods of production are well known.

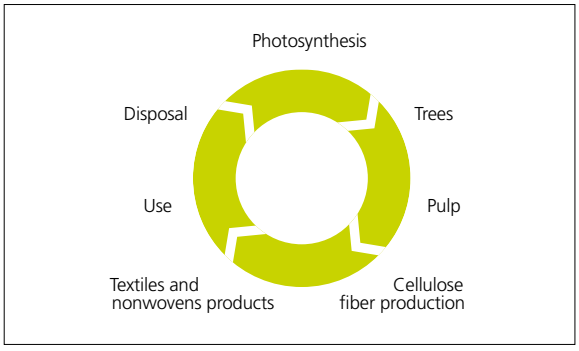

Figure 1. *Cellulose cycle.*

Using sustainable packaging materials that are part of the cellulose cycle will dramatically reduce the global usage of crude oil derivate in his area. A market study showed the strong interest in such packaging material from the retail side.

Together with partners Lenzing AG has developed sustainable nets for fruits and vegetables. This new packaging solution bears significantly positive environmental impact. Wood based cellulose nets are fully biodegradable, compostable, allowing it to re-enter the food life cycle. Studies with regard to the rate of being compostable were carried out in carefully controlled environments.

Figure 2. *Lenzing Modal® nets for packaging.*

Wood based Lenzing fibers were found completely degraded after 6 weeks in a static aerated compost pile, whereas cotton fiber suffered a weight loss of approximately only 80%. Under identical conditions, polyester, polypropylene and polyethylene show very little signs

of degradation. Upon these results big retailers have already decided to implement the concept of fruit and vegetable nets made of Lenzing Modal®.

TENCEL® New Solutions for the FootwearIndustry

The newest fiber generation developed by LENZING AG is called TENCEL®. Fibers are obtained by only dissolving the cellulose in a solvent and spinning the fiber into a waterborne spinning bath. Nearly 100% of the solvent used is recovered in the process. Contrary to other ways of cellulosic fiber manufacturing, this new technology of making fiber is based on a physical rather than a chemical process.
This technology an example of ecological soundness, received the environmental award of the European Union. It makes TENCEL® – apart from its excellent fiber characteristics – even an alternative to synthetic fibers for a wide variety of applications.
Recently introduced TENCEL® in footwear offers, in comparison to traditional materials, three remarkable benefits:

- moisture management
- performance improvement
- sustainability

Moisture management:
Fabrics and nonwovens containing TENCEL® fibers provide excellent moisture properties. An outstanding characteristic of TENCEL® fibers is the ability to absorb and release moisture, which results in a long-lasting optimal foot climate. TENCEL® fibers contribute to the reduction of odour causing bacteria within footwear components. An increased wearing comfort is guaranteed.
Lenzing and a number of renowned partners are currently innovating footwear components like lining, inner lining, thermo-adhesive lining, paddings as well as insoles, all focused on improved moisture management and requested technical performance.
Along with media attention on topics like climate change, shortage of important natural resources, declining working conditions and the abundancy of potentially harmful substances, global demand for sustainable consumer products is growing. Lenzing AG is taking ownership and developed with its supply chain partners solutions for a number of textile footwear components. Meanwhile also laces, zippers and even sewing threads can be obtained from TENCEL® fibers. Shoe manufacturer and designer can choose for a sustainable footwear parts portfolio offering enhanced

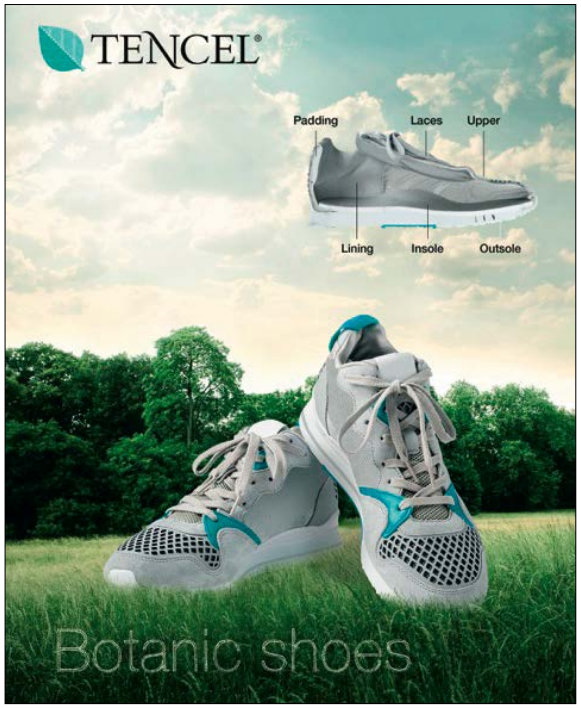

Figure 3. *Botanic shoe concept with TENCEL® fibers*

moisture management opportunities without compromising performance and longevity of the product.

TENCEL® Twines, the Sustainable Solution for Growing Fruits and Vegetables

Taking its responsibility for the environment very seriously, Lenzing AG focuses on developing products made from renewable materials. Cellulose is one of the most versatile polymers formed by nature. TENCEL®, made thereof in an environmental friendly process, is 100% compostable and 100% biodegradable, even in marine environment. Looking at the cellulose cycle, the usage of this fiber is equivalent to that, what is nowadays claimed as circular economy.

Figure 4. *TENCEL® twines for green-houses*

Agro twines produced from TENCEL® fibers, mainly for green-house use, can be tailored to keep the required strength during the growth period of the plant, but being compostable after harvesting. With this unique feature it is possible to substitute plastic twines and wire twines. After the harvesting period, no separation of the remaining plant and the twine is necessary. The residual biomass can be directly transferred to a composting site, offering time saving and as well as cost reduction is an environmentally sustainable product.

Outlook

Cellulosic fibers manufactured according to the lyocell process have a great potential to substitute standard plastics and oil based synthetic fibers. Coming from renewable origin, TENCEL® can be returned into the natural cycle without restrictions. The claim: 'from nature' to 'usage' 'back to nature' is truly fulfilled.
Currently Lenzing AG is evaluating additional promising applications where sustainability will meet demanding technical performance criteria like for carry bags, filters and even thermoplastic reinforcement and composite materials will be investigated.